

ARCHIVES OF MECHANICS

Copyright ©1999 by Institute of Fundamental Technological Research,
Polish Academy of Sciences, Warsaw, Poland

Aims and Scope

ARCHIVES OF MECHANICS provides a forum for original research on mechanics of solids, fluids and discrete systems, including the development of mathematical methods for solving mechanical problems. The journal encompasses all aspects of the field, with the emphasis placed on:

- mechanics of materials: elasticity, plasticity, time-dependent phenomena, phase transformation, damage, fracture; physical and experimental foundations, micromechanics, thermodynamics, instabilities
- methods and problems in continuum mechanics: general theory and novel applications, thermomechanics, structural analysis, porous media, contact problems
- dynamics of material systems
- fluid flows and interactions with solids

FOUNDERS

M.T. HUBER • W. NOWACKI • W. OLSZAK • W. WIERZBICKI

INTERNATIONAL COMMITTEE

J.L. AURIAULT • D.C. DRUCKER • R. DVOŘÁK • W. FISZDON • D. GROSS
V. KUKUDZHANOV • G. MAIER • G.A. MAUGIN • Z. MRÓZ
C.J.S. PETRIE • J. RYCHLEWSKI • M. SOKOŁOWSKI • W. SZCZEPIŃSKI
G. SZEFER • V. TAMUŽS • K. TANAKA • Cz. WOŹNIAK • H. ZORSKI

EDITORIAL COMMITTEE

H. PETRYK – editor • W. KOSIŃSKI • W.K. NOWACKI • M. NOWAK,
A. STYCZEK • J.J. TELEGA • S. ZAHORSKI • Z. KRAWCZYK – secretary

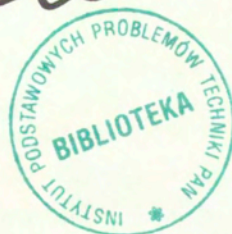
Address of the Editorial Office:
Institute of Fundamental Technological Research
Świętokrzyska 21
PL 00-049 Warsaw, Poland

Tel.: (48-22) 826 60 22, Fax: (48-22) 826 98 15
E-mail: publikac@ippt.gov.pl

P.262^a

Polish Academy of Sciences

Institute of Fundamental Technological Research



Archives of Mechanics

Archiwum Mechaniki Stosowanej

volume 51

issue 1



Agencja Reklamowo-Wydawnicza A. Grzegorzcyk

Warszawa 1999

<http://rcin.org.pl>

SUBSCRIPTIONS

Address of the Editorial Office: Archives of Mechanics

Institute of Fundamental Technological Research, Świątokrzyska 21

PL 00-049 Warsaw, Poland

Tel.: (48-22) 826 60 22, Fax: (48-22) 826 98 15, E-mail: publikac@ippt.gov.pl

Subscription orders for all journals edited by IFTR may be sent directly to the Editorial Office of the Institute of Fundamental Technological Research

Subscription rates

Annual subscription rate (1999) including postage is US \$ 174.

Please transfer the subscription fee to our bank account: Payee: IPPT PAN,

Bank: PKO SA. IV O/Warszawa,

Account no. 12401053-40054492-3000-401112-001.

All journals edited by IFTR are available also through:

- Foreign Trade Enterprise ARS POLONA Krakowskie Przedmieście 7, 00-068 Warszawa, Poland fax: (48-22) 826 86 73
- RUCH S.A. ul. Towarowa 28, 00-958 Warszawa, Poland fax:(48-22) 620 17 62
- Agencja Reklamowo-Wydawnicza A. Grzegorzcyk, Bitwy Warszawskiej 1920r. 3, 00-973 Warszawa, Poland tel./fax: (48-22) 822 49 36

Warunki prenumeraty

Redakcja przyjmuje prenumeratę na wszystkie czasopisma wydawane przez IPPT PAN.

Bieżące numery można nabyć a także zaprenumerować roczne wydanie Archiwum Mechaniki

Stosowanej bezpośrednio w Dziale Wydawnictw IPPT PAN, Świątokrzyska 21,

00-049 Warszawa, Tel.: (48-22) 826 60 22; Fax: (48-22) 826 98 15.

Cena rocznej prenumeraty z bonifikatą dla krajowego odbiorcy wynosi 120 zł.

Również można je nabyć, a także zamówić (przesyłka za zaliczeniem pocztowym) we Wzorcowni Ośrodka Rozpowszechniania Wydawnictw Naukowych PAN, 00-818 Warszawa, ul. Twarda 51/55, tel. (48-22) 697 88 35.

Wpłaty na prenumeratę przyjmują także jednostki kolportażowe RUCH S.A. Oddział Krajowej Dystrybucji Prasy, 00-958 Warszawa, ul. Towarowa 28. Konto: PBK.S.A. XIII Oddział Warszawa nr 11101053-16551-2700-1-67. Dostawa odbywa się pocztą zwykłą w ramach opłaconej prenumeraty z wyjątkiem zlecenia dostawy pocztą lotniczą, której koszt w pełni pokrywa zleceniodawca.

Tel.: (48-22) 620 10 39, fax: (48-22) 620 17 62

Arkuszy wydawniczych 10,5. Arkuszy drukarskich 10.

Papier offset, kl. III 70 g, B1

Oddano do składania w marcu 1999 r. Druk ukończono w maju 1999 r.

Skład i łamanie: G. Wasilewska. Druk i Oprawa: Drukarnia OMIKRON, Stare Babice, ul. Kutrzeby 15.

Distortion equation of motion in linear incompatible elastodynamics

R. WOJNAR

*Polish Academy of Sciences
Institute of Fundamental Technological Research
Świętokrzyska 21, 00-049 Warszawa, Poland
rwojnar@ippt.gov.pl*

THE PAPER DEALS with an initial-boundary value problem of linear incompatible elastodynamics, based on Kosevich' theory of continuously distributed defects due to prescribed plastic fields, [1, 2, 3]. In analogy to a stress formulation of linear incompatible elastodynamics with continuously distributed defects, [4], a distortion formulation is proposed. In such a formulation the tensorial initial-boundary value problem for an unknown asymmetric tensor field is to be solved. A solution to the problem generates the associated stress and rotation fields.

1. Introduction

THE STRESS FORMULATION of linear elastodynamics is a counterpart of the displacement formulation (cf. IGNACZAK [5, 6]). The stress formulation was applied to a dislocation theory by IGNACZAK and RAO in their fundamental work [4]. In the present paper we give the formulation of a problem of linear elastodynamics with defects in terms of an asymmetric distortion tensor field, and prove an appropriate uniqueness theorem. Also, we show that by a symmetrization, the problem and uniqueness theorem reduce to those of a pure stress formulation of elastodynamics with continuously distributed defects, cf. [4]. In addition, we use a solution to the distortion initial-boundary value problem to obtain a dislocation density formula from [4], see Eq.(2.11) in [4].

If the displacement field of a solid with defects is described by a vector u_i , ($u_i = u_i^T$, where u_i^T is the total displacement introduced in [4]), then the distortion tensor w_{ij} is defined as, cf. LANDAU and LIFSHITZ [2],

$$(1.1) \quad w_{ij} = u_{j,i}.$$

Of course, in general tensor w_{ij} is not symmetric, i.e. $w_{ij} \neq w_{ji}$.

In the defect theory, the integral of w_{ij} along a contour L which encloses the dislocation line D is equal to Burger's vector \tilde{b}_i , cf. Fig. 1.

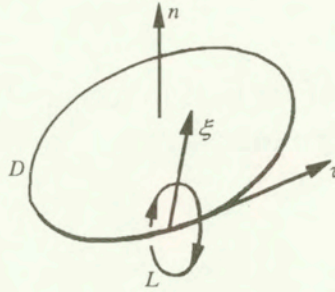


FIG. 1. The contour of integration L enclosing the dislocation line D . The direction of the contour integration and the chosen direction of the tangent vector τ to the line D are related by the corkscrew rule, after [2]. Vector \mathbf{n} is normal to the dislocation loop surface and vector ξ is a radius vector taken from the line D in the plane perpendicular to the vector τ .

Therefore, the following relation holds true:

$$(1.2) \quad \oint_L w_{ik} n_i dl = -\tilde{b}_k.$$

Using Stokes' theorem, this integral relation can be written in a differential form

$$(1.3) \quad \varepsilon_{imn} w_{nk,m} = -\tau_i \tilde{b}_k \delta(\xi),$$

where ε_{imn} is the permutation symbol (the antisymmetric unit tensor), vector τ_i denotes the unit tangent to the dislocation line D , and ξ is the two-dimensional position vector taken from the dislocation line in the plane perpendicular to the vector τ_i at the point considered; and $\delta = \delta(\xi)$ represents the Dirac delta function, cf. also the Appendix.

If we introduce, after [2], the dislocation density tensor ρ_{ik} , defined as

$$(1.4) \quad \int_{S_L} \rho_{ik} df_i = \tilde{b}_k$$

where integration is performed over a surface S_L spanned by the contour L , we write instead of relation (1.3), the following equality

$$(1.5) \quad \varepsilon_{ijm} w_{mk,j} = -\rho_{ik}.$$

Hence, tensor ρ_{ik} satisfies the condition

$$(1.6) \quad \rho_{ik,i} = 0$$

which for a single dislocation expresses the conservation of the Burgers vector along the dislocation line.

For convenience, and to make comparisons with [4] easier, we use the notation adopted in [4]

$$(1.7) \quad \alpha_{ik} \equiv -\rho_{ik}.$$

Then, Eqs. (1.5) and (1.6) take the forms

$$(1.5)' \quad \varepsilon_{ijm} w_{mk,j} = \alpha_{ik}$$

and

$$(1.6)' \quad \alpha_{ik,i} = 0.$$

Equations (1.5) or (1.5)' hold true both for dislocations which are at rest and those in motion, if only the elastic displacements are taken into account. However, the motion of a dislocation can be related to a plastic deformation, as well. An exhaustive discussion of the elastodynamic theory of defects in which plastic deformations are prescribed, and the defects are characterized in terms of a symmetric stress tensor field, is presented in [4]. In the following, we present a ramification of the results obtained in [4] in which an asymmetric distortion tensor field plays a central role.

A total distortion tensor w_{ij}^T , denoted in [2] by W_{ij} , is postulated in the form

$$(1.8) \quad w_{ij}^T = w_{ij}^E + w_{ij}^P,$$

where w_{ij}^E and w_{ij}^P represent the elastic and plastic parts of the distortion, respectively,

$$(1.9) \quad w_{ij}^T = u_{j,i}$$

and neither elastic nor plastic part of decomposition (1.8) are obtained by the gradient of a vector field. Clearly, relations (1.1) to (1.6) are valid for $w_{ij} \equiv w_{ij}^E$ and $w_{ij}^P \equiv 0$.

If, in addition, it is postulated that (1.5)' is satisfied by the elastic part w_{ij}^E only, i.e.

$$(1.10) \quad \varepsilon_{ijm} w_{mk,j}^E = \alpha_{ik}$$

then, by (1.8) and (1.9), we obtain

$$(1.11) \quad \varepsilon_{ijm} w_{mk,j}^P = -\alpha_{ik}.$$

The total deformation tensor e_{ij}^T , and elastic and plastic strain tensors e_{ij}^E and e_{ij}^P are defined in terms of w_{ij}^T , w_{ij}^E and w_{ij}^P by {cf. [4], Eqs. (2.1) – (2.2)}

$$(1.12) \quad 2e_{ij}^T = w_{ij}^T + w_{ji}^T,$$

$$(1.13) \quad 2e_{ij}^E = w_{ij}^E + w_{ji}^E (\equiv 2e_{ij}),$$

$$(1.14) \quad 2e_{ij}^P = w_{ij}^P + w_{ji}^P.$$

Other fields of the defect theory such as the dislocation moment density can be also defined in terms of the tensor w_{mn}^P , (cf. LANDAU and LIFSHITZ [2], KOSEVICH [3]).

2. Basic field equations and initial boundary value problem

Let a nonhomogeneous anisotropic linear elastic body, occupying a three-dimensional region B , be subject to a dynamic motion. Let the body forces be absent. Let the displacement be described by a vector u_i . Then the distortion tensor w_{ij}^T is defined as, cf. (1.9),

$$(2.1) \quad w_{ij}^T = u_{j,i}.$$

The relation between the strain tensor e_{ij}^T and the distortion tensor w_{ij}^T is given by (1.12), and the relation between the stress tensor s_{ij}^E and the strain tensor e_{ij}^T is given by the generalized Hooke's law, cf. SOKOLNIKOFF [7], NOWACKI [8],

$$(2.2) \quad s_{ij}^E = C_{ijmn} e_{mn}^E,$$

where C_{ijmn} is the elasticity tensor. The inverse relation reads

$$(2.3) \quad e_{ij}^E = K_{ijmn} s_{mn}^E,$$

where K_{ijmn} is the compliance tensor, *i.e.*:

$$C_{ijpq} K_{pqmn} = \delta_{i(m} \delta_{jn)} \quad \text{on } B$$

and δ_{ij} stands for Kronecker's symbol.

Thus, instead of (2.2) we can write

$$(2.4) \quad s_{ij}^E = C_{ijmn} w_{mn}^E$$

or taking into account (1.8), we get

$$(2.5) \quad s_{ij}^E = C_{ijmn} (w_{mn}^T - w_{mn}^P) (\equiv s_{ij}).$$

In Eqs. (2.2) – (2.5) the symmetry relations are postulated

$$(2.6) \quad C_{ijmn} = C_{jimn} = C_{ijnm} = C_{mni j}, \quad K_{ijmn} = K_{jimn} = K_{ijnm} = K_{mni j}.$$

The equation of motion takes the form

$$(2.7) \quad s_{ik,k}^E + b_i = \rho \ddot{u}_i,$$

where $\rho = \rho(\mathbf{x})$ and $\mathbf{b} = \mathbf{b}(\mathbf{x})$ denote the mass density and body force vector fields.

Finally, the density ρ and compliance K_{ijkl} satisfy the inequalities

$$(2.8) \quad \rho > 0, \quad K_{ijkl} \xi_{ij} \xi_{kl} > 0$$

for every tensor field $\xi_{ij}(\mathbf{x})$, $\mathbf{x} \in B$, not necessarily symmetric.

3. Distortion equation of motion

After differentiation of equation of motion (2.7) and use of definition of distortion (2.1), we get

$$(3.1) \quad (\rho^{-1} s_{ik,k}^E)_{,j} + (\rho^{-1} b_i)_{,j} = \ddot{w}_{ij}^T, \quad (\mathbf{x}, t) \in B \times [0, \infty)$$

or, by (2.5),

$$\left\{ \rho^{-1} [C_{ikmn} (w_{mn}^T - w_{mn}^P)]_{,k} \right\}_{,j} + (\rho^{-1} b_i)_{,j} = \ddot{w}_{ij}^T, \quad (\mathbf{x}, t) \in B \times [0, \infty)$$

or

$$(3.2) \quad [\rho^{-1} (C_{ikmn} w_{mn}^T)_{,k}]_{,j} + \hat{b}_{i,j} = \ddot{w}_{ij}^T, \quad (\mathbf{x}, t) \in B \times [0, \infty).$$

This is the distortion equation of elastodynamics we are to deal with. The term

$$(3.2a) \quad \hat{b}_i \equiv [b_i - (C_{ikmn} w_{mn}^P)_{,k}] / \rho$$

is to be considered as the given density of body forces distributed in a crystal, (cf. [2]).

The above field equation is subject to the initial conditions

$$(3.3) \quad w_{ij}^T(\mathbf{x}, 0) = w_{ij}^o(\mathbf{x}), \quad \dot{w}_{ij}^T(\mathbf{x}, 0) = \dot{w}_{ij}^o(\mathbf{x}) \quad \mathbf{x} \in B$$

and boundary conditions

$$(3.4) \quad \begin{aligned} u_i^0(\mathbf{x}) + t\dot{u}_i(\mathbf{x}) + \rho^{-1}t * (C_{ikmn}w_{mn}^T)_{,k}(\mathbf{x}, t) &= \mathcal{U}_i(\mathbf{x}, t) && \text{on } \partial B_{\mathcal{U}} \times [0, \infty), \\ (C_{ijmn}w_{mn}^T)n_j &= \mathcal{F}_i(\mathbf{x}, t) && \text{on } \partial B_{\mathcal{F}} \times [0, \infty), \end{aligned}$$

where $\partial B_{\mathcal{U}} \cup \partial B_{\mathcal{F}} = \partial B$, $\partial B_{\mathcal{U}} \cap \partial B_{\mathcal{F}} = \emptyset$.

The fields $w_{ij}^0(\mathbf{x})$ and $\dot{w}_{ij}^0(\mathbf{x})$ are determined by the initial displacement field $u_i(\mathbf{x}, 0) = u_i^o(\mathbf{x})$ and the initial velocity field $\dot{u}_i(\mathbf{x}, 0) = \dot{u}_i^o(\mathbf{x})$ through the relations

$$w_{ij}^0(\mathbf{x}) = u_{j,i}^o(\mathbf{x}), \quad \dot{w}_{ij}^0(\mathbf{x}) = \dot{u}_{j,i}^o(\mathbf{x}) \quad \text{on } B.$$

Moreover, the field $\mathcal{U}_i(\mathbf{x}, t)$ is expressed by the boundary displacement $\hat{u}_i(\mathbf{x}, t)$, and the initial data $u_i^o(\mathbf{x})$ and $\dot{u}_i^o(\mathbf{x})$, through

$$\mathcal{U}_i(\mathbf{x}, t) = \hat{u}_i(\mathbf{x}, t) - t\dot{u}_i^o(\mathbf{x}) - u_i^o(\mathbf{x}).$$

Finally, the field $\mathcal{F}_i(\mathbf{x}, t)$ represents the surface traction.

THEOREM 1. *(Uniqueness theorem for a distortion initial-boundary value problem of elastodynamics with defects).*

The problem (3.2) – (3.4) has at most one solution.

P r o o f. It is sufficient to show that the problem (3.2) – (3.4) corresponding to homogeneous data has a zero solution only.

Introduce the notations

$$(a) \quad s_{ij} = C_{ijmn}w_{mn}^T$$

and

$$(b) \quad W_{ij} = w_{ij}^T.$$

Then, the homogenous counterparts to Eqs. (3.2) – (3.4) read

$$(3.2)' \quad (\rho^{-1}s_{ik,k})_{,j} = \ddot{W}_{ij}, \quad (\mathbf{x}, t) \in B \times [0, \infty)$$

$$(3.3)' \quad W_{ij}(\mathbf{x}, 0) = 0, \quad \dot{W}_{ij}(\mathbf{x}, 0) = 0, \quad \mathbf{x} \in B;$$

$$(3.4)' \quad \rho^{-1}t * (C_{ikmn}W_{mn})_{,k}(\mathbf{x}, t) = 0 \quad \text{on } \partial B_{\mathcal{U}} \times [0, \infty),$$

$$C_{ijmn}W_{mn}n_j = 0 \quad \text{on } \partial B_{\mathcal{F}} \times [0, \infty).$$

Moreover, (a), (3.3)' and (3.4)' imply that

$$(b) \quad s_{ij}(\mathbf{x}, 0) = 0, \quad \dot{s}_{ij}(\mathbf{x}, 0) = 0, \quad \mathbf{x} \in B$$

and

$$(c) \quad s_{ik,k}(\mathbf{x}, t) = 0 \quad \text{on} \quad \partial B_U \times [0, \infty),$$

$$(d) \quad s_{ij}n_j = 0 \quad \text{on} \quad \partial B_F \times [0, \infty).$$

Multiply both sides of Eq. (3.2)' by \dot{s}_{ij} and integrate over B , to obtain

$$\int_B [(\rho^{-1}s_{ik,k})_{,j}] \dot{s}_{ij} dB = \int_B \ddot{W}_{ij} \dot{s}_{ij} dB.$$

Hence, by integration by parts, we get

$$\int_B \left\{ [(\rho^{-1}s_{ik,k}) \dot{s}_{ij}]_{,j} - (\rho^{-1}s_{ik,k}) \dot{s}_{ij,j} \right\} dB = \int_B \ddot{W}_{ij} \dot{s}_{ij} dB$$

or, by use of the divergence theorem,

$$\int_{\partial B} (\rho^{-1}s_{ik,k}) \dot{s}_{ij} n_j dA - \int_B [(\rho^{-1}s_{ik,k}) \dot{s}_{ij,j}] dB = \int_B \ddot{W}_{ij} \dot{s}_{ij} dB.$$

By (c) and (d), we obtain

$$- \int_B [(\rho^{-1}s_{ik,k}) \dot{s}_{ij,j}] dB = \int_B \ddot{W}_{ij} \dot{s}_{ij} dB$$

or by (a)

$$\frac{1}{2} \frac{\partial}{\partial t} \int_B [(\rho^{-1}s_{ik,k}) \dot{s}_{ij,j} + C_{ijmn} \dot{W}_{ij} \dot{W}_{mn}] dB = 0,$$

and after integration with respect to time and using the initial conditions (3.3)' and (b), we get

$$(3.5) \quad \int_B [(\rho^{-1}s_{ik,k}) s_{ij,j} + C_{ijmn} \dot{W}_{ij} \dot{W}_{mn}] dB = 0.$$

Hence

$$(e) \quad s_{ij,j} = 0$$

and

$$(f) \quad \dot{W}_{ij} + \dot{W}_{ji} = 0.$$

Insert (e) into (3.2)' to get

$$(g) \quad 0 = \ddot{W}_{ij} \quad \forall (\mathbf{x}, t) \in B \times [0, \infty).$$

Integrating the last equation twice and using the initial conditions (3.3)' we obtain the result

$$(h) \quad W_{ij} = 0 \quad \forall (\mathbf{x}, t) \in B \times [0, \infty).$$

This completes the proof of the uniqueness theorem. \square

Note that the uniqueness theorem for a pure stress initial-boundary value problem of elastodynamics in which the elasticity tensor is positive definite and the density is positive was presented in [5], while the uniqueness theorem for a pure stress initial-boundary value problem of incompressible isotropic elastodynamics was given in [9].

4. Remarks

4.1.

Let us, in addition to the fields introduced in Sec. 2, define the elastic rotation vector field

$$(4.1) \quad \omega_k = \frac{1}{2} \varepsilon_{kab} w_{ab}^E$$

and elastic rotation tensor field

$$(4.2) \quad o_{mk} = \frac{1}{2} (w_{mk}^E - w_{km}^E).$$

Also, define the elastic bend-twist tensor as

$$(4.3) \quad \kappa_{mk} = \omega_{k,m}.$$

With these definitions we find that

$$o_{mk} = \frac{1}{2} (o_{mk} - o_{km})$$

or

$$o_{mk} = \frac{1}{2} (\delta_{ma} \delta_{kb} - \delta_{mb} \delta_{ka}) o_{ab}$$

or

$$o_{mk} = \frac{1}{2} \varepsilon_{mkq} \varepsilon_{qab} o_{ab}.$$

Hence

$$o_{mk} = \varepsilon_{mkq} \omega_q$$

and, by (4.3)

$$(4.4) \quad o_{mk,j} = \varepsilon_{mkq} \kappa_{jq}.$$

Therefore, Eq. (1.5)' which, by definitions (1.13) and (4.2) can be written as

$$(4.5) \quad \varepsilon_{ijm} (e_{mk} + o_{mk})_{,j} = \alpha_{ik},$$

takes the form

$$(4.6) \quad \varepsilon_{ijm} (e_{mk,j} + \varepsilon_{mkq} \kappa_{jq}) = \alpha_{ik}$$

and this is an equation identical with Eq.(2.11)₁ in [4].

4.2.

By taking symmetric part of the distortion problem (3.1) – (3.4), we arrive at the pure stress problem of elastodynamics with continuously distributed defects discussed in [4] (cf. THEOREM 3.3 in [4]).

4.3.

If a solution of the pure stress problem discussed in 4.2. is available, then the skew part of the distortion, *i.e.* a solution of the problem obtained by taking skew part of the problem (3.1) – (3.4), can be easily obtained.

5. Conclusions

1. A pure distortion initial-boundary value problem of linear elastodynamics with continuously distributed defects has been formulated, and a uniqueness theorem for the problem has been proved.

2. By a symmetrization, the problem and uniqueness theorem reduce to those of a pure stress formulation of elastodynamics with continuously distributed defects, cf. [4].

3. By defining the elastic rotation fields in terms of the distortion tensor, a dislocation density formula from [4] has been recovered.

Appendix

To show that the integral condition (1.2) implies the local equation (1.3), Stokes' theorem is used. The proof is due to LANDAU and LIFSHITZ [2]. First, we note that for an arbitrary vector \mathbf{a} we have

$$(A.1) \quad \oint_L a_i n_i dl = \int_{S_L} \varepsilon_{imn} a_{n,m} n_i dS,$$

where S_L is a surface that spans the contour L . Substituting w_{ik} instead of a_i into (A.1) we get

$$(A.2) \quad \oint_L w_{ik} n_i dl = \int_{S_L} \varepsilon_{imn} w_{nk,m} n_i dS.$$

Next, we note that a constant vector $\tilde{\mathbf{b}}$ may be represented by an integral involving the two-dimensional delta function

$$(A.3) \quad \tilde{b}_k = \int_{S_L} \tau_i \tilde{b}_k \delta(\boldsymbol{\xi}) n_i dS,$$

where $\boldsymbol{\xi}$ is the two-dimensional radius vector taken from the axis of dislocation in the plane perpendicular to the vector $\boldsymbol{\tau}$ at the point considered, cf. Fig. 1. Substituting (A.2) and (A.3) into (1.2) we get

$$(A.4) \quad \int_{S_L} \varepsilon_{imn} w_{nk,m} n_i dS = - \int_{S_L} \tau_i \tilde{b}_k \delta(\boldsymbol{\xi}) n_i dS.$$

Since the contour L is arbitrary, from (A.4) we obtain (1.3). This completes the proof of implication (1.2) \Rightarrow (1.3).

References

1. A. M. KOSEVICH, *Equation of motion of a dislocation*, Zh. E. T. F., **43**, 637–648, 1962.
2. L. D. LANDAU and E. M. LIFSHITZ, *Teoriya uprugosti*, Izd. Nauka Glavn. Red. Fiz.-Mat. Literaturny, 3rd edition, Moskva 1965; also English translation: *Theory of elasticity*, Vol. 7 of *Course of Theoretical Physics*, Pergamon Press, Oxford 1970.
3. A. M. KOSEVICH, *Crystal dislocations and the theory of elasticity*, [in:] F.R.N. Nabarro [Ed.], *Dislocation in solids*, Vol. 1, North Holland, Amsterdam 1979.
4. J. IGNACZAK and C. R. A. RAO, *Stress characterization of elastodynamics with continuously distributed defects*, J. Elasticity, **30**, 219–250, 1993.
5. J. IGNACZAK, *Direct determination of stresses from the stress equations of motion in elasticity*, Arch. Mech. Stos., **11**, 671–678, 1959.

6. J. IGNACZAK, *A completeness problem for the stress equation of motion in the linear theory of elasticity*, Arch. Mech.Stos., **15**, 225–234, 1963.
7. I. S. SOKOLNIKOFF, *Mathematical theory of elasticity*, Second Edition, New York-Toronto-London 1956.
8. W. NOWACKI, *Theory of Elasticity* [in Polish], [in:] *Mechanika techniczna t. IV Sprężystość* [in Polish], [Ed.] M. Sokołowski, PWN, Warszawa 1978.
9. R. WOJNAR, *Uniqueness theorem for stress equations of isochoric motions of linear elasticity*, Arch. Mech., **26**, 747–750, 1974.

Received February 11, 1998; new version August 24, 1998.

Some exact solutions of steady plane MHD non-Newtonian power-law fluid flows*

I. ADLURI

*Department of Mathematics, Wheeling Jesuit University,
Wheeling, West Virginia, WV 26003 USA*

EQUATIONS of steady plane MHD flow of a non-Newtonian power-law fluid are transformed to the hodograph plane by means of the Legendre transform function of the stream-function. Results are summarized in the form of a theorem. As applications of the developed theory, four flow problems of physical interest are studied. Exact solutions and the corresponding geometry are obtained in each case.

1. Introduction

HODOGRAPH TRANSFORMATION is one of the methods of solving systems of nonlinear partial differential equations. This technique has been widely used in continuum mechanics. AMES [1] present a survey of the hodograph transformation and its applications in fluid mechanics and various other fields. In a series of papers CHANDNA *et al.* [2 – 7] have applied hodograph and Legendre transformations to investigate steady plane viscous flows, non-Newtonian flows and MHD non-Newtonian flows in the presence of constantly inclined, aligned, transverse or orthogonal magnetic field. ADLURI [8, 9] has employed this method to obtain a class of exact solutions plane MHD non-Newtonian power-law fluids and micropolar fluids. In recent years, the interest in problems of non-Newtonian fluid flows has grown considerably due to an extensive use of these fluids in many areas such as chemical processes in industries, food and construction engineering, petroleum production, power engineering and commercial applications. Since most liquid metals, non-Newtonian fluids, and many other second grade fluids to which single fluid model can be applied, accounting for electrical conductivity, makes the flow problem realistic both from the mathematical and the physical point of view.

The present paper deals with application of hodograph transformation technique to obtain a class of exact solutions of the nonlinear partial differential equations governing the steady plane flow of a power-law fluid in the presence of a transverse magnetic field. Equations of the flow are transformed to the hodograph plane interchanging the role of independent variables x, y and the

*This work is supported by Wheeling Jesuit University – 1998 Summer Research Grant

components u, v of the velocity field. Introducing a Legendre function of the stream-function, all equations in the hodograph plane are expressed in terms of this transform function. Results are summarized in the form of a theorem and finally, four interesting flow problems are studied to illustrate the developed theory. Exact solutions and geometry of the flow are obtained in each case and it is proved that a spiral flow cannot exist in a non-Newtonian power-law fluid whether or not the fluid is conducting.

2. Equations of flow

The steady plane flow of an electrically conducting non-Newtonian fluid which obeys Ostwald-de Waele power-law model

$$\tau_{ij} = 2K [2e_{kl}e_{kl}]^{\frac{(n-1)}{2}} e_{ij}$$

where

$$e_{ij} = \frac{1}{2} \left(\frac{\partial u_i}{\partial x_j} + \frac{\partial u_j}{\partial x_i} \right),$$

is governed by

$$(2.1) \quad \frac{\partial u}{\partial x} + \frac{\partial v}{\partial y} = 0,$$

$$(2.2) \quad \frac{\partial F}{\partial x} = \rho v \omega + K \left\{ \omega \frac{\partial I}{\partial y} - I \frac{\partial \omega}{\partial y} + 2 \left(\frac{\partial u}{\partial x} \frac{\partial I}{\partial x} + \frac{\partial u}{\partial y} \frac{\partial I}{\partial y} \right) \right\},$$

$$(2.3) \quad \frac{\partial F}{\partial y} = -\rho u \omega - K \left\{ \omega \frac{\partial I}{\partial x} - I \frac{\partial \omega}{\partial x} - 2 \left(\frac{\partial v}{\partial x} \frac{\partial I}{\partial x} + \frac{\partial v}{\partial y} \frac{\partial I}{\partial y} \right) \right\},$$

$$(2.4) \quad u \frac{\partial H}{\partial x} + v \frac{\partial H}{\partial y} = \frac{1}{\mu_e \sigma} \left(\frac{\partial^2 H}{\partial x^2} + \frac{\partial^2 H}{\partial y^2} \right),$$

$$(2.5) \quad \omega = \frac{\partial v}{\partial x} - \frac{\partial u}{\partial y},$$

$$(2.6) \quad I = \left[2 \left(\frac{\partial u}{\partial x} \right)^2 + 2 \left(\frac{\partial v}{\partial y} \right)^2 + \left(\frac{\partial u}{\partial y} + \frac{\partial v}{\partial x} \right)^2 \right]^{\frac{(n-1)}{2}},$$

where τ_{ij} denotes the strain rate tensor, e_{ij} – the strain tensor, $(u(x, y) \cdot v(x, y), 0)$ is the velocity vector field, $(0, 0, H(x, y))$ is the magnetic field, p is the pressure, ρ is the fluid density, μ_e is the magnetic permeability, σ is the electrical conductivity, K is the constitutive coefficient, I is the Ostwald-de Waele parameter and

$$(2.7) \quad F(x, y) = \frac{1}{2}\rho(u^2 + v^2) + p + \frac{1}{2}\mu_e H^2.$$

3. Equations in the hodograph plane

Assuming $u(x, y), v(x, y)$ to be such that the *Jacobian*

$$(3.1) \quad J(x, y) = \frac{\partial(u, v)}{\partial(x, y)} \neq 0, \quad 0 < |J| < \infty$$

in the region of the flow and considering x and y as functions of u and v , we can derive the following relations

$$J(x, y) = \frac{\partial(u, v)}{\partial(x, y)} = \left[\frac{\partial(x, y)}{\partial(u, v)} \right]^{-1} = \bar{J}(u, v),$$

$$(3.2) \quad \frac{\partial u}{\partial x} = J \frac{\partial y}{\partial v}, \quad \frac{\partial u}{\partial y} = -J \frac{\partial x}{\partial v}, \quad \frac{\partial v}{\partial y} = J \frac{\partial x}{\partial u},$$

$$\frac{\partial f}{\partial x} = \frac{\partial(f, y)}{\partial(x, y)} = \bar{J} \frac{\partial(\bar{f}, y)}{\partial(u, v)}, \quad \frac{\partial f}{\partial y} = -\frac{\partial(f, x)}{\partial(u, v)} = \bar{J} \frac{\partial(x, \bar{f})}{\partial(u, v)},$$

where $f = f(x, y) = f(u(x, y), v(x, y)) = \bar{f}(u, v)$ is any continuously differentiable function.

Employing these relations to Eqs. (2.1) – (2.7) we obtain the following equations in the (u, v) – plane:

$$(3.3) \quad \frac{\partial x}{\partial u} + \frac{\partial y}{\partial v} = 0,$$

$$(3.4) \quad \bar{J} \frac{\partial(\bar{F}, y)}{\partial(u, v)} = \rho v \bar{\omega} + K \bar{J} \left\{ \bar{\omega} Q_1 - \bar{I} P_1 + 2 \bar{J} \left(Q_2 \frac{\partial y}{\partial v} - Q_1 \frac{\partial x}{\partial v} \right) \right\},$$

$$(3.5) \quad \bar{J} \frac{\partial(x, \bar{F})}{\partial(u, v)} = -\rho u \omega - K \bar{J} \left\{ \bar{\omega} Q_2 - \bar{I} P_2 + 2 \bar{J} \left(Q_2 \frac{\partial y}{\partial u} - Q_1 \frac{\partial x}{\partial u} \right) \right\},$$

$$(3.6) \quad u N_1 + v N_2 = \frac{1}{\mu_e \sigma} \left\{ \frac{\partial(\bar{J} N_1, y)}{\partial(u, v)} + \frac{\partial(x, \bar{J} N_2)}{\partial(u, v)} \right\},$$

$$(3.7) \quad \bar{\omega} = \bar{J} \left(\frac{\partial x}{\partial v} - \frac{\partial y}{\partial u} \right),$$

$$(3.8) \quad \bar{I} = (\bar{J})^{(n-1)} \left\{ 2 \left(\frac{\partial x}{\partial u} \right)^2 + 2 \left(\frac{\partial y}{\partial v} \right)^2 + \left(\frac{\partial x}{\partial v} + \frac{\partial y}{\partial u} \right)^2 \right\}^{\frac{(n-1)}{2}}$$

where

$$(3.9) \quad \begin{aligned} P_1(u, v) &= \frac{\partial(x, \bar{w})}{\partial(u, v)}, & P_2(u, v) &= \frac{\partial(\bar{w}, y)}{\partial(u, v)}, \\ Q_1(u, v) &= \frac{\partial(x, \bar{I})}{\partial(u, v)}, & Q_2(u, v) &= \frac{\partial(\bar{I}, y)}{\partial(u, v)}, \\ N_1(u, v) &= \frac{\partial(\bar{H}, y)}{\partial(u, v)}, & N_2(u, v) &= \frac{\partial(x, \bar{H})}{\partial(u, v)}. \end{aligned}$$

Equations (3.3) – (3.8) is a system of six equations in six unknown functions $x(u, v), y(u, v), \bar{w}, \bar{I}, \bar{H}$ and \bar{F} . Once a solution of this is obtained, we can determine $u(x, y), v(x, y)$ and all other flow variables in the physical plane. Eq. (3.6) is the diffusion equation for a finitely conducting fluid for infinitely conducting fluid flows it should be replaced by

$$(3.10) \quad uN_1 + vN_2 = 0.$$

4. Legendre transformation function and $\bar{H}(u, v)$

The continuity Eq. (2.1) implies the existence of a stream-function $\psi(x, y)$ such that

$$(4.1) \quad d\psi = -vdx + udy, \quad \frac{\partial\psi}{\partial x} = v, \quad \frac{\partial\psi}{\partial y} = u$$

and Eq. (3.3) implies the existence of a function $L(u, v)$ called the Legendre transform function of the stream-function $\psi(x, y)$ such that

$$(4.2) \quad dL = -ydu + xdv, \quad \frac{\partial L}{\partial u} = -y, \quad \frac{\partial L}{\partial v} = x.$$

Functions $L(u, v)$ and $\psi(x, y)$ are related by

$$(4.3) \quad L(u, v) = vx - uy + \psi(x, y).$$

Using Eq. (4.2), we can transform Eqs. (3.4) – (3.9), respectively, to

$$(4.4) \quad \bar{J} \frac{\partial \left(\frac{\partial L}{\partial u}, \bar{F} \right)}{\partial(u, v)} = \rho v \omega + K \bar{J} (\bar{w} Q_1 - \bar{I} P_1 - 2 \bar{J} R_1),$$

$$(4.5) \quad \bar{J} \frac{\partial \left(\frac{\partial L}{\partial v}, \bar{F} \right)}{\partial(u, v)} = -\rho u \omega - K \bar{J} \left(\bar{\omega} Q_2 - \bar{I} P_2 - 2 \bar{J} R_2 \right),$$

$$(4.6) \quad u N_1 + v N_2 = \frac{1}{\mu_e \sigma} \left\{ \frac{\partial \left(\frac{\partial L}{\partial u}, \bar{J} N_1 \right)}{\partial(u, v)} + \frac{\partial \left(\frac{\partial L}{\partial v}, \bar{J} N_2 \right)}{\partial(u, v)} \right\},$$

$$(4.7) \quad \bar{J} = \left[\frac{\partial^2 L}{\partial u^2} \cdot \frac{\partial^2 L}{\partial v^2} - \left(\frac{\partial^2 L}{\partial u \partial v} \right)^2 \right]^{-1},$$

$$\bar{\omega} = \bar{J} \left(\frac{\partial^2 L}{\partial u^2} + \frac{\partial^2 L}{\partial v^2} \right),$$

$$(4.8) \quad \bar{I} = (\bar{J})^{(n-1)} \left\{ \left(\frac{\partial^2 L}{\partial u^2} - \frac{\partial^2 L}{\partial v^2} \right)^2 + 4 \left(\frac{\partial^2 L}{\partial u \partial v} \right)^2 \right\}^{\frac{(n-1)}{2}},$$

where

$$P_1(u, v) = \frac{\partial \left(\frac{\partial L}{\partial v}, \bar{\omega} \right)}{\partial(u, v)}, \quad P_2(u, v) = \frac{\partial \left(\frac{\partial L}{\partial u}, \bar{\omega} \right)}{\partial(u, v)},$$

$$Q_1(u, v) = \frac{\partial \left(\frac{\partial L}{\partial v}, \bar{I} \right)}{\partial(u, v)}, \quad Q_2(u, v) = \frac{\partial \left(\frac{\partial L}{\partial u}, \bar{I} \right)}{\partial(u, v)},$$

$$(4.9) \quad N_1(u, v) = \frac{\partial \left(\frac{\partial L}{\partial u}, \bar{H} \right)}{\partial(u, v)}, \quad N_2(u, v) = \frac{\partial \left(\frac{\partial L}{\partial v}, \bar{H} \right)}{\partial(u, v)},$$

$$R_1(u, v) = Q_1 \frac{\partial^2 L}{\partial v^2} + Q_2 \frac{\partial^2 L}{\partial u \partial v}, \quad R_2 = Q_1 \frac{\partial^2 L}{\partial u \partial v} + Q_2 \frac{\partial^2 L}{\partial u^2}.$$

To eliminate $\bar{F}(u, v)$ from Eqs. (4.4) and (4.5), we use the integrability condition

$$\begin{aligned} & \left(\bar{J} \frac{\partial^2 L}{\partial u \partial v} \frac{\partial}{\partial v} - \bar{J} \frac{\partial^2 L}{\partial v^2} \frac{\partial}{\partial u} \right) \left(\bar{J} \frac{\partial \left(\frac{\partial L}{\partial u}, \bar{F} \right)}{\partial(u, v)} \right) \\ &= \left(\bar{J} \frac{\partial^2 L}{\partial u^2} \frac{\partial}{\partial v} - \bar{J} \frac{\partial^2 L}{\partial u \partial v} \frac{\partial}{\partial u} \right) \left(\bar{J} \frac{\partial \left(\frac{\partial L}{\partial v}, \bar{F} \right)}{\partial(u, v)} \right) \end{aligned}$$

and obtain

$$(4.10) \quad \rho(vP_1 + uP_2) + K(\bar{\omega}W_1 - \bar{I}W_2 - 2W_3) = 0,$$

where

$$\begin{aligned} (4.11) \quad W_1 &= \frac{\partial \left(\frac{\partial L}{\partial v}, \bar{J}Q_1 \right)}{\partial(u, v)} + \frac{\partial \left(\frac{\partial L}{\partial u}, \bar{J}Q_2 \right)}{\partial(u, v)}, \\ W_2 &= \frac{\partial \left(\frac{\partial L}{\partial v}, \bar{J}P_1 \right)}{\partial(u, v)} + \frac{\partial \left(\frac{\partial L}{\partial u}, \bar{J}P_2 \right)}{\partial(u, v)}, \\ W_3 &= \frac{\partial \left(\frac{\partial L}{\partial v}, \bar{J}^2 R_1 \right)}{\partial(u, v)} + \frac{\partial \left(\frac{\partial L}{\partial u}, \bar{J}^2 R_2 \right)}{\partial(u, v)}. \end{aligned}$$

We can summarize the above results in the form of a theorem:

THEOREM: *If $L(u, v)$ is the Legendre transform function of a stream-function of a steady plane transverse finitely conducting non-Newtonian power-law fluid flow and $\bar{H}(u, v)$ is the transformed magnetic field, then functions $L(u, v)$ and $\bar{H}(u, v)$ have to satisfy Eqs. (4.6) and (4.10) where $\bar{\omega}$, \bar{I} , \bar{J} , P_i , Q_i , R_i and W_i are given by (4.7) – (4.9) and (4.11).*

To solve $L(u, v)$ and $\bar{H}(u, v)$ from Eqs. (4.6) and (4.10), it is convenient to express Eqs. (4.6) – (4.11) in polar coordinates (q, θ) in the hodograph plane by defining

$$(4.12) \quad u = q \cos \theta, \quad v = q \sin \theta, \quad q^2 = u^2 + v^2, \quad \theta = \tan^{-1} \left(\frac{v}{u} \right).$$

Using (4.12), Eqs. (4.6) – (4.11) can be transformed to

$$(4.13) \quad q(N_1^* \cos \theta + N_2^* \sin \theta) = \frac{1}{\mu_e \sigma q} \left\{ \frac{\partial \left(\cos \theta \frac{\partial L^*}{\partial q} - \frac{\sin \theta}{q} \frac{\partial L^*}{\partial \theta}, J^* N_1^* \right)}{\partial(q, \theta)} + \frac{\partial \left(\sin \theta \frac{\partial L^*}{\partial q} + \frac{\cos \theta}{q} \frac{\partial L^*}{\partial \theta}, J^* N_2^* \right)}{\partial(q, \theta)} \right\},$$

$$(4.14) \quad \rho(P_1^* \sin \theta + P_2^* \cos \theta) + K(\omega^* W_1^* - I^* W_2^* - 2W_3^*) = 0,$$

$$(4.15) \quad \omega^*(q, \theta) = J^* \left(\frac{\partial^2 L^*}{\partial q^2} + \frac{1}{q} \frac{\partial L^*}{\partial q} + \frac{1}{q^2} \frac{\partial^2 L^*}{\partial \theta^2} \right),$$

$$(4.16) \quad I^*(q, \theta) = (J^*)^{(n-1)} \left\{ \left(\frac{\partial^2 L^*}{\partial q^2} - \frac{1}{q} \frac{\partial L^*}{\partial q} - \frac{1}{q^2} \frac{\partial^2 L^*}{\partial \theta^2} \right)^2 + \frac{4}{q^4} \left(\frac{\partial L^*}{\partial \theta} - q \frac{\partial^2 L^*}{\partial q \partial \theta} \right)^2 \right\}^{\frac{(n-1)}{2}},$$

$$(4.17) \quad J^*(q, \theta) = q^4 \left\{ q^2 \frac{\partial^2 L^*}{\partial q^2} \left(q \frac{\partial L^*}{\partial q} + \frac{\partial^2 L^*}{\partial \theta^2} \right) - \left(\frac{\partial L^*}{\partial \theta} - q \frac{\partial^2 L^*}{\partial q \partial \theta} \right)^2 \right\}^{-1},$$

$$P_1^*(q, \theta) = \frac{1}{q} \frac{\partial \left(\sin \theta \frac{\partial L^*}{\partial q} + \frac{\cos \theta}{q} \frac{\partial L^*}{\partial \theta}, \omega^* \right)}{\partial(q, \theta)},$$

$$P_2^*(q, \theta) = \frac{1}{q} \frac{\partial \left(\cos \theta \frac{\partial L^*}{\partial q} - \frac{\sin \theta}{q} \frac{\partial L^*}{\partial \theta}, \omega^* \right)}{\partial(q, \theta)},$$

(4.18)

$$Q_1^*(q, \theta) = \frac{1}{q} \frac{\partial \left(\sin \theta \frac{\partial L^*}{\partial q} + \frac{\cos \theta}{q} \frac{\partial L^*}{\partial \theta}, I^* \right)}{\partial(q, \theta)},$$

$$Q_2^*(q, \theta) = \frac{1}{q} \frac{\partial \left(\cos \theta \frac{\partial L^*}{\partial q} - \frac{\sin \theta}{q} \frac{\partial L^*}{\partial \theta}, I^* \right)}{\partial(q, \theta)},$$

$$\begin{aligned}
 R_1^*(q, \theta) &= Q_2^* \left(\sin \theta \cos \theta \frac{\partial^2 L^*}{\partial q^2} - \frac{\sin \theta \cos \theta}{q} \frac{\partial L^*}{\partial q} - \frac{\cos 2\theta}{q^2} \frac{\partial L^*}{\partial \theta} \right. \\
 &\quad \left. + \frac{\cos 2\theta}{q} \frac{\partial^2 L^*}{\partial q \partial \theta} - \frac{\sin \theta \cos \theta}{q^2} \frac{\partial^2 L^*}{\partial \theta^2} \right) + Q_2^* \left(\sin \theta \cos \theta \frac{\partial^2 L^*}{\partial q^2} - \frac{\sin \theta \cos \theta}{q} \frac{\partial L^*}{\partial q} \right. \\
 &\quad \left. - \frac{\cos 2\theta}{q^2} \frac{\partial L^*}{\partial \theta} + \frac{\cos 2\theta}{q} \frac{\partial^2 L^*}{\partial q \partial \theta} - \frac{\sin \theta \cos \theta}{q^2} \frac{\partial^2 L^*}{\partial \theta^2} \right), \\
 (4.19) \quad R_2^*(q, \theta) &= Q_1^* \left(\sin \theta \cos \theta \frac{\partial^2 L^*}{\partial q^2} - \frac{\sin \theta \cos \theta}{q} \frac{\partial L^*}{\partial q} - \frac{\cos 2\theta}{q^2} \frac{\partial L^*}{\partial \theta} \right. \\
 &\quad \left. + \frac{\cos 2\theta}{q} \frac{\partial^2 L^*}{\partial q \partial \theta} - \frac{\sin \theta \cos \theta}{q^2} \frac{\partial^2 L^*}{\partial \theta^2} \right) \\
 &\quad + Q_2^* \left(\cos^2 \theta \frac{\partial^2 L^*}{\partial q^2} + \frac{\sin^2 \theta}{q} \frac{\partial L^*}{\partial q} + \frac{\sin 2\theta}{q^2} \frac{\partial L^*}{\partial \theta} - \frac{\sin 2\theta}{q^2} \frac{\partial^2 L^*}{\partial q \partial \theta} + \frac{\sin^2 \theta}{q^2} \frac{\partial^2 L^*}{\partial \theta^2} \right),
 \end{aligned}$$

$$W_1^*(q, \theta) = \frac{1}{q} \left\{ \frac{\partial \left(\sin \theta \frac{\partial L^*}{\partial q} + \frac{\cos \theta}{q} \frac{\partial L^*}{\partial \theta}, J^* Q_1^* \right)}{\partial(q, \theta)} \right. \\
 \left. + \frac{\partial \left(\cos \theta \frac{\partial L^*}{\partial q} - \frac{\sin \theta}{q} \frac{\partial L^*}{\partial \theta}, J^* Q_2^* \right)}{\partial(q, \theta)} \right\},$$

$$(4.20) \quad W_2^*(q, \theta) = \frac{1}{q} \left\{ \frac{\partial \left(\sin \theta \frac{\partial L^*}{\partial q} + \frac{\cos \theta}{q} \frac{\partial L^*}{\partial \theta}, J^* P_1^* \right)}{\partial(q, \theta)} \right. \\
 \left. + \frac{\partial \left(\cos \theta \frac{\partial L^*}{\partial q} - \frac{\sin \theta}{q} \frac{\partial L^*}{\partial \theta}, J^* P_2^* \right)}{\partial(q, \theta)} \right\},$$

$$W_3^*(q, \theta) = \frac{1}{q} \left\{ \frac{\partial \left(\sin \theta \frac{\partial L^*}{\partial q} + \frac{\cos \theta}{q} \frac{\partial L^*}{\partial \theta}, J^{*2} R_1^* \right)}{\partial(q, \theta)} \right. \\
 \left. + \frac{\partial \left(\cos \theta \frac{\partial L^*}{\partial q} - \frac{\sin \theta}{q} \frac{\partial L^*}{\partial \theta}, J^{*2} R_2^* \right)}{\partial(q, \theta)} \right\},$$

$$(4.21) \quad N_1^*(q, \theta) = \frac{1}{q} \frac{\partial \left(\cos \theta \frac{\partial L^*}{\partial q} - \frac{\sin \theta}{q} \frac{\partial L^*}{\partial \theta}, H^* \right)}{\partial(q, \theta)},$$

$$N_2^*(q, \theta) = \frac{1}{q} \frac{\partial \left(\sin \theta \frac{\partial L^*}{\partial q} + \frac{\cos \theta}{q} \frac{\partial L^*}{\partial \theta}, H^* \right)}{\partial(q, \theta)}$$

where $L^*(q, \theta) = L(u, v)$, $\omega^*(q, \theta) = \omega(u, v)$, $I^*(q, \theta) = I(u, v)$, and $J^*(q, \theta) = J(u, v)$.

Once $L^*(q, \theta)$ and $H^*(q, \theta)$ are determined, we use relations

$$(4.22) \quad x = \sin \theta \frac{\partial L^*}{\partial q} + \frac{\cos \theta}{q} \frac{\partial L^*}{\partial \theta}, \quad y = \cos \theta \frac{\partial L^*}{\partial q} - \frac{\sin \theta}{q} \frac{\partial L^*}{\partial \theta}$$

to find the velocity components and the remaining flow variables in the physical plane.

5. Applications

In this section, we investigate some flow problems of physical interest as applications of the theorem.

5.1 Hyperbolic flow

Let

$$(5.1) \quad L(u, v) = A_1 u^2 + B_1 v^2 + C_1 u + D_1 v + E_1$$

be the Legendre transform function where $A_1 \neq B_1 \neq 0$, C_1 , D_1 and E_1 are arbitrary constants.

Substituting (5.1) in (4.6) – (4.9) we have

$$(52) \quad \bar{J} = \frac{1}{4A_1 B_1}, \quad \bar{\omega} = \frac{A_1 + B_1}{2A_1 B_1}, \quad P_1 = 0, \quad P_2 = 0,$$

$$\bar{I} = \left(\frac{A_1 - B_1}{2A_1 B_1} \right)^{(n-1)}, \quad Q_1 = 0, \quad Q_2 = 0, \quad R_1 = 0, \quad R_2 = 0,$$

$$N_1 = 2A_1 \frac{\partial \bar{H}}{\partial v}, \quad N_2 = -2B_1 \frac{\partial \bar{H}}{\partial u}.$$

Finitely conducting fluid flow: Substituting (5.2) in Eqs. (4.6) and (4.10), we find that (4.10) is satisfied identically and (4.6) simplifies to

$$(5.3) \quad A_1 u \frac{\partial \bar{H}}{\partial v} - B_1 v \frac{\partial \bar{H}}{\partial u} = \frac{\mu_e \sigma}{2A_1 B_1} \left(B_1^2 \frac{\partial^2 \bar{H}}{\partial u^2} + A_1^2 \frac{\partial^2 \bar{H}}{\partial v^2} \right).$$

Solving this equation we get

$$(5.4) \quad \bar{H}(u, v) = A_1 u^2 + B_1 v^2, \quad A_1 = -B_1,$$

and

$$(5.5) \quad L(u, v) = A_1(u^2 - v^2) + C_1 u + D_1 v + E_1.$$

Substitution of (5.5) in (4.1) and (4.3) yields

$$(5.6) \quad u(x, y) = -\frac{(y + C_1)}{2A_1}, \quad v(x, y) = -\frac{(x - D_1)}{2A_1}.$$

Using (5.6) in (5.4), (2.2), (2.3), (2.6) and (4.1), we get the flow variables $H(x, y)$, $I(x, y)$ and $p(x, y)$ in the physical plane in the following form:

$$(5.7) \quad H(x, y) = \frac{(y + C_1)^2 - (x - D_1)^2}{4A_1^2},$$

$$(5.8) \quad I(x, y) = \frac{(-1)^{(n-1)}}{A_1^{(n-1)}},$$

$$(5.9) \quad p(x, y) = -\frac{\rho}{2} \left\{ \frac{(x - D_1)^2 + (y + C_1)^2}{4A_1^2} \right\} - \frac{\mu_e}{2} \left\{ \frac{(y + C_1)^2 - (x - D_1)^2}{4A_1^2} \right\}^2 + \pi_1$$

where π_1 is an arbitrary constant.

Infinitely conducting fluid flow: In this case, Eq. (4.10) is again satisfied identically and Eq. (3.10) simplifies to

$$(5.10) \quad A_1 u \frac{\partial \bar{H}}{\partial v} - B_1 v \frac{\partial \bar{H}}{\partial u} = 0.$$

A general solution of Eq. (5.10) is $\bar{H}(u, v) = f(u^2 + v^2)$, but without loss of generality, we can take

$$(5.11) \quad \bar{H}(u, v) = A_1 u^2 + B_1 v^2.$$

Proceeding as in the case of finitely conducting fluid flow, we obtain

$$(5.12) \quad u(x, y) = -\frac{(y + C_1)}{2A_1}, \quad v(x, y) = \frac{(x - D_1)}{2B_1},$$

$$(5.13) \quad H(x, y) = \frac{(x - D_1)^2}{4B_1} + \frac{(y + C_1)^2}{4A_1},$$

$$(5.14) \quad I(x, y) = \frac{1}{2^{(n-1)}} \left(\frac{1}{A_1} + \frac{1}{B_1} \right)^{(n-1)},$$

$$(5.15) \quad p(x, y) = -\frac{\rho}{2} \left\{ \frac{(x - D_1)^2}{4B_1^2} + \frac{(y + C_1)^2}{4A_1^2} \right\} - \frac{\mu_e}{2} \left\{ \frac{(x - D_1)^2}{4B_1} + \frac{(y + C_1)^2}{4A_1} \right\}^2 + \pi_2$$

where π_2 is arbitrary constant.

If $L(u, v) = A_1u^2 + B_1v^2 + C_1u + D_1v + E_1$ is the Legendre transform function of a stream-function of a steady plane transverse flow of a finitely conducting non-Newtonian power-law fluid, then the flow variables are given by (5.6) – (5.9) and the stream-lines are hyperbolas

$$(5.16) \quad \frac{(x - D_1)^2}{4A_1} - \frac{(y + C_1)^2}{4A_1} = \text{const.}$$

If the fluid is infinitely conducting, the flow in the physical plane is given by (5.12) – (5.15) with stream-lines

$$(5.17) \quad \frac{(x - D_1)^2}{4B_1} + \frac{(y + C_1)^2}{4A_1} = \text{const.}$$

5.2. Parabolic flow

Letting

$$(5.18) \quad L(u, v) = (A_2v + B_2u)u + C_2u + D_2,$$

where $A_2 \neq 0$, B_2 , C_2 and D_2 are arbitrary constants, and using it in (4.7) – (4.9) we can obtain

$$\bar{J} = -\frac{1}{A_2^2}, \quad \bar{\omega} = -\frac{2B_2}{A_2^2}, \quad \bar{I} = (-2)^{(n-1)} \left(\frac{A_2^2 + B_2^2}{A_2^4} \right)^{\frac{(n-1)}{2}}, \quad (5.18)$$

$$(5.19) \quad P_1 = 0, \quad P_2 = 0, \quad Q_1 = 0, \quad Q_2 = 0, \quad R_1 = 0, \quad R_2 = 0,$$

$$N_1 = 2B_2 \frac{\partial \bar{H}}{\partial v} - A_2 \frac{\partial \bar{H}}{\partial u}, \quad N_2 = A_2 \frac{\partial \bar{H}}{\partial v}.$$

Finitely conducting fluid flows: Results (5.19) satisfy Eq. (4.10) identically and simplify (4.6) to

$$(5.20) \quad (2B_2u + A_2v) \frac{\partial \bar{H}}{\partial v} - A_2u \frac{\partial \bar{H}}{\partial u} = -\frac{1}{\mu_e \sigma} \left\{ \frac{\partial^2 \bar{H}}{\partial u^2} - \frac{4B_2}{A_2} \frac{\partial^2 \bar{H}}{\partial u \partial v} + \left(1 + \frac{4B_2^2}{A_2^2} \right) \frac{\partial^2 \bar{H}}{\partial v^2} \right\}.$$

Solving the above equation we get

$$(5.21) \quad \bar{H}(u, v) = c_1 \int e^{\frac{(A_2 \sigma \mu_e u^2)}{2}} du + c_2$$

where c_1 and c_2 are arbitrary constants.

Proceeding as in the previous application, we find

$$(5.22) \quad u(x, y) = \frac{x}{A_2}, \quad v(x, y) = -\left(\frac{2B_2}{A_2^2} x + \frac{y}{A_2} + \frac{C_2}{A_2} \right),$$

$$(5.23) \quad H(x, y) = \frac{c_1}{A_2} \int e^{\frac{x^2}{2A_2 \sigma \mu_e}} dx + c_2,$$

$$(5.24) \quad p(x, y) = -\frac{\rho}{2} \left\{ \frac{(x^2 + y^2) + (y + C_2)^2}{A_2^2} \right\} - \frac{\mu_e}{2} \left\{ \frac{c_1}{A_2} \int e^{\frac{x^2}{2A_2 \sigma \mu_e}} dx + c_2 \right\}^2 + \pi_3,$$

where π_3 is an arbitrary constant.

Infinitely conducting fluid: In this case, Eq. (4.10) is again satisfied identically and Eq. (5.19) takes the form

$$(5.25) \quad (2B_2u + A_2v) \frac{\partial \bar{H}}{\partial v} - A_2u = 0.$$

A general solution of this equation is

$$(5.26) \quad \bar{H}(u, v) = \Phi(B_2u^2 + A_2uv)$$

which, on substituting the velocity components given in (5.22), becomes

$$(5.27) \quad H(x, y) = \Phi \left(-\frac{B_2}{A_2^2}x^2 - \frac{xy}{A_2} - \frac{C_2}{A_2}x \right),$$

where Φ is an arbitrary function of argument.

The pressure function is given by

$$(5.28) \quad p(x, y) = -\frac{\rho}{2} \left\{ \frac{(x^2 + y^2) + (y + C_2)^2}{A_2^2} \right\} - \frac{\mu_e}{2} \left[\Phi \left(-\frac{B_2}{A_2^2}x^2 - \frac{xy}{A_2} - \frac{C_2}{A_2} \right) \right]^2 + \pi_4$$

where π_4 is an arbitrary constant.

If $L(u, v) = (A_2v + B_2u)u + C_2u + D_2$ is the Legendre transform function of a steady plane transverse flow of a non-Newtonian power-law fluid of finite conductivity, the flow variables are given by (5.22) – (5.24) and the streamlines are parabolic curves

$$(5.29) \quad B_2x^2 + A_2xy + A_2C_2x = \text{const.}$$

In case of infinitely conducting fluid flow, Eqs. (5.22), (5.27) and (5.28) express the flow variables in the physical plane with streamlines given by (5.29).

5.3. Radial flow

Let

$$(5.30) \quad L^*(q, \theta) = A_3\theta + B_3$$

where A_3 and B_3 are arbitrary constants in the Legendre transform function of stream-function.

Using (5.30) in (4.15) – (4.21), we obtain

$$(5.31) \quad J^* = -\frac{q^4}{A_3^2}, \quad \omega^* = 0, \quad I^* = \frac{2^{(n-1)}q^{2(n-1)}}{A_3^{(n-1)}}, \quad P_2^* = 0,$$

$$Q_1^* = \frac{A_3 I^{*'} \sin \theta}{q^2}, \quad Q_2^* = \frac{A_3 I^{*'} \cos \theta}{q^2},$$

$$R_1^* = -\frac{A_3^2 I^{*'} \cos \theta}{q^4}, \quad R_2^* = \frac{A_3^2 I^{*'} \sin \theta}{q^4},$$

$$W_1^* = \frac{I^{*'}}{q} - \frac{1}{q^2}(q^2 I^{*'})', \quad W_2^* = 0, \quad W_3^* = 0,$$

$$N_1^* = \frac{A_3 \cos \theta}{q^2} \frac{\partial H^*}{\partial q} + \frac{A_3 \sin \theta}{q^3} \frac{\partial H^*}{\partial \theta}, \quad N_2^* = \frac{A_3 \sin \theta}{q^2} \frac{\partial H^*}{\partial q} - \frac{A_3 \cos \theta}{q^3} \frac{\partial H^*}{\partial \theta}.$$

Finitely conducting fluid flows: Using results (5.31) in (4.13) and (4.14), we find that (4.14) is satisfied identically and (4.13) becomes

$$(5.32) \quad \frac{\partial^2 H^*}{\partial q^2} + (1 + A_3 \mu_e \sigma) \frac{1}{q} \frac{\partial H^*}{\partial q} + \frac{1}{q^2} \frac{\partial^2 H^*}{\partial \theta^2} = 0.$$

Assuming the solution of Eq. (5.32) in the form $H^*(q, \theta) = h_1(q) + h_2(\theta)$ we can obtain

$$(5.33) \quad H^*(q, \theta) = c_3 \left(\frac{1}{2} \theta^2 + \frac{1}{A_3 \mu_e \sigma} \ln q \right) + c_4 q^{-A_3 \mu_e \sigma} + c_5 \theta + c_6,$$

where $c_3, c_4, c_5,$ and c_6 are arbitrary constants.

Proceeding as in the previous applications, we obtain the flow variables in the physical plane in the form

$$(5.34) \quad u(x, y) = \frac{A_3 x}{(x^2 + y^2)}, \quad v(x, y) = \frac{A_3 y}{(x^2 + y^2)},$$

$$(5.35) \quad H(x, y) = \frac{c_3}{2} \left\{ \left(\tan^{-1} \frac{y}{x} \right)^2 + \frac{1}{A_3 \mu_e \sigma} \ln(x^2 + y^2) \right\} \\ + c_4 (x^2 + y^2)^{-\frac{A_3 \mu_e \sigma}{2}} + c_5 \tan^{-1} \frac{y}{x} + c_6,$$

$$(5.36) \quad I(x, y) = \frac{2^{(n-1)}}{A_3^{(n-1)}} (x^2 + y^2)^{(n-1)},$$

$$(5.37) \quad p(x, y) = -\frac{2^n(n-1)K}{(n-2)A_3^{(n-2)}}(x^2 + y^2)^{(n-2)} - \frac{\rho A_3^2}{2(x^2 + y^2)} - \frac{\mu_e}{2}H^2 + \pi_4,$$

where π_4 is an arbitrary constant.

Infinitely conducting fluid flows: In this case, the diffusion equation reduces to

$$(5.38) \quad \frac{\partial H^*}{\partial q} = 0$$

which yields

$$(5.39) \quad H^*(q, \theta) = \Psi(\theta),$$

where Ψ is an arbitrary function of θ .

The expressions of velocity components and $I(x, y)$ remain the same whereas $H(x, y)$ and $p(x, y)$ are given by

$$(5.40) \quad H(x, y) = \Psi\left(\tan^{-1}\frac{y}{x}\right),$$

$$(5.41) \quad p(x, y) = -\frac{2^n K(n-1)}{A_3^{(n-2)}(n-2)}(x^2 + y^2)^{(n-2)} - \frac{\rho A_3^2}{2(x^2 + y^2)} - \frac{\mu_e}{2}\left\{\Psi\left(\tan^{-1}\frac{y}{x}\right)\right\}^2 + \pi_5,$$

where π_5 is an arbitrary constant.

If $L^*(q, \theta) = A_3\theta + B_3$, $A_3 \neq 0$ is the Legendre transform function of a stream-function of a steady plane transverse flow of a finitely conducting non-Newtonian fluid of power-law model, then the Eqs. (5.34) – (5.37) express the flow variables in the physical plane. If the fluid conductivity is infinite, the flow variables are given by (5.34), (5.36), (5.40) and (5.41).

5.4. Spiral flow

$$(5.42) \quad L^*(q, \theta) = A_4 \ln q + B_4\theta, \quad A_4 \neq 0, \quad B_4 \neq 0$$

and proceeding as in the previous applications, we can obtain

$$(5.43) \quad J^* = -\frac{q^4}{(A_4^2 + B_4^2)}, \quad \omega^* = 0, \quad I^* = \frac{(-2)^{(n-1)}q^{(2n-2)}}{(A_4^2 + B_4^2)^{\frac{(n-1)}{2}}}, \quad P_1^* = 0, \quad P_2^* = 0,$$

$$Q_1^* = -\frac{I^{*'}}{q^2}(A_4 \cos \theta - B_4 \sin \theta), \quad Q_2^* = \frac{I^{*'}}{q^2}(A_4 \sin \theta - B_4 \cos \theta),$$

$$(5.43) \quad R_1^* = -\frac{I^{*'}}{q^4} (A_4^2 + B_4^2) \cos \theta, \quad R_2^* = \frac{I^{*'}}{q^4} (A_4^2 + B_4^2) \sin \theta,$$

[cont.]

$$N_1^* = \frac{1}{q^2} (A_4 \sin \theta + B_4 \cos \theta) \frac{\partial H^*}{\partial q} - \frac{1}{q^3} (A_4 \cos \theta - B_4 \sin \theta) \frac{\partial H^*}{\partial \theta},$$

$$N_2^* = -\frac{1}{q^2} (A_4 \cos \theta - B_4 \sin \theta) \frac{\partial H^*}{\partial q} - \frac{1}{q^3} (A_4 \sin \theta + B_4 \cos \theta) \frac{\partial H^*}{\partial \theta}.$$

These equations together with (5.42) yield

$$(5.44) \quad W_1^* = 0, \quad W_2^* = 0, \quad W_3^* = \frac{A_4}{(A_4^2 + B_4^2)} \left\{ \frac{(I^{*'} q^A)'}{q^2} - I^{*'} q \right\}.$$

Employing (5.43) and (5.44), Eq. (4.414) simplifies to

$$(5.45) \quad \frac{4A_4 K (-2)^{(n-1)} n(n-1)}{(A_4^2 + B_4^2)^{\frac{(n+1)}{2}}} q^{(2n-2)} = 0.$$

From this equation it follows that a steady plane flow of a non-Newtonian power-law fluid cannot be spiral whether the fluid conductivity is finite or infinite. However, a spiral can exist in a steady plane viscous fluid ($n = 1$) whether it is conducting or non-conducting. In the case of finitely conducting fluid, Eq. (5.45) is identically satisfied and Eq. (4.13) becomes

$$(5.46) \quad \frac{\partial^2 H^*}{\partial q^2} + (1 + B_4 \mu_e \sigma) \frac{1}{q} \frac{\partial H^*}{\partial q} - \frac{A_4 \mu_e \sigma}{q^2} \frac{\partial H^*}{\partial \theta} + \frac{1}{q^2} \frac{\partial^2 H^*}{\partial \theta^2} = 0.$$

Assuming the solution of this equation in the form $H^*(q, \theta) = g_1(q) + g_2(\theta)$, where g_1 and g_2 are arbitrary functions, we obtain

$$(5.47) \quad H^*(q, \theta) = \frac{\lambda_1}{\mu_e \sigma} \left(\frac{\ln q}{B_4} + \frac{\theta}{A_4} \right) + d_1 q^{-B_4 \sigma \mu_e} + d_2 e^{A_4 \sigma \mu_e \theta} + d_3,$$

where λ_1 , d_1 , d_2 and d_3 are arbitrary constants.

Proceeding as in the previous applications, we can determine $u(x, y)$, $v(x, y)$ and $p(x, y)$ in the following form:

$$(5.48) \quad u(x, y) = \frac{(B_4 x - A_4 y)}{(x^2 + y^2)}, \quad v(x, y) = \frac{(A_4 x + B_4 y)}{(x^2 + y^2)},$$

$$(5.49) \quad p(x, y) = -\frac{\rho (A_4^2 + B_4^2)}{2 (x^2 + y^2)} - \frac{\mu_e}{2} \left\{ \frac{\lambda_1}{\mu_e \sigma} \left(\frac{\ln q}{B_4} + \frac{\theta}{A_4} \right) + d_1 q^{-B_4 \mu_e \sigma} + d_2 e^{A_4 \mu_e \sigma \theta} + d_3 \right\}^2 + \pi_6,$$

where π_6 is an arbitrary constant.

If the viscous fluid is infinitely conducting, the the diffusion Eq. (4.13) reduces to

$$(5.50) \quad \frac{B_4}{q} \frac{\partial H^*}{\partial q} - \frac{A_4}{q^2} \frac{\partial H^*}{\partial \theta} = 0.$$

A solution of this equation is

$$(5.51) \quad H^*(q, \theta) = \lambda_1 \left(\frac{\ln q}{B_4} + \frac{\theta}{A_4} \right) + d_4,$$

where d_4 is an arbitrary constant.

The pressure function is given by

$$(5.52) \quad p(x, y) = -\frac{\rho (A_4^2 + B_4^2)}{2 (x^2 + y^2)} - \frac{\mu_e}{2} \left\{ \lambda_1 \left(\frac{\ln q}{B_4} + \frac{\theta}{A_4} \right) + d_4 \right\}^2 + \pi_7,$$

where π_7 is an arbitrary constant.

6. Discussion

In each of the applications studied, the velocity components $\omega(x, y)$ and $I(x, y)$ are independent of the effect of electrical conductivity. Therefore, the solutions of the flow equations of steady plane flow of a non-Newtonian power-law non-conducting fluid can be derived as special cases of the problems investigated by discarding the term $-\mu_e H^2/2$ from the pressure functions. A steady plane flow of a non-Newtonian power-law fluid cannot be a spiral flow whether or not it is conducting. The solution of the problem of steady plane flow of an ordinary viscous fluid can be obtained by setting $n = 1$.

Acknowledgement

The author thanks the reviewer for his helpful comments.

References

1. W.F. AMES, *Non-linear partial differential equations*, Academic Press, New York 1965.
2. O.P. CHANDNA, R.M. BARRON and A.C. SMITH, *Rotational plane steady flow of a viscous fluid*, SIAM J. Appl. Math., **42**, 1323-1336, 1982.

3. A.M. SIDDIQUI, Q. M. KALONI and O.P. CHANDNA, *Hodograph transformation method in non-Newtonian fluid flows*, J. Engng Math., **19**, 203–216, 1985.
4. O.P. CHANDNA and P.V. NGUYEN, *Hodograph method in non-Newtonian MHD transverse fluid flows*, J. Engng Math., **23**, 119–139, 1989.
5. P.V. NGUYEN and O.P. CHANDNA, *Hodograph study of non-Newtonian MHD aligned steady plane flows*, Int. J. Math. And Math. Sci., **13**, 93–114, 1990.
6. P.V. NGUYEN and O.P. CHANDNA, *Hodograph transformation method and solution in aligned MHD plane flows*, Int. J. Engng Sci., **28**, 973, 1990.
7. P.V. NGUYEN and O.P. CHANDNA, *Hodograph study of MHD constantly inclined fluid flows*, Int. J. Engng Sci., **30**, 69–82, 1992.
8. I. ADLURI, *Hodograph method in plane MHD non-Newtonian fluid flows*, Arch. Mech., **45**, 121–134, 1993.
9. I. ADLURI, *Hodographic study of plane micropolar fluid flows*, Int. J. Math. and Math. Sci., **18**, 357–364, 1995.

Received June 8, 1998; new version November 10, 1998.

Frequency dependence on space-time for electromagnetic propagation in dispersive medium

A. CIARKOWSKI

Polish Academy of Sciences

Institute of Fundamental Technological Research

Świętokrzyska 21, 00-049 Warszawa, Poland

PROPAGATION OF AN ELECTROMAGNETIC HIGH-FREQUENCY modulated signal in a lossy dispersive Lorentz medium is reconsidered. A new approximate solution is found to the equation relating complex frequency of the propagating signal and the space-time point. This solution is compared numerically with the solution to the saddle point equation in the special case of the Brillouin medium parameters.

1. Introduction

INTEREST IN PROPAGATION OF ELECTROMAGNETIC SIGNAL through dispersive media dates back to early 1900's. Fundamental works in this field are due to SOMMERFELD [1] and BRILLOUIN [2, 3]. They studied the evolution of a signal propagating in a Lorenz medium that accurately models some real lossy media. On the grounds of asymptotic considerations, the authors showed that the main change in the form of an electromagnetic signal propagating in this medium takes place at the initial stage of propagation, while at higher penetration depths the pulse form is almost unchanged. They revealed that two different precursors precede the steady state signal. At every space-time point, the precursors' speed of oscillations and their dumping are functions of complex frequencies, which in turn are determined by the locations of saddle points in the integral defining the signal. The works of Sommerfeld and Brillouin are very important because they gave insight into the mechanism of electromagnetic pulse evolution as it propagates in a dispersive medium, and they provided approximate analytic description of this evolution in the mature dispersion regime.

More recently, OUGHSTUN and SHERMAN, in a series of papers [4, 5, 6, 7, 8, 9, 10], reexamined the classical theory of Sommerfeld and Brillouin. Equipped with modern asymptotic methods and access to powerful computers, they were able to improve the classical asymptotic results by extending them to special instances of the pulse dynamics, and to provide better understanding of physical phenomena associated with propagation of various signals in a dispersive material.

In short terms, asymptotic analysis of a signal propagation in the dispersive medium reduces to asymptotic evaluation of a contour integral that describes the signal dynamics in the medium. A key step in this approach is to find, at each space point and at each time instant, the complex frequencies that determine the way in which particular parts of the signal oscillate and are dumped in the medium. These frequencies are derived from the equation which determines the locations of saddle points corresponding to the phase function in the integral. Because of the complex form of the equation, it seems to be impossible to solve the equation exactly. Brillouin found four families of saddle points in the complex frequency plane and obtained approximate analytical formulas describing them. Those formulas fail to hold in some instances of pulse evolution. New, better approximation to these frequencies was found by OUGHSTUN and SHERMAN in [4].

In this paper we obtain still other approximate formulas for the complex frequencies that govern the dynamics of the signal propagating in the dispersive medium. By numerical comparison we show that in vast range of the space and time coordinates, our approximation surpasses those obtained by Brillouin and Oughstun and Sherman.

2. Formulation of the problem

Motivated by the works of SOMMERFELD [1], BRILLOUIN [2, 3] and OUGHSTUN and SHERMAN [4], we reconsider the problem of propagation of an arbitrary electromagnetic signal in a linear, homogeneous, isotropic, temporary dispersive medium filling the half-space $z > 0$. Let $A(z, t)$ represent any scalar component of the electromagnetic field or its potential. Assume further that

$$A(0, t) = f(t)$$

is known for all time t , where $f(t)$ is zero for $t < 0$. Then, (see OUGHSTUN and SHERMAN [4]),

$$(2.1) \quad A(z, t) = \frac{1}{2\pi} \int_C \tilde{f}(\omega) \exp \left[\frac{z}{c} \phi(\omega, \theta) \right] d\omega,$$

where

$$\tilde{f}(\omega) = \int_0^{\infty} f(t) e^{-i\omega t} dt$$

is the Laplace transform of the signal evolution at the plane $z = 0$,

$$\phi(\omega, \theta) = i \frac{c}{z} [\tilde{k}(\omega)z - \omega t] = i\omega[n(\omega) - \theta]$$

is the phase function, and

$$\theta = \frac{ct}{z}$$

is a dimensionless parameter corresponding to a space-time point. The quantity $n(\omega)$ stands for the complex index of refraction of the medium and in the Lorentz model it is equal to

$$(2.2) \quad n(\omega) = \left(1 - \frac{b^2}{\omega^2 - \omega_0^2 + 2i\delta\omega} \right)^{1/2}.$$

Here, b , ω_0 and δ are medium parameters ([12]). Brillouin chose the following numerical values for those parameters:

$$b^2 = 20.0 \times 10^{32} \text{ s}^{-1}, \quad \omega_0 = 4.0 \times 10^{16} \text{ s}^{-1}, \quad \delta = 0.28 \times 10^{16} \text{ s}^{-1},$$

which are characteristic of a dispersive, lossy medium. His choice has become a standard in works by many other authors.

Asymptotic evaluation of the integral in (2.1) for large values of the phase in the integrand requires that the saddle points of $\phi(\omega, \theta)$ are known. At those points the phase function is stationary, i.e. it satisfies the equation $\phi'(\omega, \theta) = 0$, or equivalently,

$$(2.3) \quad n(\omega) + \omega n'(\omega) - \theta = 0.$$

By using explicit form of $n(\omega)$ in this equation one arrives at

$$(2.4) \quad \left[\omega^2 - \omega_1^2 + 2i\delta\omega + \frac{b^2\omega(\omega + i\delta)}{\omega^2 - \omega_0^2 + 2i\delta\omega} \right]^2 = \theta^2(\omega^2 - \omega_1^2 + 2i\delta\omega)(\omega^2 - \omega_0^2 + 2i\delta\omega),$$

where $\omega_1^2 = \omega_0^2 + b^2$. This equation determines the exact locations of saddle points in the ω -complex plane. It does not seem possible to solve this equation exactly. Instead, approximate solutions were constructed (BRILLOUIN [2, 3], OUGHSTUN and SHERMAN [4]).

In this paper we find still another approximation to the function relating the location of the saddle points to particular values of θ . Below, we summarize the results known in the literature and present the new approximate solution to Eq. (2.3).

3. Approximate solutions to the saddle point equation

3.1. Brillouin's solution

Brillouin's study of the saddle-point Eq. (2.3) led to the conclusion that for each θ there are four distinct saddle points, situated symmetrically with respect to

the imaginary axis in the ω complex plane. Two of the four simple saddle points, pertaining to the Brillouin precursor in the signal, move along the imaginary axis as θ increases from 1 to θ_1 , one downwards (crossing the real axis) and the other upwards, and coalesce into one second-order saddle point at $\theta = \theta_1$. When θ increases any further, this saddle point divides into two simple saddle points which detach from the axis and move outwards, approaching in the limit, as $\omega \rightarrow \infty$, the respective points ω_+ and ω_- . The limiting points are located in the third and the fourth quadrant, respectively, of the complex frequency plane and are defined by

$$(3.1) \quad \omega_{\pm} = \pm(\omega_0^2 - \delta^2)^{1/2} - i\delta.$$

For any $\theta \geq 1$ these saddle points vary in the regions $|\omega| \leq |\omega_0|$. Therefore in the literature they are referred to as the near saddle points.

The remaining simple saddle points appear in the lower ω half-plane and are related to the Sommerfeld precursor in the signal. As θ increases from 1 to infinity, those points move inwards from $+\infty - 2i\delta$ to ω'_+ and from $-\infty - 2i\delta$ to ω'_- , respectively, where

$$(3.2) \quad \omega'_{\pm} = \pm(\omega_1^2 - \delta^2)^{1/2} - i\delta.$$

Since they vary in the regions $|\omega| \geq |\omega_1|$, they are referred to as the distant saddle points.

The points ω_{\pm} and ω'_{\pm} are the branch points of $n(\omega)$. In particular, if $\omega = \omega_{\pm}$,

$$(3.3) \quad \omega^2 - \omega_0^2 - 2i\delta\omega = 0$$

and if $\omega = \omega'_{\pm}$,

$$(3.4) \quad \omega^2 - \omega_1^2 - 2i\delta\omega = 0.$$

In the region $|\omega| \geq |\omega_1|$ Brillouin approximated the complex index of refraction by

$$(3.5) \quad n(\omega) \approx 1 - \frac{b^2}{2\omega(\omega + 2i\delta)}.$$

By substituting this approximation into Eq. (2.3) and solving for ω , he obtained the following approximate formula for the distant saddle points:

$$(3.6) \quad \omega_{SPD}^{\pm}(\theta) \approx \pm \frac{b}{[2(\theta - 1)]^{1/2}} - 2i\delta.$$

According to this formula, when $\theta = 1$, the distant saddle points lie at infinity, their locations being given by $\pm\infty - 2i\delta$. As θ increases to infinity, this formula incorrectly states that they move towards the imaginary ω axis along the line

$\omega = -2i\delta$. As a consequence, Eq. (3.6) does not provide a good approximation for the distant saddle point locations in the vicinity of the limiting points ω'_{\pm} .

In the region $|\omega| \leq |\omega_0|$ Brillouin adopted the following approximation for the complex index of refraction:

$$(3.7) \quad n(\omega) \approx \frac{\omega_1}{\omega_0} + \frac{b^2}{2\omega_1\omega_0^3}\omega(\omega + 2i\delta) - \frac{\delta^2 b^2(4\omega_1^2 - b^2)}{2\omega_1^3\omega_0^5}\omega^2.$$

(In fact, the final term in this expression was appended by OUGHSTUN and SHERMAN [4] to assure that the approximation is correct to ω^2). With (3.7) used in Eq. (2.3) its approximate solutions are

$$(3.8) \quad \omega_{SPN}^{\pm} \approx \pm \frac{1}{3} \left[6 \frac{\theta_0 \omega_0^4}{\alpha b^2} (\theta - \theta_0) - 4 \frac{\delta^2}{\alpha^2} \right]^{1/2} - i \frac{2\delta}{3\alpha},$$

where

$$(3.9) \quad \alpha = 1 - \frac{\delta^2(4\omega_1^2 - b^2)}{\omega_0^2\omega_1^2},$$

$$(3.10) \quad \theta_0 = \frac{\omega_1}{\omega_0} = (1 + b^2/\omega_0^2)^{1/2}.$$

According to (3.8) there are two near saddle points which, as θ increases from 1 to θ_1 , move towards each other along the imaginary ω axis. The “upper” saddle point crosses the real ω axis at $\theta = \theta_0$. Both saddle points coalesce into a saddle point of the order 2 at $\theta = \theta_1 > \theta_0$. The value of θ_1 follows from equating the square root in (3.8) to zero, which yields

$$(3.11) \quad \theta_1 = \theta_0 + \frac{2\delta^2 b^2}{3\alpha\theta_0\omega_0^2}.$$

The corresponding location of the saddle point of the order 2 is by (3.8) equal to $\omega = -i2\delta/3\alpha$.

For higher values of θ the formula (3.8) incorrectly states that two simple saddle points move off the imaginary ω axis towards infinity along the line $\omega = -i2\delta/3\alpha$. In particular, it does not predict that the points tend to ω_{SPN}^{\pm} as $\theta \rightarrow \infty$.

3.2. Oughstun and Sherman’s solution of the saddle point equation

The starting point in Oughstun and Sherman’s approach was the Eq. (2.4). Crucial step in their procedure consisted in expanding the rational term in the square bracket into a sum of integer powers of ω (positive or negative, depending on which region in the complex ω plane was under consideration).

In particular, for the saddle points varying in the distant regions $|\omega| \geq |\omega_1|$, the terms of the order ω^{-2} and higher were dropped from the expansion of the rational function as $\omega \rightarrow \infty$. With that approximation the saddle point equation Eq. (2.4)) was reduced to a cubic equation which could be solved exactly. Appropriate solutions of that equation were further simplified to give finally

$$(3.12) \quad \omega_{SP_D}^{\pm}(\theta) \cong \pm \xi(\theta) - i\delta[1 + \eta(\theta)],$$

where

$$(3.13) \quad \xi(\theta) = \left(\omega_0^2 - \delta^2 + \frac{b^2\theta^2}{\theta^2 - 1} \right)^{1/2},$$

$$(3.14) \quad \eta(\theta) = \frac{\delta^2/27 + b^2/(\theta^2 - 1)}{\xi^2(\theta)}.$$

If θ is close to unity, $\xi(\theta) \cong b/[2(\theta - 1)]^{1/2}$, $\eta(\theta) \cong 1$, and thus the approximation (3.6) is recovered. If, on the other hand, θ is large, $\xi(\theta) \cong (\omega_1^2 - \delta^2)^{1/2}$, $\eta(\theta) \cong \delta^2/[27(\omega_1^2 - \delta^2)] \cong 0$, and hence

$$(3.15) \quad \omega_{SP_D}(\theta) \cong \pm(\omega_1^2 - \delta^2)^{1/2} - \delta i = \omega'_{\pm} \quad \text{as } \theta \rightarrow \infty,$$

i.e. present approximation and the Brillouin's one (3.6) are very close to each other.

In case when the saddle points vary in the region $|\omega| \leq |\omega_0|$, Oughstun and Sherman replaced the rational functions by their power expansions as $\omega \rightarrow 0$, up to the order $O(\omega^3)$. This again reduced the saddle point equation to a cubic equation. Since the cubic term is small in comparison to other terms, at least for ω not too great, the authors deleted that term and finally obtained a further simplified quadratic equation whose solutions are given by

$$(3.16) \quad \omega_{SP_N}^{\pm} \cong \pm\psi(\theta) - \frac{2}{3}i\delta\zeta(\theta),$$

where

$$(3.17) \quad \psi(\theta) = \left[\frac{\omega_0^2(\theta^2 - \theta_0^2)}{\theta^2 - \theta_0^2 + \frac{3b^2}{\omega_0^2}\alpha} - \delta^2 \left(\frac{\theta^2 - \theta_0^2 + \frac{2b^2}{\omega_0^2}}{\theta^2 - \theta_0^2 + \frac{3b^2}{\omega_0^2}\alpha} \right)^2 \right]^{1/2},$$

$$(3.18) \quad \zeta(\theta) = \frac{3}{2} \frac{\theta^2 - \theta_0^2 + \frac{2b^2}{\omega_0^2}}{\theta^2 - \theta_0^2 + \frac{3b^2}{\omega_0^2}\alpha}$$

and

$$(3.19) \quad \alpha = 1 - \frac{\delta^2}{3\omega_0^2\omega_1^2}(4\omega_1^2 + b^2).$$

If θ is close to θ_0 , (3.16) reduces to (3.8). On the other hand, if θ tends to infinity then (3.16) approaches ω_{\pm} , as it happens in the case of the exact solution.

Approximate value of θ_1 as predicted by (3.16) follows from equating $\psi(\theta)$ to zero. With some additional simplifications it appears to be

$$(3.20) \quad \theta_1 \cong \theta_0 + \frac{2\delta^2 b^2}{\theta_0 \omega_0^2 (3\alpha \omega_0^2 - 4\delta^2)}.$$

Oughstun and Sherman’s approximation for the location of the saddle points appeared to be quite satisfactory, both because of its accuracy and its simplicity. However, as it will be shown in the next section, a different approximation can be constructed, which provides better accuracy over a wide range of θ values.

3.3. Alternative solution to the saddle point equation

Unlike in the Oughstun and Sherman approach, our starting point is the original saddle point equation (2.3). We formulate this equation in terms of the complex index of refraction n . If approximate solutions are found for n from that equation, corresponding values for the frequencies can be obtained from (2.2) to give

$$(3.21) \quad \begin{aligned} \omega^+ &= -i + \sqrt{\omega_0^2 - \delta^2 - \frac{b^2}{n^2 - 1}}, \\ \omega^- &= -(\omega^+)^* = -i\delta - \sqrt{\omega_0^2 - \delta^2 - \frac{b^2}{(n^*)^2 - 1}}. \end{aligned}$$

Here the asterisk denotes complex conjugate.

With $n'(\omega)$ determined from (2.2), the saddle point equation formulated in terms of n now reads

$$(3.22) \quad n + \frac{(n^2 - 1)^2}{b^2 n} \left[-i\delta \left(\omega_0^2 - \delta^2 - \frac{b^2}{n^2 - 1} \right)^{1/2} + \omega_0^2 - \delta^2 - \frac{b^2}{n^2 - 1} \right] = \theta.$$

As mentioned earlier, for θ increasing from 1 to ∞ , the near saddle points tend to ω_{\pm} , and the distant saddle points tend to ω'_{\pm} , respectively. On the other hand, $|n(\omega)|$ tends to infinity as ω approaches ω_{\pm} , and $|n(\omega)|$ decreases to zero as it comes near ω'_{\pm} . This suggests that in the vicinity of those limiting points, the saddle point equation can be approximated by asymptotically expanding its both sides for $|n| \rightarrow \infty$ or $|n| \rightarrow 0$, respectively. (The right-hand side of the equation is left intact, as it is independent of n). Now we consider both cases in turn.

First, consider the case of the distant saddle point, i.e. the case of $|n| < 1$. Let the l.h.s. of the Eq. (3.22) be expanded in positive powers of n as $n \rightarrow 0$, and terms higher than cubic are neglected. Then the saddle point equation takes the following approximate form

$$(3.23) \quad an^4 + cn^2 + dn + e \sim 0,$$

where

$$(3.24) \quad a = \left[\omega_0^2 - \delta^2 + \frac{i\delta b^2}{\sqrt{\omega_1^2 - \delta^2}} - i\delta\sqrt{\omega_1^2 - \delta^2} - \frac{i\delta b^2[3b^2 + 4(\omega_0^2 - \delta^2)]}{8(\omega_1^2 - \delta^2)^{3/2}} \right] \frac{1}{b^2},$$

$$(3.25) \quad c = -\frac{i\delta}{2\sqrt{\omega_1^2 - \delta^2}} - \frac{2}{b^2} \left(\omega_0^2 - \delta^2 - i\delta\sqrt{\omega_1^2 - \delta^2} \right),$$

$$(3.26) \quad d = -\theta,$$

and

$$(3.27) \quad e = \frac{\omega_1^2 - \delta^2 - i\delta\sqrt{\omega_1^2 - \delta^2}}{b^2}.$$

Appropriate solution to this equation is not too complicated (presumably because the term proportional to n^3 is missing from the equation) and is given by

$$(3.28) \quad n \cong g - \sqrt{\frac{1}{4a} \left(\frac{\theta}{g} - 2c \right) - g^2},$$

where

$$(3.29) \quad g = \frac{1}{2\sqrt{3a}} \sqrt{\frac{2^{-1/3}}{(u + \sqrt{u^2 - v^3})^{1/3}} \left[(u + \sqrt{u^2 - v^3})^{2/3} + v \right] - 2c},$$

$$(3.30) \quad u = 2c^3 - 72ace + 27a\theta^2,$$

$$(3.31) \quad v = 2^{2/3}(c^2 - 12ae).$$

Here, the parameter θ appears directly under the square root sign and in g via the variable u .

As θ approaches infinity, g behaves like $\theta^{1/3}/(2a^{1/3})$ and both components in (3.28) cancel out, thus making n tend to zero. Consequently, by (3.21), as $\theta \rightarrow \infty$ the distant saddle points tend to ω_{\pm} . This agrees with Brillouin's and Oughstun and Sherman's results. For sufficiently small n , powers of n higher than 1 can be

disregarded in Eq. (3.23). If n so approximated is used in (3.21), the following result is obtained:

$$(3.32) \quad \omega \cong -i\delta \pm \sqrt{(\omega_1^2 - \delta^2) \left(1 + \frac{1}{\theta}\right) - i\delta \frac{\sqrt{\omega_1^2 - \delta^2}}{\theta}},$$

valid for $\theta \rightarrow \infty$. It shows the rate at which distant saddle points tend to their limiting values as θ increases to infinity.

Now consider the near saddle points locations corresponding to the case of $|n| > 1$. By expanding the l.h.s. of the Eq. (3.22) asymptotically as $n \rightarrow \infty$, and disregarding powers of n higher than n^{-1} , the saddle point equation reduces to the same form as in (3.22), with partly modified coefficients:

$$(3.33) \quad a = \frac{\omega_0^2 - \delta^2 - i\delta\sqrt{\omega_0^2 - \delta^2}}{b^2},$$

$$(3.34) \quad c = \frac{i\delta}{2\sqrt{\omega_0^2 - \delta^2}} - \frac{2}{b^2} \left(\omega_0^2 - \delta^2 - i\delta\sqrt{\omega_0^2 - \delta^2}\right),$$

$$(3.35) \quad d = -\theta,$$

and

$$(3.36) \quad e = \left[\omega_1^2 - 2 - \frac{i\delta b^2}{\sqrt{\omega_0^2 - \delta^2}} - i\delta\sqrt{\omega_0^2 - \delta^2} + \frac{i\delta b^2 [b^2 + 4(\omega_0^2 - \delta^2)]}{8(\omega_0^2 - \delta^2)^{3/2}} \right] \frac{1}{b^2}.$$

It is interesting to note that real parts of the coefficients are the same as in the case of the distant saddle points. For the medium parameters proposed by Brillouin, the imaginary parts are only slightly different, as it can be seen from

$$(3.37) \quad (0.79608 - 0.05586i)n^4 + (-1.59216 + 0.14681i)n^2 - \theta n$$

$$+ 1.79608 - 0.07993i \sim 0$$

which applies in the case of near saddle points, and

$$(3.38) \quad (0.79608 - 0.05730i)n^4 + (-1.59216 + 0.14446i)n^2 - \theta n$$

$$+ 1.79608 - 0.08390i \sim 0$$

appropriate in the case of distant saddle points.

Now, the appropriate solution to the fourth degree Eq. (3.23) is

$$(3.39) \quad n \cong g + \sqrt{\frac{1}{4a} \left(\frac{\theta}{g} - 2c \right) - g^2},$$

i.e. it differs from (3.28) in the sign preceding the second term. As θ tends to infinity, n behaves like $a^{-1/3}\theta^{1/3}$. Therefore, the last term under the square root sign in (3.21) vanishes in the limit and the near saddle points attain the values ω_{\pm} . This again agrees with Brillouin's and Oughstun and Sherman's results.

As it will be seen in the following section, the approximation of saddle point locations given here are pretty good in a wide range of changing θ , except for very small values of this parameter, about 1.5 and below. In this exceptional subregion we propose a very simple, local approximation obtained by expanding the l.h.s. of the Eq. (3.22) about $n = \sqrt{1 + b^2/\omega_0^2}$, which corresponds to $\omega = 0$. By retaining only the first term in the expansion we obtain

$$(3.40) \quad n \approx \frac{1}{2} \left(\frac{\omega_1}{\omega_0} + \theta \right),$$

and consequently

$$(3.41) \quad \omega \approx -i\delta + \sqrt{\omega_0^2 - \delta^2 - \frac{4b^2}{(\omega_1/\omega_0 + \theta)^2 - 1}},$$

the approximation being valid for small ω .

3.4. Numerical results

Results obtained in the previous section will now be compared with the exact ones and those obtained by Oughstun and Sherman.

In Fig. 1a,b the real and imaginary parts of the distant saddle points are displayed as functions of the parameter θ . It is seen that the approximate values obtained in this work are almost undistinguishable from the exact ones, even at small values of θ .

Figure 2a,b presents real and imaginary parts of the near saddle points as functions of θ . Again, the accuracy of the present result is very good, except at very small values of θ . For θ around 1 and slightly above this value, Oughstun-Sherman's result is better. This follows, on the one hand, from the fact that their approximation is constructed under the assumption of small values of ω , and hence θ . On the other hand, the approximation method used here is not well suited for small θ because $d\omega/dn$ blows up at θ equal 1 or $\sqrt{b^2/(\omega_0^2 - \delta^2) + 1}$.

In Fig. 3a,b the local approximation proposed in (3.41) is compared with exact solution of the saddle point equation and the Oughstun-Sherman's approximation. It is very simple but not as good as the latter result.

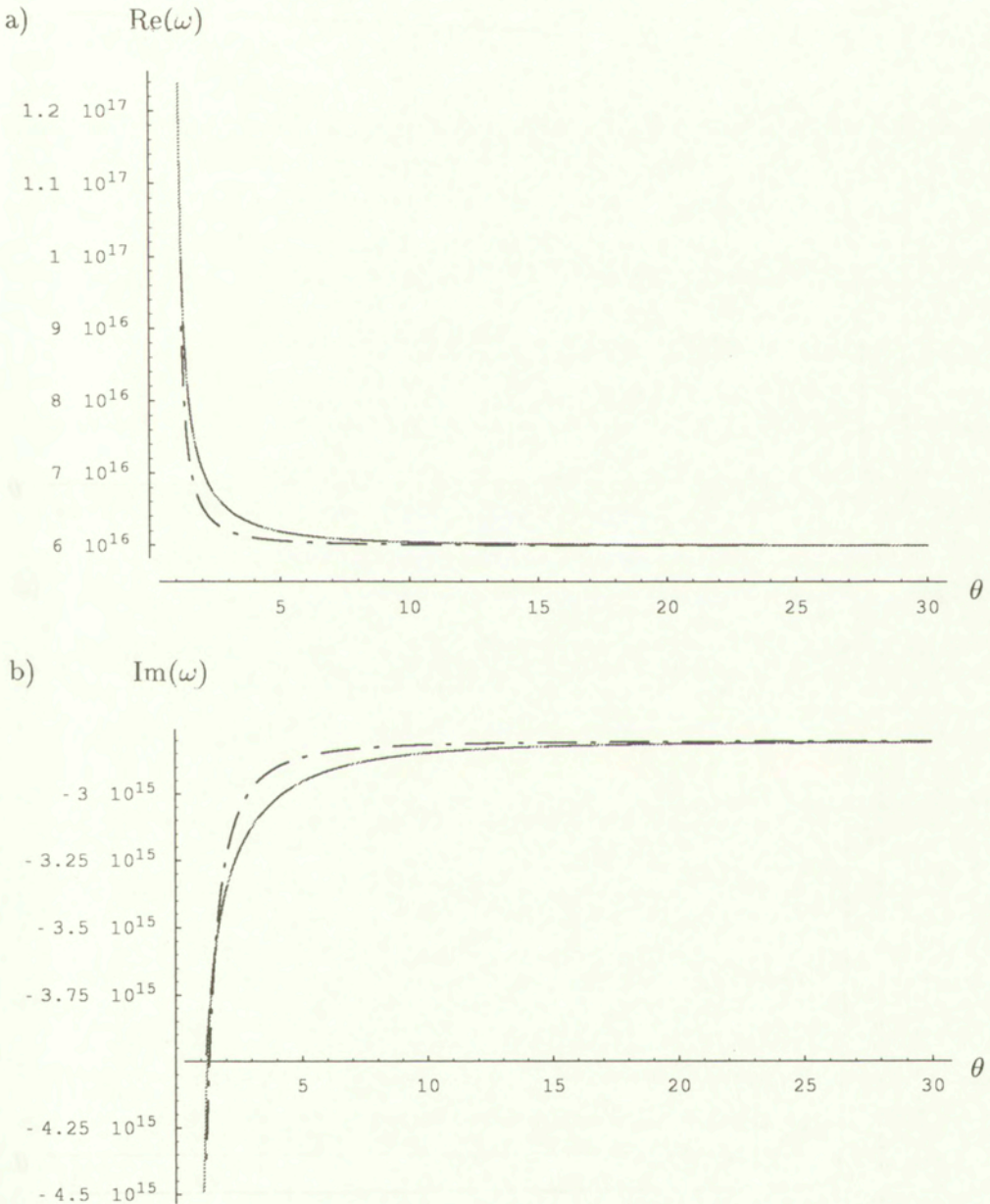


FIG. 1. a) $\text{Re}(\omega)$ versus θ for distant saddle points. —·— Oughstun-Sherman's approximate solution, — exact solution and the approximate solution based on Eq. (3.28) (both plots are undistinguishable except for values of θ below 1.5); b) $\text{Im}(\omega)$ versus θ for distant saddle points. The same caption as in Fig. 1a.

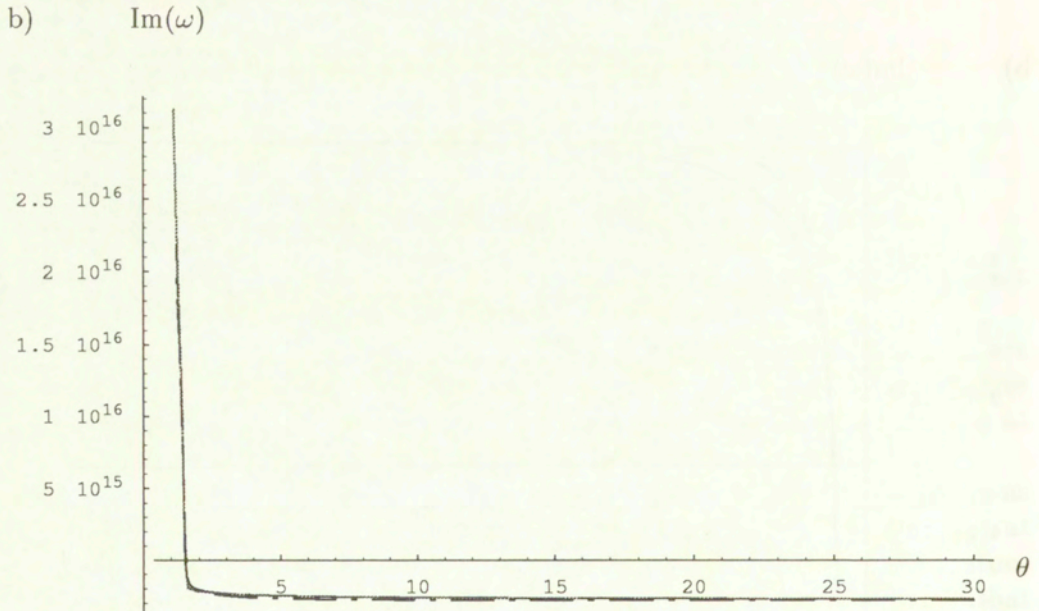
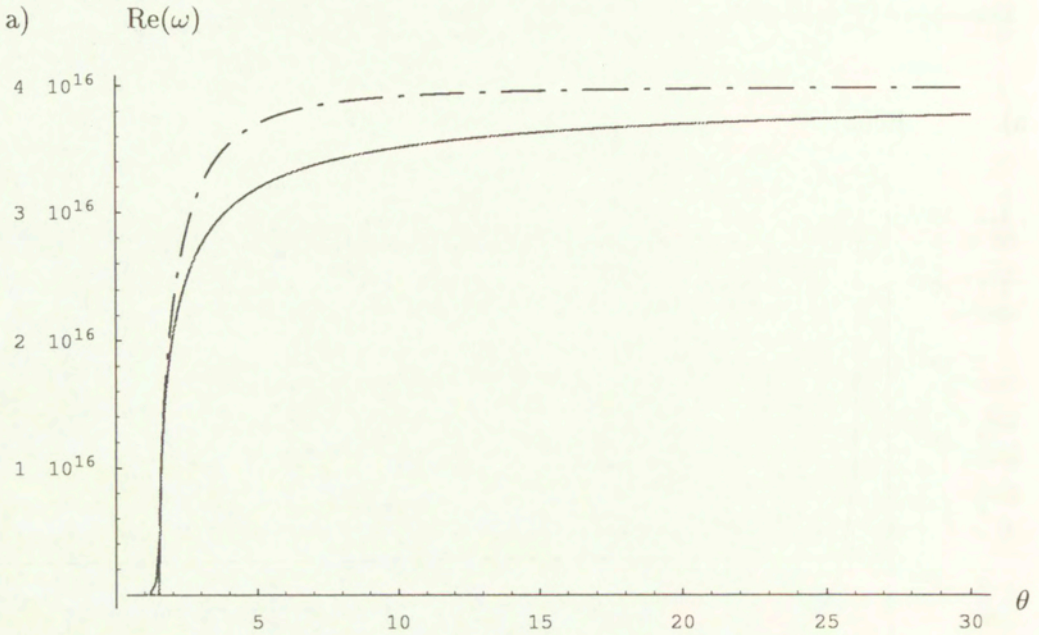


FIG. 2. a) $\text{Re}(\omega)$ versus θ for near saddle points. — · — Oughstun-Sherman's approximate solution, — exact solution and the approximate solution based on Eq. (3.39) (both plots are undistinguishable except for values of θ below 1.5); b) $\text{Im}(\omega)$ versus θ for near saddle points. The same caption as in Fig. 2a.

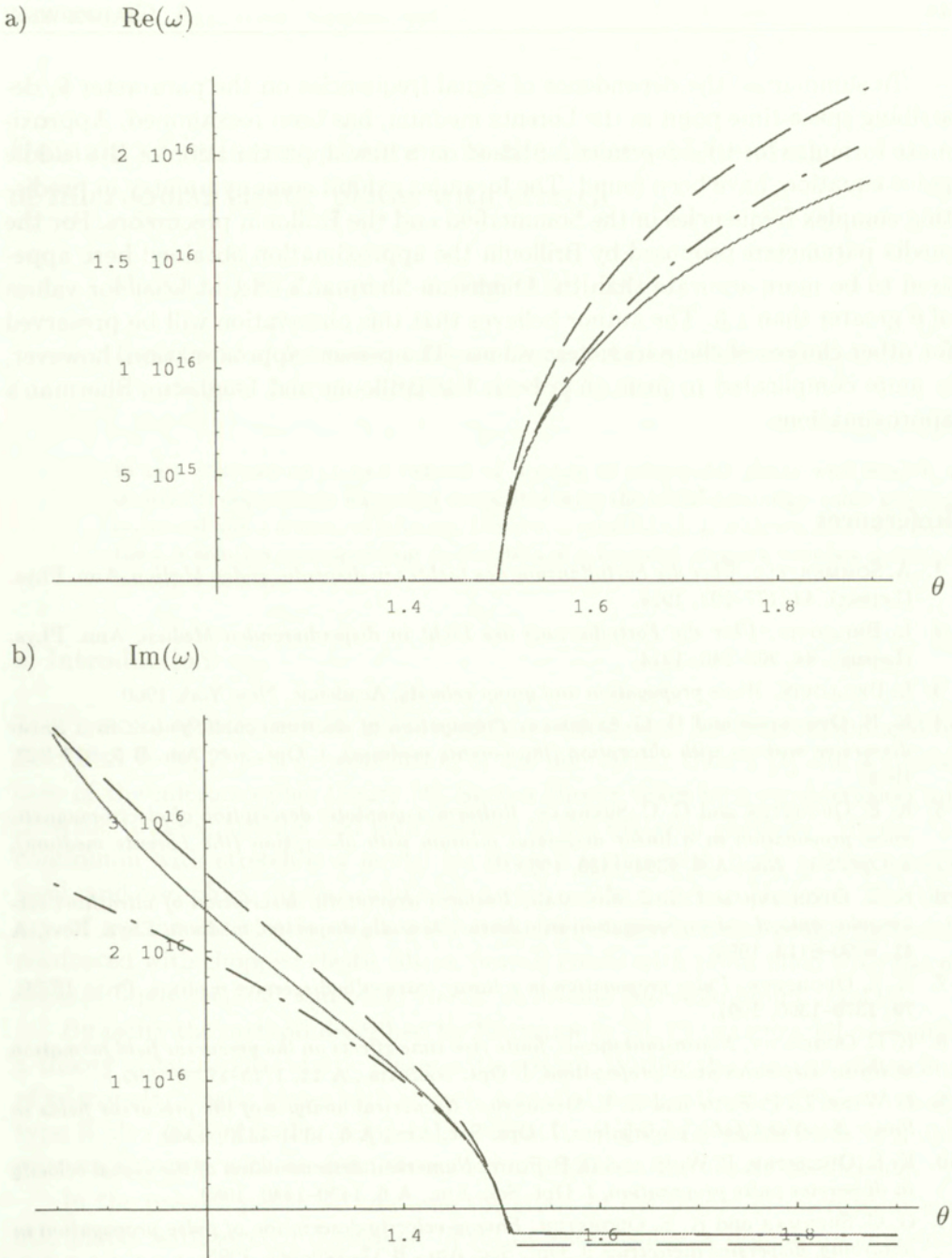


FIG. 3. a) $\text{Re}(\omega)$ versus θ for near saddle points at small values of θ . — exact solution, — — — Oughstun-Sherman's approximate solution, — · — present approximate solution; b) $\text{Im}(\omega)$ versus θ for near saddle points at small values of θ . Same caption as in Fig. 3a.

To summarize, the dependence of signal frequencies on the parameter θ , describing space-time point in the Lorentz medium, has been reexamined. Approximate formulas for this dependence, based on a new approximation of the saddle point equation, have been found. The formulas exhibit some symmetry in predicting complex frequencies in the Sommerfeld and the Brillouin precursors. For the media parameters proposed by Brillouin the approximation obtained here appeared to be more accurate than the Oughstun-Sherman's one, at least for values of θ greater than 1.5. The author believes that this observation will be preserved for other choices of the parameters values. The present approximation, however, is more complicated in form than both the Brillouin and Oughstun-Sherman's approximations.

References

1. A. SOMMERFELD, *Über die Fortpflanzung des Lichtes in disperdierenden Medien*, Ann. Phys. (Lepzig), **44**, 177–202, 1914.
2. L. BRILLOUIN, *Über die Fortpflanzung des Licht in disperdierenden Medien*, Ann. Phys. (Lepzig), **44**, 203–240, 1914.
3. L. BRILLOUIN, *Wave propagation and group velocity*, Academic, New York 1960.
4. K. E. OUGHSTUN and G. C. SHERMAN, *Propagation of electromagnetic pulses in a linear dispersive medium with absorption (the Lorentz medium)*, J. Opt. Soc. Am. **B 5**, 817–849, 1988.
5. K. E. OUGHSTUN and G. C. SHERMAN, *Uniform asymptotic description of electromagnetic pulse propagation in a linear dispersive medium with absorption (the Lorentz medium)*, J. Opt. Soc. Am., **A 6**, 1394–1420, 1989.
6. K. E. OUGHSTUN and G. C. SHERMAN, *Uniform asymptotic description of ultrashort rectangular optical pulse propagation in a linear, causally dispersive medium*, Phys. Rev., **A 41**, 6090–6113, 1990.
7. K. E. OUGHSTUN, *Pulse propagation in a linear, casually dispersive medium*, Proc. IEEE, **79**, 1379–1390, 1991.
8. K. E. OUGHSTUN, *Noninstantaneous, finite rise-time effects on the precursor field formation in linear dispersive pulse propagation*, J. Opt. Soc. Am., **A 12**, 1715–1729, 1995.
9. P. WYNS, D. P. FOTY and K. E. OUGHSTUN, *Numerical analysis of the precursor fields in linear dispersive pulse propagation*, J. Opt. Soc. Am., **A 6**, 1394–1420, 1989.
10. K. E. OUGHSTUN, P. WYNS and D. P. FOTY, *Numerical determination of the signal velocity in dispersive pulse propagation*, J. Opt. Soc. Am., **A 6**, 1430–1440, 1989.
11. G. C. SHERMAN and K. E. OUGHSTUN, *Energy-velocity description of pulse propagation in absorbing, dispersive dielectrics*, J. Opt. Soc. Am., **B 12**, 229–247, 1995.
12. J. A. STRATTON, *Electromagnetic theory*, Mc Graw Hill, New York 1941, Sec. 5.14.

Received June 19, 1998; revised version November 18, 1998.

Domain of influence theorem in the theory of bending of micropolar elastic plates with stretch

M. CIARLETTA and F. PASSARELLA

*Department of Information Engineering and Applied Mathematics,
University of Salerno - I-84084 Fisciano (Sa), Italy*

IN THE CONTEXT OF LINEAR THEORY of bending of micropolar plates with stretch, a domain of dependence inequality associated with the initial-boundary value problem is derived and a domain of influence theorem is established. It is shown that for a finite time, a solution corresponding to the data of a bounded support vanishes outside a bounded domain.

1. Introduction

THE THEORY OF MICROPOLAR ELASTIC SOLIDS with stretch has been introduced by ERINGEN in [1, 2] as a generalization of the micropolar theory [3] and a special case of the micromorphic theory [4]. Such a theory takes into consideration microstructural expansions and contractions of the material particles. Micropolar continuum with stretch is a model for Bravais lattice with basis on the atomic level, and two-phase dipolar solid with a core on the macroscopic level. The theory of micropolar elastic solids with stretch characterizes composite materials reinforced with chopped elastic fibers, porous media with pores filled with gas or inviscid liquid, asphalt and other elastic inclusions and solid-liquid crystals.

By using the method described by ERINGEN in [5], CIARLETTA [6] presented a theory of micropolar elastic plates with stretch. Within the context of bending of micropolar elastic plates with stretch, a spatial decay estimate of Saint-Venant type is also derived and a reciprocal theorem is established which leads to a uniqueness theorem with no definiteness assumptions on the elastic coefficients.

In the present paper we continue the study of the theory of micropolar elastic plates with stretch developed in [6] by establishing a domain of influence theorem of the type discussed in [7, 8]. To this aim we first establish a domain of dependence inequality associated with the initial-boundary value problem of micropolar plate with stretch, in the sense of [9]. Then we prove that, provided the given data of the initial-boundary value problem have a bounded support on the time interval $[0, t]$, the corresponding dynamic process vanishes outside a certain bounded domain.

Finally, we note that the domain of influence theorem has been studied in connection with various theories of continua (see e.g. [10] – [14]).

2. Basic equations

We consider a homogeneous and isotropic micropolar elastic solid with stretch that at time $t = 0$ occupies the right cylinder \bar{B} of length $2h$ with cross-section $\bar{\Sigma}$ and the smooth lateral boundary Π . We call B and Σ be the interiors of \bar{B} and $\bar{\Sigma}$ and denote by n_i the components of the outward unit normal to the boundary of \bar{B} . We assume that Σ is a simply connected region and we denote by L the boundary of Σ .

We refer the motion of continuum to the system of rectangular Cartesian axes Ox_k ($k = 1, 2, 3$) chosen in such a way that

$$B = \{\tilde{\mathbf{x}} = (x_1, x_2, x_3) : (x_1, x_2, 0) \in \Sigma, -h < x_3 < h\},$$

and

$$\Pi = \{\tilde{\mathbf{x}} = (x_1, x_2, x_3) : (x_1, x_2, 0) \in L, -h < x_3 < h\}.$$

We denote the tensor components of order $p \geq 1$ by Latin subscripts, ranging over $\{1, 2, 3\}$, or by Greek subscripts, ranging over $\{1, 2\}$. Summation over repeated subscripts is implied. Superposed dots or subscripts preceded by a comma mean partial derivative with respect to the time or the corresponding coordinates.

In the context of the theory of micropolar elastic solids with stretch, we consider the following set of the independent variables:

$$\mathcal{U} = (u_i, \varphi_i, \psi)$$

where u_i are the components of the displacement vector, φ_i are the components of the microrotation vector and ψ is the microstretch function. We suppose that the fields $u_i, \varphi_i, \psi \in C^{2,2}(B \times T) \cap C^{1,1}(\bar{B} \times [0, \infty))$, where $T = (0, \infty)$.

In the considered theory, the equations of motion are

$$t_{ji,j} + f_i = \rho \ddot{u}_i,$$

$$m_{ji,j} + \varepsilon_{irs} t_{rs} + g_i = j \ddot{\varphi}_i,$$

$$\lambda_{j,j} - s + H = J \ddot{\psi}, \quad \text{on } B \times T,$$

where t_{ij} is the stress tensor, m_{ij} is the couple stress tensor, $\lambda_i/3$ is the microstress vector, $s/3$ is the microstress function, f_i , g_i and H are the body loads, ρ is the reference mass density, j is a coefficient of inertia, $J = 3j/2$ and ε_{irs} is the

alternating symbol. We assume that ρ and j are given strictly positive constants and that the surface tractions $t_i = t_{ji}n_j$, $m_i = m_{ji}n_j$, $p = \lambda_j n_j$ at regular points are assigned on the surfaces $x_3 = \pm h$, i.e. the functions t_{3i} , m_{3i} , λ_3 are prescribed.

We call a state of bending on $B \times T$ a process \mathcal{U} that satisfies the following relations [5]:

$$\begin{aligned}
 u_\alpha(x_1, x_2, x_3, t) &= -u_\alpha(x_1, x_2, -x_3, t), \\
 u_3(x_1, x_2, x_3, t) &= u_3(x_1, x_2, -x_3, t), \\
 \varphi_\alpha(x_1, x_2, x_3, t) &= \varphi_\alpha(x_1, x_2, -x_3, t), \\
 \varphi_3(x_1, x_2, x_3, t) &= -\varphi_3(x_1, x_2, -x_3, t), \\
 \psi(x_1, x_2, x_3, t) &= -\psi(x_1, x_2, -x_3, t), \quad (x_1, x_2, x_3, t) \in B \times T.
 \end{aligned}$$

In accordance with the theories established by ERINGEN in [1, 2] and CIARLETTA in [6], we assume that the body loads obey the relations

$$\begin{aligned}
 f_\alpha(x_1, x_2, x_3, t) &= -f_\alpha(x_1, x_2, -x_3, t), \\
 f_3(x_1, x_2, x_3, t) &= f_3(x_1, x_2, -x_3, t), \\
 g_\alpha(x_1, x_2, x_3, t) &= g_\alpha(x_1, x_2, -x_3, t), \\
 g_3(x_1, x_2, x_3, t) &= -g_3(x_1, x_2, -x_3, t), \\
 H(x_1, x_2, x_3, t) &= -H(x_1, x_2, -x_3, t).
 \end{aligned}$$

In the context of the theory of bending of micropolar elastic plates with stretch, we have the following independent variables (see [5, 6] for physical meaning of various quantities):

$$\begin{aligned}
 v_\alpha &= \frac{1}{I} \int_{-h}^h x_3 u_\alpha dx_3, & w &= \frac{1}{2h} \int_{-h}^h u_3 dx_3, \\
 \psi_\alpha &= \frac{1}{2h} \int_{-h}^h \varphi_\alpha dx_3, & u &= \frac{1}{I} \int_{-h}^h x_3 \psi dx_3,
 \end{aligned}$$

where $I = \frac{2}{3}h^3$.

Following [6], we consider the state of bending characterized by

$$\begin{aligned} u_\alpha &= x_3 v_\alpha(x_1, x_2, t), & u_3 &= w(x_1, x_2, t), \\ \varphi_\alpha &= \psi_\alpha(x_1, x_2, t), & \varphi_3 &= 0, & \psi &= x_3 u(x_1, x_2, t), \quad \text{on } B \times T. \end{aligned}$$

On the basis of the theory established in [6], we obtain the fundamental system of field equations consisting of the equations of motion

$$(2.1) \quad \begin{aligned} \tau_{\alpha 3, \alpha} + F &= \rho \ddot{w}, \\ \mu_{\beta \alpha, \beta} + \varepsilon_{\beta \alpha 3}(\tau_{3\beta} - \tau_{\beta 3}) + K_\alpha &= j \ddot{\psi}_\alpha, \\ M_{\beta \alpha, \beta} - 2h\tau_{3\alpha} + H_\alpha &= \rho I \ddot{v}_\alpha, \\ Q_{\alpha, \alpha} - 2h\pi_3 - S + P &= \zeta \ddot{u}, \quad \text{on } \Sigma \times T, \end{aligned}$$

the constitutive equations

$$(2.2) \quad \begin{aligned} \tau_{\alpha 3} &= (\mu + \kappa)\varepsilon_{\alpha 3} + \mu\varepsilon_{3\alpha}, & \tau_{3\alpha} &= (\mu + \kappa)\varepsilon_{3\alpha} + \mu\varepsilon_{\alpha 3}, \\ \mu_{\alpha\beta} &= \alpha\eta_{\rho\rho}\delta_{\alpha\beta} + \beta\eta_{\beta\alpha} + \gamma\eta_{\alpha\beta}, \\ M_{\alpha\beta} &= I[\lambda\varepsilon_{\rho\rho}\delta_{\alpha\beta} + (\mu + \kappa)\varepsilon_{\alpha\beta} + \mu\varepsilon_{\beta\alpha} + \alpha u\delta_{\alpha\beta}], \\ Q_\alpha &= \sigma I\xi_\alpha, & \pi_3 &= \sigma u, & S &= I(a\varepsilon_{\rho\rho} + bu), \end{aligned}$$

and the geometrical equations

$$(2.3) \quad \begin{aligned} \varepsilon_{\alpha\beta} &= v_{\beta, \alpha}, & \varepsilon_{\alpha 3} &= w_{, \alpha} + \varepsilon_{3\alpha\beta}\psi_{\beta}, & \varepsilon_{3\alpha} &= v_\alpha - \varepsilon_{3\alpha\beta}\psi_{\beta}, \\ \eta_{\alpha\beta} &= \psi_{\beta, \alpha}, & \xi_\alpha &= u_{, \alpha}. \end{aligned}$$

In these equations we have used the notations [5, 6]

$$(2.4) \quad \begin{aligned} \tau_{ij} &= \frac{1}{2h} \int_{-h}^h t_{ij} dx_3, & \mu_{ij} &= \frac{1}{2h} \int_{-h}^h m_{ij} dx_3, \\ M_{ij} &= \int_{-h}^h x_3 t_{ij} dx_3, & Q_i &= \int_{-h}^h x_3 \lambda_i dx_3, \\ \pi_i &= \frac{1}{2h} \int_{-h}^h \lambda_i dx_3, & S &= \int_{-h}^h x_3 s dx_3, & \zeta &= \frac{3}{2} j I; \end{aligned}$$

the loads F , K_α , H_α and P are defined by

$$\begin{aligned}
 F &= F_3 + q, & q &= \frac{1}{h}t_{33}(x_1, x_2, h, t), & F_3 &= \int_{-h}^h f_3 dx_3, \\
 K_\alpha &= G_\alpha + \eta_\alpha, & \eta_\alpha &= \frac{1}{h}m_{3\alpha}(x_1, x_2, h, t), & G_\alpha &= \int_{-h}^h g_\alpha dx_3, \\
 H_\alpha &= q_\alpha + L_\alpha, & q_\alpha &= 2ht_{3\alpha}(x_1, x_2, h, t), & L_\alpha &= \int_{-h}^h x_3 f_\alpha dx_3, \\
 P &= \chi + R, & \chi &= 2h\lambda_3(x_1, x_2, h, t), & R &= \int_{-h}^h x_3 H dx_3;
 \end{aligned}$$

moreover, the coefficients λ , μ , κ , a , $\alpha\beta$, γ , σ and b are constitutive constants. The loads F , K_α , H_α and P are prescribed.

Together with the system of field equations (2.1) – (2.3) in the variables v_α , w , ψ_α , u , we consider the following initial-boundary conditions:

$$\begin{aligned}
 v_\alpha(x_1, x_2, 0) &= v_\alpha^0(x_1, x_2), & w(x_1, x_2, 0) &= w^0(x_1, x_2), \\
 \psi_\alpha(x_1, x_2, 0) &= \psi_\alpha^0(x_1, x_2), & u(x_1, x_2, 0) &= u^0(x_1, x_2), \\
 \dot{v}_\alpha(x_1, x_2, 0) &= \nu_\alpha(x_1, x_2), & \dot{w}(x_1, x_2, 0) &= \omega(x_1, x_2), \\
 \dot{\psi}_\alpha(x_1, x_2, 0) &= \chi_\alpha(x_1, x_2), & \dot{u}(x_1, x_2, 0) &= v(x_1, x_2), & \text{on } \bar{\Sigma},
 \end{aligned}
 \tag{2.5}$$

and

$$\begin{aligned}
 M_{\beta\alpha}n_\beta &= \tilde{M}_\alpha, & \tau_{\alpha 3}n_\alpha &= \tilde{\tau}, \\
 \mu_{\beta\alpha}n_\beta &= \tilde{\mu}_\alpha, & Q_\alpha n_\alpha &= \tilde{Q}, & \text{on } L \times T.
 \end{aligned}
 \tag{2.6}$$

The terms on the right-hand sides of the equations (2.5) and (2.6) stand for the (sufficiently smooth) assigned function; with F , K_α , H_α , P , these are the (external) data of the mixed problem considered. An array field $\mathcal{Q} = \{v_\alpha, w, \psi_\alpha, u\}$ satisfying all equations (2.1) – (2.3) and (2.5) – (2.6), for some assignment of the data, will be referred to as a (regular) *solution* of the problem of bending.

Of interest in the sequel will be the internal energy W of the plate due to bending (see [6])

$$(2.7) \quad 2W = 2 \int_{-h}^h W^* dx_3 = M_{\alpha\beta} \epsilon_{\alpha\beta} + Q_\alpha \xi_\alpha + Su \\ + 2h(\tau_{\alpha 3} \epsilon_{\alpha 3} + \tau_{3\alpha} \epsilon_{3\alpha} + \pi_3 u + \mu_{\alpha\beta} \eta_{\alpha\beta}),$$

in which W^* is the strain energy density of the micropolar elastic solid with stretch [2]. In what follows, we suppose that W^* is a positive definite quadratic form; thus, there exists a strictly positive constant ξ (it is maximum elastic modulus) such that [15]

$$(2.8) \quad \frac{1}{\xi} (t_{ij} t_{ij} + m_{ij} m_{ij} + \lambda_i \lambda_i + s^2) \leq 2W^*,$$

and [6]

$$(2.9) \quad \frac{1}{\xi} \left[\frac{1}{I} (M_{\alpha\beta} M_{\alpha\beta} + Q_\alpha Q_\alpha) + 2h(\tau_{\alpha 3} \tau_{\alpha 3} + \mu_{\alpha\beta} \mu_{\alpha\beta}) \right] \leq 2W.$$

3. Domain of influence

Having fixed a solution Q of the problem (2.1) – (2.3) and (2.5) – (2.6) and a time $t \in T$, we denote by $D_0(t)$ the support of initial and boundary data and body loads of the problem in concern; $D_0(t)$ is the set of the point $\mathbf{x} \in \bar{\Sigma}$ such that

(i) if $\mathbf{x} \in \Sigma$, then $v_\alpha^0(\mathbf{x}) \neq 0$ or $w^0(\mathbf{x}) \neq 0$ or $\psi_\alpha^0(\mathbf{x}) \neq 0$ or $u^0(\mathbf{x}) \neq 0$ or $\nu_\alpha(\mathbf{x}) \neq 0$ or $\omega(\mathbf{x}) \neq 0$ or $\chi_\alpha(\mathbf{x}) \neq 0$ or $v(\mathbf{x}) \neq 0$ or there exists $\tau \in [0, t]$ such that $F(\mathbf{x}, \tau) \neq 0$ or $K_\alpha(\mathbf{x}, \tau) \neq 0$ or $H_\alpha(\mathbf{x}, \tau) \neq 0$ or $P(\mathbf{x}, \tau) \neq 0$;

(ii) if $\mathbf{x} \in L$, then there exists $\tau \in [0, t]$ such that $\tilde{M}_\alpha(\mathbf{x}, \tau) \neq 0$ or $\tilde{\tau}(\mathbf{x}, \tau) \neq 0$ or $\tilde{\mu}_\alpha(\mathbf{x}, \tau) \neq 0$ or $\tilde{Q}(\mathbf{x}, \tau) \neq 0$.

By a domain of influence of the data at time t for mixed problem (2.1) – (2.3) and (2.5) – (2.6) we mean the set

$$(3.1) \quad D(t) = \{\mathbf{x}_0 \in \bar{\Sigma} : D_0(t) \cap \overline{S(\mathbf{x}_0, ct)} \neq \emptyset\},$$

where $\overline{S(\mathbf{x}_0, d)}$ is the closed disc of radius d and the center \mathbf{x}_0 , and c is given by

$$(3.2) \quad c = \left\{ \frac{\xi}{m} \right\}^{1/2} \quad \text{with} \quad m = \min\{\rho, j\}.$$

We put

$$\Sigma(\mathbf{x}_0, d) = \Sigma \cap S(\mathbf{x}_0, d), \quad L(\mathbf{x}_0, d) = L \cap S(\mathbf{x}_0, d),$$

in which $S(\mathbf{x}_0, d)$ is the interior of $\overline{S(\mathbf{x}_0, ct)}$.

In order to approach the proof of the domain of influence theorem, we have to show first the

THEOREM. *Let Q be a solution of the initial-boundary value problem (2.1) – (2.3) and (2.5) – (2.6), and U be the function defined by*

$$(3.3) \quad U = W + \frac{1}{2}(\rho I \dot{v}_\alpha \dot{v}_\alpha + \zeta \dot{u}^2 + 2h\rho \dot{w}^2 + 2hj \dot{\psi}_\alpha \dot{\psi}_\alpha).$$

Then, for each $t \in T$ and any positive constant R we have

$$(3.4) \quad \int_{\Sigma(\mathbf{x}_0, R)} U(\mathbf{x}, t) da \leq \int_{\Sigma(\mathbf{x}_0, R+ct)} U(\mathbf{x}, 0) da$$

$$+ \int_0^t \int_{\Sigma(\mathbf{x}_0, R+c(t-r))} (H_\beta \dot{v}_\beta + P \dot{u} + F \dot{w}_i + K_\beta \dot{\psi}_\beta) da dr$$

$$+ \int_0^t \int_{L(\mathbf{x}_0, R+c(t-r))} (M_{\beta\alpha} \dot{v}_\alpha + Q_\beta \dot{u} + 2h(\tau_{\beta 3} \dot{w} + \mu_{\beta\alpha} \dot{\psi}_\alpha)) n_\beta ds dr,$$

where c is given by (3.2).

P r o o f. At a fixed $(\mathbf{x}_0, t) \in \mathbb{R}^2 \times T$ and a positive constant R , we introduce the function

$$G(\mathbf{x}, r) = G_\delta \left\{ \frac{1}{c} [R + c(t - r) - |\mathbf{x} - \mathbf{x}_0|] \right\}, \quad (\mathbf{x}, r) \in \mathbb{R}^2 \times T,$$

where G_δ is a smooth, nondecreasing function on \mathbb{R} , such that

$$G_\delta(\iota) = 0 \quad \text{if } \iota \in (-\infty, 0], \quad \text{and} \quad G_\delta(\iota) = 1 \quad \text{if } \iota \in [\delta, \infty).$$

The support of G is $\Omega = \bigcup_{r \leq t} S(\mathbf{x}_0, R + c(t - r))$. We may prove that G is identically equal to 1 on the set $\Omega_0 = \bigcup_{r \leq t} S(\mathbf{x}_0, R + ct - cr - c\delta)$ and, consequently, $\text{grad } G$ vanishes on Ω_0 .

Of course, we must choose δ small enough to assume that $R + ct - cr - c\delta > 0$ for any $r \in [0, t]$.

From the equations (2.2) and (2.3), we can note that

$$(3.5) \quad \begin{aligned} G\dot{U} = G & \left(M_{\beta\alpha} \dot{v}_{\alpha,\beta} + Q_{\beta} \dot{u}_{,\beta} + S\dot{u} + 2h(\tau_{\beta 3} \dot{w}_{,\beta} \right. \\ & + \varepsilon_{3\beta\alpha} \tau_{\beta 3} \dot{\psi}_{\alpha} + \tau_{3\alpha} \dot{v}_{\alpha} - \varepsilon_{3\beta\alpha} \tau_{\beta 3} \dot{\psi}_{\alpha} + \pi_{3\dot{u}} + \mu_{\beta\alpha} \dot{\psi}_{\alpha,\beta}) \\ & \left. + \rho I \ddot{v}_{\alpha} \dot{v}_{\alpha} + \zeta \ddot{u} \dot{u} + 2h\rho \ddot{w} \dot{w} + 2hj \ddot{\psi}_{\alpha} \dot{\psi}_{\alpha} \right), \end{aligned}$$

and, taking into account the equations (2.1) and (3.5), we can write

$$(3.6) \quad \begin{aligned} \int_0^t \int_{\Sigma} \frac{\partial A}{\partial r} da dr &= \int_0^t \int_{\Sigma} \left(U \frac{\partial G}{\partial r} \right) (\mathbf{x}, r) da dr \\ &+ \int_0^t \int_{\Sigma} G \left(H_{\alpha} \dot{v}_{\alpha} + P\dot{u} + 2hF\dot{w} + 2hK_{\alpha} \dot{\psi}_{\alpha} \right) da dr \\ &+ \int_0^t \int_{\Sigma} G \left[M_{\beta\alpha} \dot{v}_{\alpha} + Q_{\beta} \dot{u} + 2h(\tau_{\beta 3} \dot{w} + \mu_{\beta\alpha} \dot{\psi}_{\alpha}) \right]_{,\beta} da dr, \end{aligned}$$

where $A = GU$. Using the equation (3.6) and the divergence theorem, we get

$$(3.7) \quad \begin{aligned} \int_{\Sigma} A(\mathbf{x}, t) da &= \int_{\Sigma} A(\mathbf{x}, 0) da + \int_0^t \int_{\Sigma} \left(U \frac{\partial G}{\partial r} \right) (\mathbf{x}, r) da dr \\ &+ \int_0^t \int_{\Sigma} G \left(H_{\alpha} \dot{v}_{\alpha} + P\dot{u} + 2hF\dot{w} + 2hK_{\alpha} \dot{\psi}_{\alpha} \right) da dr \\ &- \int_0^t \int_{\Sigma} G_{,\beta} \left[2h(\tau_{\beta 3} \dot{w} + \mu_{\beta\alpha} \dot{\psi}_{\alpha}) + M_{\beta\alpha} \dot{v}_{\alpha} + Q_{\beta} \dot{u} \right] da dr \\ &+ \int_0^t \int_L G \left[2h(\tau_{\beta 3} \dot{w} + \mu_{\beta\alpha} \dot{\psi}_{\alpha}) + M_{\beta\alpha} \dot{v}_{\alpha} + Q_{\beta} \dot{u} \right] n_{\beta} ds dr. \end{aligned}$$

If we denote by

$$G'_{\delta} = \frac{dG_{\delta}(y)}{dy}, \quad y = \frac{1}{c} [R + c(t - r) - |\mathbf{x} - \mathbf{x}_0|],$$

then we can write

$$(3.8) \quad G_{,\beta} = -\zeta_{\beta} \frac{1}{c} G'_{\delta}, \quad \zeta_{\beta} = \frac{(x_{\beta} - x_{\beta}^0)}{|\mathbf{x} - \mathbf{x}_0|},$$

and

$$(3.9) \quad \frac{\partial G}{\partial r} = -G'_{\delta}.$$

Thus, we have

$$(3.10) \quad -G_{,\beta} \left[M_{\beta\alpha} \dot{v}_{\alpha} + Q_{\beta} \dot{u} + 2h(\tau_{\beta 3} \dot{w} + \mu_{\beta\alpha} \dot{\psi}_{\alpha}) \right] = G'_{\delta} \left[M_{\beta\alpha} \zeta_{\beta} \frac{\dot{v}_{\alpha}}{c} + Q_{\beta} \zeta_{\beta} \frac{\dot{u}}{c} + 2h \left(\tau_{\beta 3} \zeta_{\beta} \frac{\dot{w}}{c} + \mu_{\beta\alpha} \zeta_{\beta} \frac{\dot{\psi}_{\alpha}}{c} \right) \right].$$

If we apply the Schwarz inequality and the arithmetic-geometric inequality, the equation (3.10) implies that

$$(3.11) \quad -G_{,\beta} \left[M_{\beta\alpha} \dot{v}_{\alpha} + Q_{\beta} \dot{u} + 2h(\tau_{\beta 3} \dot{w} + \mu_{\beta\alpha} \dot{\psi}_{\alpha}) \right] \leq \frac{1}{2} G'_{\delta} \left[\frac{1}{I\xi} M_{\beta\alpha} M_{\beta\alpha} + \frac{I\xi}{c^2} \dot{v}_{\alpha} \dot{v}_{\alpha} + \frac{1}{I\xi} Q_{\beta} Q_{\beta} + \frac{I\xi}{c^2} \dot{u}^2 + \frac{2h}{\xi} \tau_{\beta 3} \tau_{\beta 3} + \frac{2h\xi}{c^2} \dot{w}^2 + \frac{2h}{\xi} \mu_{\beta\alpha} \mu_{\beta\alpha} + \frac{2h\xi}{c^2} \dot{\psi}_{\alpha} \dot{\psi}_{\alpha} \right].$$

Taking into account the relations (2.9), (3.2), (3.3) and (2.4)₇, the equation (3.11) implies that

$$(3.12) \quad -G_{,\beta} \left[M_{\beta\alpha} \dot{v}_{\alpha} + Q_{\beta} \dot{u} + 2h(\tau_{\beta 3} \dot{w} + \mu_{\beta\alpha} \dot{\psi}_{\alpha}) \right] \leq G'_{\delta} U.$$

With the help of (3.9) and (3.12), we get

$$(3.13) \quad \int_0^t \int_{\Sigma} U \frac{\partial G}{\partial r} - G_{,\beta} \left[M_{\beta\alpha} \dot{v}_{\alpha} + Q_{\beta} \dot{u} + 2h(\tau_{\beta 3} \dot{w} + \mu_{\beta\alpha} \dot{\psi}_{\alpha}) \right] da dr \leq 0.$$

Thus, from (3.7) we have

$$\begin{aligned}
 (3.14) \quad \int_{\Sigma} A(x, t) da &\leq \int_{\Sigma} A(x, 0) da \\
 &+ \int_0^t \int_{\Sigma} G \left(H_{\alpha} \dot{v}_{\alpha} + P \dot{u} + 2hF\dot{w} + 2hK_{\alpha} \dot{\psi}_{\alpha} \right) da dr \\
 &+ \int_0^t \int_L G \left[M_{\beta\alpha} \dot{v}_{\alpha} + Q_{\beta} \dot{u} + 2h(\tau_{\beta 3} \dot{w} + \mu_{\beta\alpha} \dot{\psi}_{\alpha}) \right] n_{\beta} ds dr.
 \end{aligned}$$

We note that passage to the limit $\delta \rightarrow 0$ is permissible in the integrals in (3.14) by virtue of the Lebesgue dominated convergence theorem, since G tends boundedly to the characteristic function of the set Ω . If we take the limit in (3.14) as $\delta \rightarrow 0$, then we obtain (3.4). ■

The set $D(t)$ covers a domain of elastic disturbances produced by the data at time t ; in fact, following [11, 12], we prove the

DOMAIN OF INFLUENCE THEOREM: *Let \mathcal{Q} be a solution of the initial-boundary value problem (2.1) – (2.3) and (2.5) – (2.6), and $D(t)$ be domain of influence of its data at time t . Then,*

$$v_{\alpha} = 0, \quad w = 0, \quad \psi_{\alpha} = 0, \quad u = 0, \quad \text{on } (\bar{\Sigma} - D(t)) \times [0, t].$$

P r o o f. If we put in the inequality (3.4) $t = \tau$ and $R = c(t - \tau)$, we obtain

$$\begin{aligned}
 (3.15) \quad \int_{\Sigma(\mathbf{x}_0, c(t-\tau))} U(\mathbf{x}, \tau) da &\leq \int_{\Sigma(\mathbf{x}_0, ct)} U(\mathbf{x}, 0) da \\
 &+ \int_0^{\tau} \int_{\Sigma(\mathbf{x}_0, c(t-\tau))} \left(H_{\alpha} \dot{v}_{\alpha} + P \dot{u} + 2hF\dot{w} + 2hK_{\alpha} \dot{\psi}_{\alpha} \right) da dr \\
 &+ \int_0^{\tau} \int_{L(\mathbf{x}_0, c(t-\tau))} \left[M_{\beta\alpha} \dot{v}_{\alpha} + Q_{\beta} \dot{u} + 2h(\tau_{\beta 3} \dot{w} + \mu_{\beta\alpha} \dot{\psi}_{\alpha}) \right] n_{\beta} ds dr.
 \end{aligned}$$

At fixed $(\mathbf{x}_0, \tau) \in (\bar{\Sigma} - D(t)) \times [0, t]$, we have

$$\begin{aligned}
 \bar{v}_{\alpha}(\mathbf{x}, 0) &= 0, & w(\mathbf{x}, 0) &= 0, & \psi_{\alpha}(\mathbf{x}, 0) &= 0, \\
 u(\mathbf{x}, 0) &= 0, & v_{\alpha, \beta}(\mathbf{x}, 0) &= 0, & w_{, \beta}(\mathbf{x}, 0) &= 0, \\
 \psi_{\alpha, \beta}(\mathbf{x}, 0) &= 0, & u_{, \beta}(\mathbf{x}, 0) &= 0, & \mathbf{x} \in \Sigma(\mathbf{x}_0, ct), &
 \end{aligned}$$

and

$$\begin{aligned}
 F(\mathbf{x}, \tau) &= 0, & K_\alpha(\mathbf{x}, \tau) &= 0, \\
 H_\alpha(\mathbf{x}, \tau) &= 0, & P(\mathbf{x}, \tau) &= 0, & (\mathbf{x}, \tau) \in \Sigma(\mathbf{x}_0, ct) \times [0, t].
 \end{aligned}$$

Thus, we get

$$\begin{aligned}
 &\int_{\Sigma(\mathbf{x}_0, ct)} U(\mathbf{x}, 0) da = 0. \\
 (3.16) \quad &\int_0^\tau \int_{\Sigma(\mathbf{x}_0, c(t-\tau))} \left(H_\alpha \dot{v}_\alpha + P \dot{u} + 2RF\dot{w} + 2RK_\alpha \dot{\psi}_\alpha \right) da d\tau = 0.
 \end{aligned}$$

If we consider $\tau \leq t$ and $\Sigma(\mathbf{x}_0, ct) \subset \bar{\Sigma} - D(t)$, the last integral of Eq. (3.15) also vanishes. Then, the equation (3.15) becomes

$$(3.17) \quad \int_{\Sigma(\mathbf{x}_0, c(t-\tau))} U(\mathbf{x}, \tau) da \leq 0.$$

With the aid of the equations (3.3), (2.8) and (3.17), we conclude that

$$\begin{aligned}
 \dot{v}_\alpha(\mathbf{x}_0, \tau) &= 0, & \dot{w}(\mathbf{x}_0, \tau) &= 0, \\
 \dot{\psi}_\alpha(\mathbf{x}_0, \tau) &= 0, & \dot{u}(\mathbf{x}_0, \tau) &= 0, & (\mathbf{x}_0, \tau) \in (\bar{\Sigma} - D(t)) \times [0, t];
 \end{aligned}$$

taking into account that

$$\begin{aligned}
 v_\alpha(\mathbf{x}_0, 0) &= 0, & w(\mathbf{x}_0, 0) &= 0, \\
 \psi_\alpha(\mathbf{x}_0, 0) &= 0, & u(\mathbf{x}_0, 0) &= 0, & \mathbf{x}_0 \in \bar{\Sigma} - D(t),
 \end{aligned}$$

we obtain the desired result. ■

References

1. A. C. ERINGEN, *Micropolar elastic solids with stretch*. [In:] Prof. Dr. Mustafa Inan Anisina, 1-18. Ari Kitabevi Matbaasi, Istanbul 1971.
2. A. C. ERINGEN, *Theory of thermo-microstretch elastic solids*, Int. J. Engng. Sci., **28**, 1291-1301, 1990.

3. A. C. ERINGEN, *Linear theory of micropolar elasticity*, J. Math. Mech., **15**, 909–923, 1966.
4. A. C. ERINGEN, *Mechanics of micromorphic materials*, [In:] Proceedings of the 11th International Congress of Applied Mechanics, 1964, Munich (Edited by H. Görtler), 131–138. Springer, Berlin 1966.
5. A. C. ERINGEN, *Theory of micropolar plates*, ZAMP, **18**, 12–30, 1967.
6. M. CIARLETTA, *On the bending of microstretch elastic plates*, Int. J. Engng. Sci., to appear.
7. L. T. WHEELER and E. STERNBERG, *Some theorems in classical elastodynamics*. Arch. Rat. Mech. Anal., **31**, 51–90, 1968.
8. M. E. GURTIN, *The linear theory of elasticity*, [In:] Flügge's Handbuch der Physik, vol. VI a/2 (Editor by C. Truesdell), 1–295, Springer, Berlin 1972.
9. B. CARBONARO and R. RUSSO, *Energy inequalities and the domain of influence theorem in classical elastodynamics*, J. Elasticity, **14**, 163–174, 1984.
10. J. IGNACZAK, *Domain of influence theorem in linear thermoelasticity*, Int. J. Engng. Sci., **16**, 139–145, 1978.
11. J. IGNACZAK and J. BIALY, *Domain of influence theorem in thermoelasticity with one relaxation time*, J. Thermal Stresses, **3**, 391–399, 1980.
12. J. IGNACZAK, B. CARBONARO and R. RUSSO, *Domain of influence theorem in thermoelasticity with one relaxation time*, J. Thermal Stresses, **9**, 79–91, 1986.
13. I. LUCA, *Domain of influence and uniqueness in viscothermoelasticity of integral type*, Continuum Mech. Thermodyn., **1**, 213–226, 1989.
14. B. CARBONARO and J. IGNACZAK, *Some theorems in temperature-rate-dependent thermoelasticity for unbounded domains*, J. Thermal Stresses, **10**, 193–220, 1987.
15. D. IESAN and A. SCALIA, *On Saint-Venant's principle for microstretch elastic bodies*, Int. J. Engng. Sci., **35**, 1277–1290, 1997.

Received April 14, 1998; revised version September 7, 1998.

Two-point Padé approximants to the effective heat conduction coefficient of non-uniform media

S. MAY

Polish Academy of Sciences

Institute of Fundamental Technological Research

Świętokrzyska 21, 00-049 Warszawa, Poland

IN [3] THE TWO-POINT PADÉ APPROXIMANTS were used to obtain the lower and upper bounds to the effective heat transfer coefficient in the composite with inclusions in the form of densely packed cylinder array. The effective heat transfer coefficient fulfils the Keller symmetry condition, however the asymptotic formula (MCPHEDRAN *et al.* [4]) used to build the approximants does not agree with this condition. By using the Keller symmetry explicitly we transform the asymptotic formula to the symmetric form and obtain better bounds than those in [3].

1. Introduction

ONE OF IMPORTANT PROBLEMS of the theory of dispersive media is the theoretical determination of the effective transport coefficient of non-uniform media on the basis of geometrical structure and physical properties of the media. In the paper we consider the effective heat conduction coefficient λ_{ef} of two-component composite with a regular square array of infinite circular cylinders immersed in an infinite matrix. The coefficients of heat conduction of inclusions and matrix are λ_d and λ_c , respectively, and the volume fraction of inclusions is φ . Our considerations are not bounded to the heat conduction theory but may be applied to other physical theories governed by the Laplace equation, such as the theory of electric conduction, dielectric constant, etc.

In most methods of investigation of the effective transport coefficient, the infinite system of algebraic equations, known as the Rayleigh equations [1], is used as the departure point. Upon truncation these equations can be solved numerically. Another method of solution is based on using the power series. However, the solution is non-analytic for $h = \lambda_d/\lambda_c$ tending to 0 or ∞ and $\varphi \rightarrow \varphi_{\max} = \pi/4$. As a consequence, both methods lose their accuracy for nearly touching cylinders, and large or small h – the power series converges very slowly in this range of parameters. In fact, while using $h - 1$ or $1/(h - 1)$ as the power series argument, one obtains the power series divergent in some part of the physical region. By changing the power series argument to $\alpha = (1 - h)/(1 + h)$ one obtains the series

that converges for $|\alpha| < 1$, however the problem of slow convergence remains. Some improvement may be achieved by using the rational approximations in the form of continued fractions or Padé approximants [2]. This is due to the fact that the solution of the problem is a Stieltjes function of $h - 1$ and has a set of singularities (single poles) for real $h < -1$, outside the physically meaningful region of parameters. The rational functions give better approximations to such functions. However, for $\varphi \rightarrow \varphi_{\max}$ and $h \rightarrow \infty$ an essential singularity appears and the above method fails near this singular point. For such a case MCPHEDRAN *et al.* [4] gave the asymptotic solution. There exists yet a certain gap between the solution originating from the power series at $h = 1$ (and resulting from these power series rational approximations) and the asymptotic solution. To fulfil this gap, a new approach was developed using the two-point Padé approximants. These approximants, built from the power series at $h = 1$ and the asymptotic development for $h \rightarrow \infty$ were used in [3]. There is yet a certain drawback in the method applied there. It is known [5] that the solution of our problem should fulfil the symmetry condition

$$(1.1) \quad \lambda_{ef}(1/h)\lambda_{ef}(h) = \text{const}$$

known as the Keller symmetry. Of course, the power series solution agree with the Keller symmetry, however the asymptotic solution [4], found for $h \rightarrow \infty$ (but not for $h \rightarrow 0$) fails in this respect. The same is true for the two-point Padé approximants considered in [3] and based on this asymptotic solution. In the present investigation we take into account the Keller symmetry as an additional condition. Owing to this we obtain the correct asymptotic transition not only for $h \rightarrow \infty$ but also for $h \rightarrow 0$; moreover, the approximants fulfilling the symmetry condition give better bounds to the solution than those found in [3]. The influence of analytical properties of functions, such as the Keller symmetry, on the bounds of effective properties of materials was investigated in [10] for a more general class of composites. However the type of bounds, considered in the present paper, and based on the asymptotic solution, was not particularly treated there.

2. The problem formulation and the power series solution

We consider an infinite regular system of circular cylinders in the form of a square array. Let the distance between the neighbouring cylinder axes be 1 and the cylinder radius ρ . The temperature distribution in the medium is governed by the Eq. (2.1)

$$(2.1) \quad \nabla \cdot (\lambda_c + (\lambda_d - \lambda_c)\theta_d)\nabla T = 0,$$

where θ_d is the characteristic function of cylinders. Besides the heat transfer

equation one should take into account the conditions of continuity of temperature and normal component of heat flux $\mathbf{q} = (\lambda_c + (\lambda_d - \lambda_c)\theta_d)\nabla T$ on the cylinder border

$$(2.2) \quad T(\rho_-) = T(\rho_+), \quad \mathbf{q}(\rho_-) \cdot \mathbf{n} = \mathbf{q}(\rho_+) \cdot \mathbf{n},$$

where \mathbf{n} is the unit normal vector, and the indices minus and plus correspond to the internal and external side of cylinder surface, respectively. To determine the effective heat transfer coefficient we introduce a constant external temperature gradient in the direction of the Ox -axis. The temperature distribution in the medium can be considered as the sum of the systematic $T^{(0)}$ and periodic $T^{(p)}$ components: $T = T^{(0)} + T^{(p)}$. In the problem the amplitude of $T^{(0)}$ is not important, and without any loss of generality we may put $T^{(0)} = x$. For the periodic component $T^{(p)}$ we consider the periodicity conditions on the border of elementary cell

$$(2.3) \quad \mathbf{n} \cdot \nabla T^{(p)} = 0.$$

It is convenient to seek the solution of Eq. (2.1) with the boundary conditions (2.2) and (2.3) in the functional basis derived from the Wigner potential ([2, 3, 9]). The elements of this basis fulfil the boundary conditions (2.3).

The effective heat transfer coefficient is defined as

$$(2.4) \quad \lambda_d = \left\langle (\lambda_c + (\lambda - \lambda_c)\theta_d) \frac{\partial T}{\partial x} \right\rangle,$$

where $\langle \dots \rangle = S^{-1} \int \dots dS$ means the average over the elementary cell. Expressing the temperature in the referred basis, one can define a very simple algorithm for finding the effective heat transfer coefficient as a power series of $h - 1$. The algorithm was used in [3], and described in more details in [9]. Using this algorithm one can determine numerically the coefficients of the power series (2.5):

$$(2.5) \quad \frac{\lambda_{ef}}{\lambda_c} = c_0 + c_1(h - 1) + c_2(h - 1)^2 + \dots$$

3. Padé approximants and the Keller symmetry

The rational function

$$(3.1) \quad [M/M]_n = \frac{A_0 + A_1 z + \dots + A_M z^M}{1 + B_1 z + \dots + B_M z^M},$$

is the two-point Padé approximant to the Stieltjes function $f(z)$ if $f(z)$ can be developed to the formal power series in 0 and infinity (convergence radius can be equal to 0) and

1. The first n coefficients of the expansion of $[M/M]_n$ to the power series of the argument $1/z$ are equal to the corresponding coefficients of the power expansion of $f(z)$ at infinity;

2. The $2M + 1 - n$ first coefficients of the expansion of $[M/M]_n$ to the power series of z are equal to the corresponding coefficients of the power expansion of $f(z)$ at $z = 0$.

For n even or odd, the approximants give a lower or upper bound of $f(z)$, respectively. In the following we shall only consider the approximants $[M/M]_2$. They fulfil [11] the following inequality:

$$(3.2) \quad [M/M]_2 \leq [M + 1/M + 1]_2 \leq f(z)$$

for $z \geq 0$ and natural M . As a consequence of (3.2), the larger is M , the better is the bound for $f(z)$.

Using the algorithm mentioned in the previous section one can obtain λ_{ef} as a power series of $h - 1$. On the other hand, the asymptotic formula given in [4] makes it possible to find the first two coefficients of the asymptotic expansion of λ_{ef} with the argument $1/h$. Using merely the two first terms of the series one may replace the argument $1/h$ in the asymptotic expansion by $1/(h - 1)$. The extra terms introduced by this replacement of arguments, being of the order $O(h^{-2})$, are omitted in the given approximation. For the given approximants of both series of arguments $h - 1$ and $1/(h - 1)$ one can obtain the Padé approximants using for example the algorithm *QD*, described in [8]. Such a method, used in [3], has yet a certain deficiency. It has the same fault as the asymptotic formula in [4] – it does not agree with the Keller symmetry (1.1): it is valid for $h \rightarrow \infty$ but not for $h \rightarrow 0$. To make use of the Keller symmetry, let us introduce a new argument α instead of h

$$(3.3) \quad \alpha = \frac{1 - h}{1 + h}$$

and new functions β_c and β_d , instead of λ_{ef}

$$(3.4) \quad \beta_c = \alpha \varphi \frac{1 + \lambda_{ef}/\lambda_c}{1 - \lambda_{ef}/\lambda_d},$$

$$\beta_d = \alpha(1 - \varphi) \frac{(1 + \alpha)\lambda_{ef}/\lambda_c + (1 - \alpha)}{(1 + \alpha)\lambda_{ef}/\lambda_c - (1 - \alpha)}.$$

Solving (3.4) with respect to λ_{ef}/λ_c and λ_{ef}/λ_d we obtain

$$(3.5) \quad \begin{aligned} \frac{\lambda_{ef}}{\lambda_c} &= 1 - \frac{2\alpha\varphi}{1 + \alpha\varphi + \beta_c}, \\ \frac{\lambda_{ef}}{\lambda_d} &= 1 + \frac{2\alpha(1 - \varphi)}{1 - \alpha(1 - \varphi) + \beta_d}. \end{aligned}$$

For β_c and β_d equal to 0 the formulae (3.5) transform to the Maxwell-Garnett formula, independent of the geometrical structure of the composite. The whole information about geometrical structure of the composite is comprised in β_c or β_d . It follows from (3.5) that the lower bound of β_c and β_d give the lower and upper bounds of λ_{ef} , respectively. Using (1.1) and (3.4) one may easily check that $\beta_i(\alpha) = \beta_i(-\alpha)$ for $i = c, d$ as a consequence of the Keller symmetry; therefore $\beta_i = \beta_i(\alpha^2)$. For $1/h \ll \sqrt{1 - 4\varphi/\pi} \ll 1$ the asymptotic expression of λ_{ef} from [4] simplifies to the form:

$$(3.6) \quad \left(\frac{\lambda_{ef}}{\lambda_c}\right)^{as} = 1 + q_0 + \frac{q_1}{h} + O(h^{-2}),$$

where

$$(3.7) \quad \begin{aligned} q_0 &= \pi(\sigma - 1), \\ q_1 &= -2\pi\sigma(\sigma - 1)\ln\sigma, \\ \sigma &= \frac{1}{\sqrt{1 - \frac{4\varphi}{\pi}}}. \end{aligned}$$

Inserting (3.6) to (3.4) one finds the asymptotic expressions for β_c and β_d :

$$(3.8) \quad \begin{aligned} \beta_c^{as} &= c_{c0} + \frac{c_{c1}}{h} + O(h^{-2}), \\ \beta_d^{as} &= c_{d0} + \frac{c_{d1}}{h} + O(h^{-2}), \end{aligned}$$

where

$$(3.9) \quad \begin{aligned} c_{c0} &= \frac{2\varphi}{\pi} \left(\frac{\pi}{2} + \frac{1}{\sigma - 1} \right), & c_{d0} &= -\varphi, \\ c_{cd} &= \frac{4\varphi}{\pi} \left(\frac{\sigma \ln \sigma - 1}{\sigma - 1} - \frac{\pi}{2} \right), & c_{d1} &= 2\pi(1 - \varphi)(\sigma - 1). \end{aligned}$$

The formulae (3.8) are valid for $h \rightarrow \infty$ what corresponds to $\alpha \rightarrow -1$, and do not fulfil the Keller symmetry. To transform (3.8) to the symmetric form let us note that for $h \rightarrow \infty$ the following relation $1 - \alpha^2 = 4/h + O(h^{-2})$ results from (3.3). Using this relation one can transform the asymptotic formula (3.8) to the symmetrical form (3.10):

$$(3.10) \quad \begin{aligned} \beta_c^{as} &= c_{c0} + \frac{1}{4}c_{c1}(1 - \alpha^2) + O\left((1 - \alpha^2)^2\right), \\ \beta_d^{as} &= c_{d0} + \frac{1}{4}c_{d1}(1 - \alpha^2) + O\left((1 - \alpha^2)^2\right). \end{aligned}$$

Eqs. (3.10) give the first two terms of the asymptotic power series of the argument $1 - \alpha^2$. They give correct asymptotic result for $h \rightarrow \infty$ and for $h \rightarrow 0$: in both cases $\alpha^2 \rightarrow 1$. For $h \rightarrow \infty$, Eqs. (3.8) and (3.10) differ by the terms $O(h^{-2})$. Upon inserting the asymptotic expressions (3.10) to (3.6) we obtain the asymptotic expression for the effective heat transfer coefficient, valid for both $h \rightarrow \infty$ and $h \rightarrow 0$ (more exactly: for $h(1 - 4\varphi/\pi)^{1/2} \rightarrow \infty$ and $h(1 - 4\varphi/\pi)^{1/2} \rightarrow 0$ because of the limited region of applicability of the asymptotic formula (3.6)). The argument α^2 has a certain disadvantage because the functions $\beta_c(\alpha^2)$ and $\beta_d(\alpha^2)$ are not the Stieltjes functions – their poles corresponding to $h < -1$ are now located on the positive semi-axis $\alpha^2 > 1$ – while the formula (3.2) for the two-point Padé approximants is valid for the Stieltjes functions. To obtain β_c and β_d as Stieltjes functions, let us introduce a new argument t

$$(3.11) \quad t = h + \frac{1}{h} - 2 = \frac{4\alpha^2}{1 - \alpha^2},$$

hence

$$(3.12) \quad \alpha^2 = 1 - \frac{1}{1 - t/4}.$$

The negative values of t correspond to $h < 1$. Expressing α as a function of t and inserting it into (3.10) one obtains the following formulae for $\beta_c(\alpha^2)$ and $\beta_d(\alpha^2)$:

$$(3.13) \quad \begin{aligned} \beta_c^{as} &= c_{c0} + \frac{c_{c1}}{t} + O(t^{-2}), \\ \beta_d^{as} &= c_{d0} + \frac{c_{d1}}{t} + O(t^{-2}). \end{aligned}$$

To obtain the power expansion of β_c and β_d at $t = 0$, let us remark that

$$(3.14) \quad h - 1 = -\frac{2\alpha}{1 + \alpha},$$

as it follows from (3.3). Expanding the right-hand side of (3.14) into the power series and inserting it into (2.4) one obtains λ_{ef}/λ_c as a power series of α . Upon inserting this power series into (3.4) one finds β_c and β_d as power series of α . As a consequence of the Keller symmetry, the coefficients of the odd powers of α in the series are equal to 0. Now using (3.12) and expanding α^2 into the power series of t , we obtain β_c and β_d as a power series of t

$$(3.15) \quad \begin{aligned} \beta_c &= a_0 + a_1 t + a_2 t^2 + \dots \\ \beta_d &= b_0 + b_1 t + b_2 t^2 + \dots \end{aligned}$$

Taking as the departure point the power series (3.15) and using the algorithm *FG* given in [8], we obtain the two-point Padé approximants $[M/M]_2$ (see (2.1)) of β_c and β_d . Because we take into account the even number of terms of the asymptotic development (3.13) (namely two), the Padé approximants give accordingly to (3.2) lower bounds of β_c and β_d . Inserting these bounds to (3.5) we obtain upper and lower bounds for λ_{ef} , respectively.

4. Numerical results

Numerical calculations were performed for nearly touching cylinders corresponding to $\varphi \geq 0.785$. For smaller φ the one-point Padé approximants and the continued fractions give satisfactory results. The region of φ for which the two-point Padé approximants give good results is determined by the region in which the asymptotic formula (3.6) is valid (i.e. for $\varphi_{\max} - \varphi \ll 1$). There is yet another restraint: in the series (3.6) we consider two first terms only – it is difficult to make this formula symmetric while using more terms (and it is doubtful whether the further terms in the asymptotic expansion are correct). Therefore, although we consider the values of φ near φ_{\max} in some sense, there is no possibility of the limit transition $\varphi \rightarrow \varphi_{\max}$ because all derivatives of λ_{ef}/λ_c with respect to h tend to infinity for $h \rightarrow \infty$ and $\varphi \rightarrow \varphi_{\max}$, and the formula based on a finite number of derivatives can not be a good approximant for φ too near to φ_{\max} . The asymptotic values of lower and upper bounds of λ_{ef} for $h \rightarrow \infty$ and $\varphi < \varphi_{\max}$ are always correct and equal one to another – it follows from the nature of the method. For φ very near to φ_{\max} , there appears however an intermediate region of large h in which the lower and upper bounds may considerably differ, and their difference tends to infinity while $\varphi \rightarrow \varphi_{\max}$ ($\varphi_{\max} = 0.785398163\dots$). On the other hand, if φ is too small the method becomes unstable. Both these constraints determine the limits within which the method is useful. The situation is analogous to that in [3] but in our case the bounds for λ_{ef} are better.

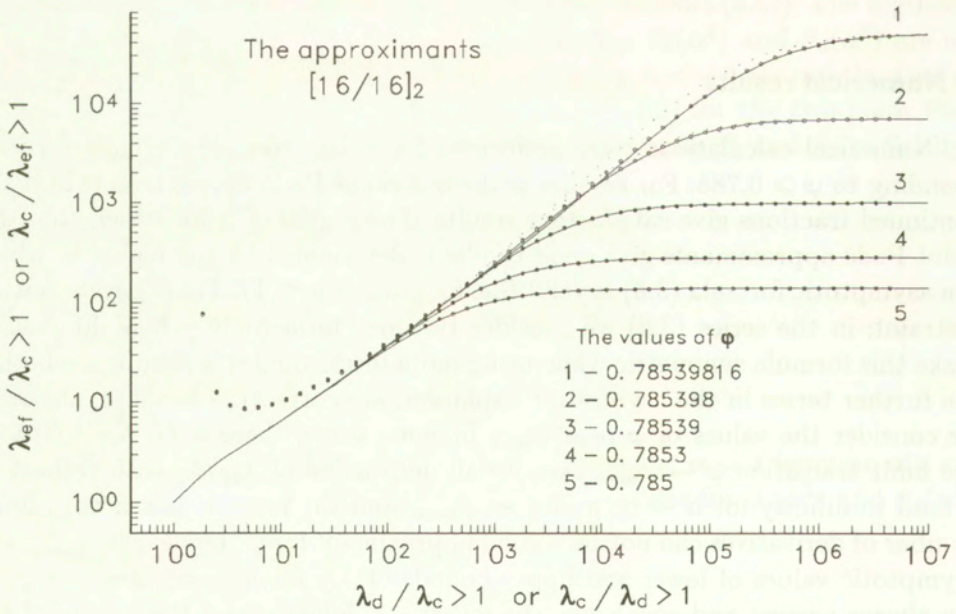
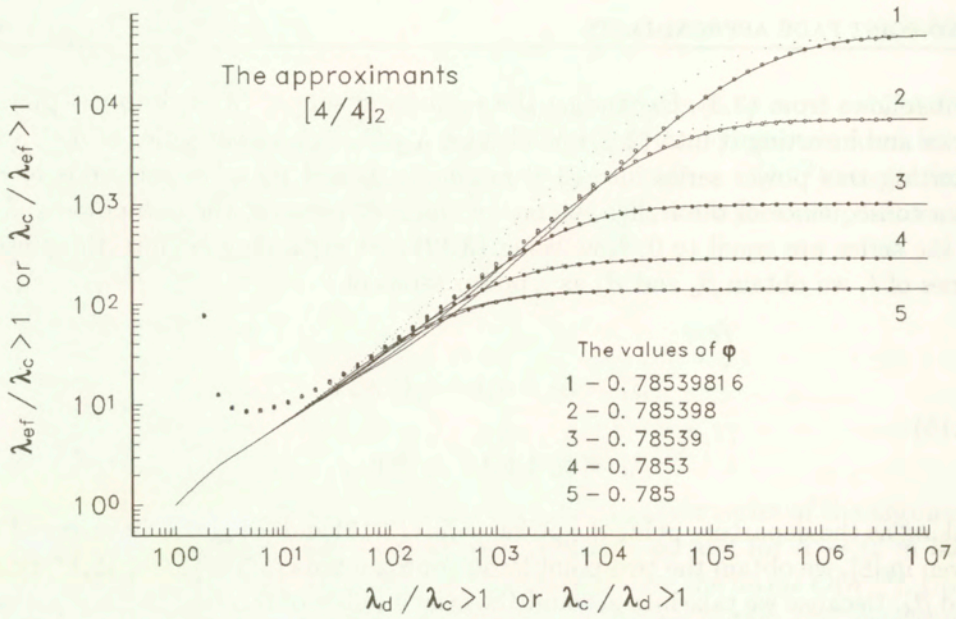


FIG. 1. The upper (dotted lines) and lower (solid lines) bounds to the effective heat transfer coefficient for the square array of nearly touching cylinders obtained from the two-point Padé approximants $[4/4]_2$ and $[16/16]_2$. For comparison, the asymptotic results (MCPHEDRAN *et al.* [6]) are shown by small solid squares.

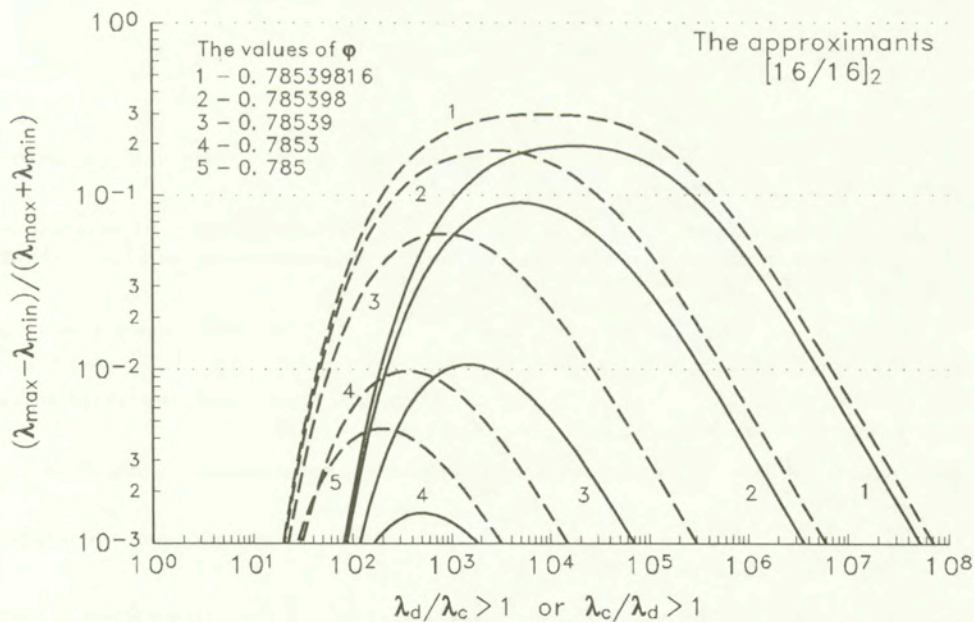
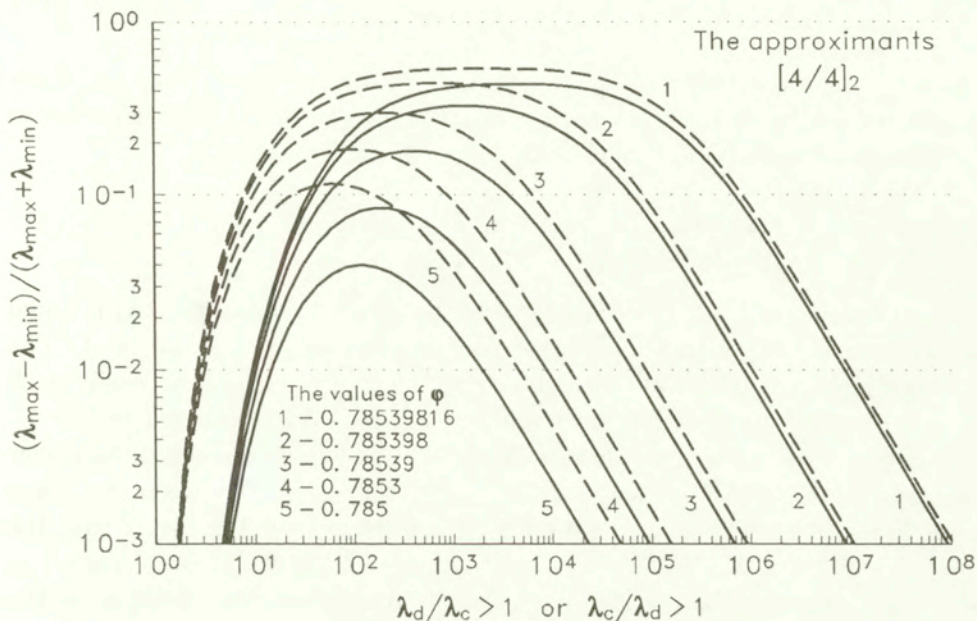


FIG. 2. The relative differences between the upper and lower bounds from Fig. 1 (solid lines) as compared with the corresponding results calculated without using the Keller symmetry [3] (dashed lines).

In the Fig. 1 the lower and upper bounds of λ_{ef} obtained from the Padé approximants $[4/4]_2$ and $[16/16]_2$ are shown. It follows from the Keller symmetry (1.1) that in the right-hand side of both equalities (4.1)

$$(4.1) \quad \frac{\lambda_{ef}}{\lambda_c} = f\left(\frac{\lambda_d}{\lambda_c}\right), \quad \frac{\lambda_c}{\lambda_{ef}} = f\left(\frac{\lambda_c}{\lambda_d}\right)$$

appears the same function f . Because one of the ratios λ_d/λ_c and λ_c/λ_d is equal or larger than 1, the values less than 1 are not shown in the plot of f . The asymptotic values from [4] are also shown in the figure. It may be easily seen that the lower bounds are much more precise than the upper bounds (for $h > 1$).

To compare the presented results with those of [3], which disregard the Keller symmetry, the relative difference $(\lambda_{\max} - \lambda_{\min})/(\lambda_{\max} + \lambda_{\min})$ between the upper and the lower bounds is shown in the Fig. 2. It is seen from the Fig. 2 that the discrepancy between the lower and upper bounds is largest in some region of large h , and increases with φ . Of course, this discrepancy is much smaller for the $[16/16]_2$ approximants than for $[4/4]_2$. The comparison of our results with those from [3] shows that our bounds are more accurate. For the values of h not very large, the difference may be even of one order of magnitude or more.

References

1. J.B. RAYLEIGH, *On the influence of obstacles arranged in rectangular order on the properties of the medium*, Phil. Mag., ser. 5, **34**, 481–502, 1892.
2. S. MAY, S. TOKARZEWSKI, A. ZACHARA, B. CICHOCKI, *Continued fraction representation for the effective thermal conductivity of a regular two component composite*, Int. J. Heat and Mass Transfer, **37**, 2165–2173, 1994.
3. S. TOKARZEWSKI, J. BŁAWZDZIEWICZ, I.V. ANDRIANOV, *Effective conductivity of densely packed conducting cylinders*, Appl. Phys., **A**, 601–604, 1994.
4. R.C. MCPHEDRAN, L. POLADIAN, G.W. MILTON, *Asymptotic studies of closely spaced highly conducting cylinders*, Proc. R. Soc. London, **A 415**, 185–196, 1988.
5. J.W. KELLER, *A theorem on the conductivity of a composite medium*, J.Math. Phys., **5**, 448–449, 1994.
6. S. TOKARZEWSKI, J. BŁAWZDZIEWICZ, I.V. ANDRIANOV, *Two-point Padé approximants for Stieltjes series*, IFTR Reports, 30/993.
7. S. MAY, S. TOKARZEWSKI, A. ZACHARA, B. CICHOCKI, *The effective conductivity of two-component composite of a regular two-dimensional structure [in Polish]*, IFTR Reports, 24/192.
8. W.B. JONES, W.J. THRON, *Continued fractions, analytic theory and applications*, Addison-Wesley, 1980.
9. S. MAY, S. TOKARZEWSKI, A. ZACHARA, *The Wigner potential method in the investigation of thermal properties of regular composites*, Arch. Mech., **48**, 2, 429–442, 1996.

10. K.E. CLARC and G.W. MILTON, *Optimal bounds correlating electric, magnetic and thermal properties of two-phase, two-dimensional composites.*, Proc. Roy. Soc., London A **448**, 61–190, 1995.
11. S. TOKARZEWSKI and J.J. TELEGA, *Inequalities for two-point Padé approximants to the expansions of Stieltjes functions in real domain.*, Acta Applicanda Mathematicae, **48**, 285–297, 1997.

Received September 14, 1998; new version December 18, 1998

Influence of finite deformations on the growth mechanism of microvoids contained in structural metals

W. DORNOWSKI

*Military University of Technology
Kaliskiego 2, 01-489 Warszawa, Poland*

IN THIS PAPER an analysis of the growth mechanism of the single microvoid for finite deformations is presented. A hollow sphere model is assumed. Such a model has been considered in many previous papers, however on the assumption that the strains remain small. The material surrounding the microvoid is assumed to be work-hardening, viscoplastic, described by the constitutive equations formulated by PERZYNA [1]. Quantitative and qualitative distinctions between the presented solution and geometrically linear solution are discussed. On the basis of the obtained solution, constitutive functions of a certain damage evolution equation for the complex stress state have been identified. A numerical example of the fracture analysis for a structural element is presented.

1. Introduction

PHENOMENA such as nucleation, growth and coalescence of microvoids play a very important role in the ductile fracture process of structural metals. Domains of localized strains determine the places of void nucleation. In these domains, the voids generally nucleate by decohesion of second phase particles or by transgranular and intergranular cracking. The localized plastic deformation controls the growth and coalescence processes (neck, shear band).

Micromechanics analysis of void nucleation and coalescence, as well as of void growth, establishes the basis of constitutive modeling for porous plastic solids. Such relations play an important role in the theoretical description and in numerical analysis of the deformation and fracture processes for structural elements. Prediction of ductile fracture behavior requires the knowledge of the relation between the growth of a void and the imposed stress and strain histories.

MCCCLINTOCK'S [2] analysis of the expansion of a long cylindrical hole in an ideally plastic solid marks the beginning of the recently appearing, extensive literature on the micromechanics of ductile fracture. Moreover, this paper showed that a precise mechanics analysis of a carefully chosen continuum model could help us to quantify the complex microstructural behavior. The imposed axial strain rate and the transverse stress were considered. The linearized geometri-

cal relations were assumed. McClintock's exact solution exhibits an exponential increase in the void growth rate with positive transverse stress.

RICE and TRACEY [3] analyzed the growth of an isolated spherical void surrounded by an ideally plastic matrix. This void was subjected to a general stress state. The approximate solution has been obtained by using the Rayleigh-Ritz method. The influence of viscoplastic properties of the matrix on the growth of a spherical void has been analyzed in [4]. For the limiting case (rigid-ideally plastic solid) the solution presented in [4] reduces to the solution obtained in [3]. Finite element results for the growth of an isolated spherical void in an ideally plastic solid have been obtained in paper [5]. The model of a single void immersed in the infinite material space is a characteristic mark of the void growth analysis reported in papers [2 – 5]. This approach does not take into account the void interaction effects.

A different approach taking into account void interaction effects has been presented by CAROLL and HOLT [6]. In their paper, the description of the growth mechanism has been obtained by an analysis of the collapse of a hollow sphere made of incompressible elastic-plastic material. JOHNSON [7] has analyzed the same hollow sphere model problem. The viscoplastic effects have been taken into account. Other generalizations allowed for the work-hardening effects. The void growth process for a linear, work-hardening viscoplastic material has been analyzed by PERZYNA [8]. In Perzyna's model, EFTIS and NEMES [9] have assumed the non-linear work-hardening rule. The influence of thermal effects on the growth mechanism for the discussed model has been investigated in [10].

In all papers quoted above the void growth analysis was based on the simplifying assumption that the strains in the material surrounding an isolated void remain small. In this paper we give up this assumption and consider the finite deformation of the matrix material. Such conditions can be realized in many technological problems of structural metals.

Section 2 is focused on an analysis of the growth mechanism of a single void for finite strains. The model of the hollow sphere proposed in [6] and [7] is assumed. It has been assumed that the matrix material is described by Perzyna's viscoplastic law and by the non-linear work-hardening rule. Quantitative and qualitative distinctions between the presented solution and the geometrically linearized solution [9] are discussed. In Section 3 the damage evolution equation for the complex state of stress [11] is discussed. A numerical example of fracture analysis for the structural element is presented in Section 4. The last section brings final conclusions and comments.

2. The growth mechanism of the isolated spherical void for finite deformations

We consider a rectangular volume element containing a representative distribution of voids as shown in Fig. 1. Let us assume a uniform hydrostatic tension \bar{p} acting over the surface of this element [7].

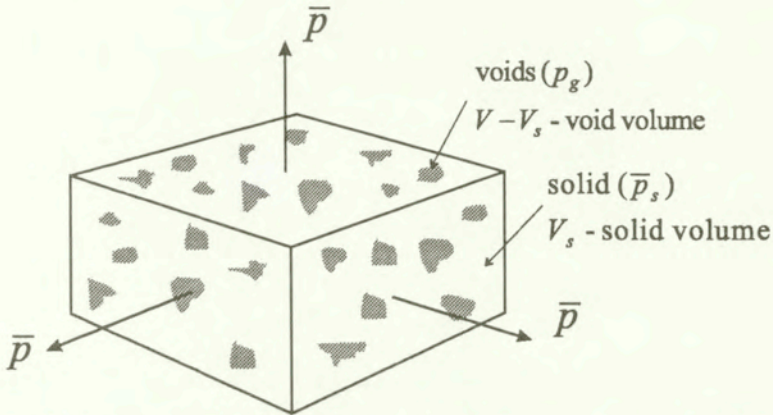


FIG. 1. Material element containing voids: \bar{p} is the average mean stress acting over the element face, p_g is the gas pressure in the voids, \bar{p}_s is the average mean stress in the solid material.

The equilibrium of forces acting on the cross-sectional area A occupied by the voids is expressed by the following equation [7]:

$$(2.1) \quad A_s \bar{p}_s + (A - A_s) p_g = A \bar{p},$$

where \bar{p}_s is the mean stress (spatial average) in the solid material which acts on the average area A_s on the plane of total area A , and p_g is the internal gas pressure (for reactive media). For a random distribution of hole shapes and sizes $A_s/A = V_s/V$, and we obtain that the mean stress in the solid constituent is

$$(2.2) \quad \bar{p}_s = \frac{1}{1 - \xi} \bar{p} - \frac{\xi}{1 - \xi} p_g,$$

where

$$(2.3) \quad \xi = \frac{V - V_s}{V}$$

is the porosity parameter describing the ratio of the voids volume to the volume of the aggregate.

A simplified model of the porous element is now assumed. Let us consider a single spherical void of initial radius a_0 in a sphere of initial radius b_0 . In the

actual configuration, the void is subjected to internal pressure p_g and external stress \bar{p}_s (Fig. 2.)

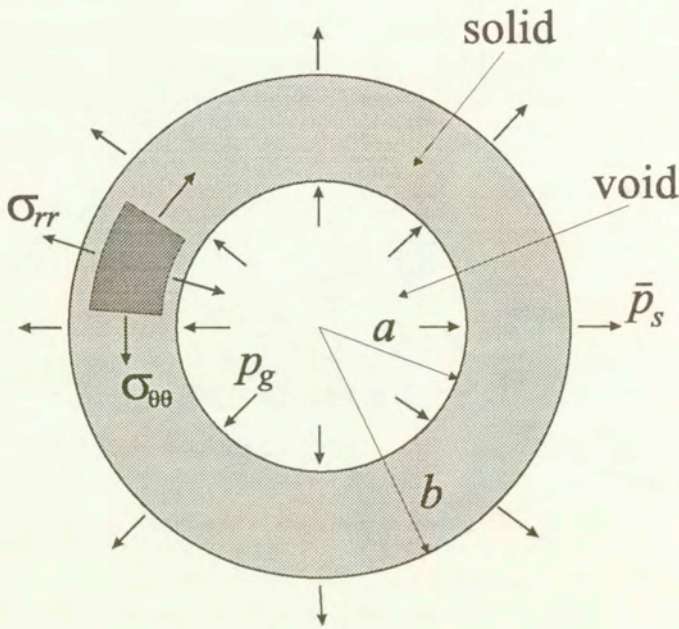


FIG. 2. Porous material model.

For these assumptions the porosity parameters, namely the initial and actual ones, are determined by relations

$$(2.4) \quad \xi_0 = \frac{a_0^3}{b_0^3}, \quad \xi = \frac{a^3}{b^3}.$$

We carry out the analysis of the spherical void growth in the Eulerian polar coordinate system $\{r, \theta, \varphi\}$. The Lagrangian coordinates of the material point are denoted by $\{R, \Theta, \Phi\}$, and the corresponding Eulerian coordinates are as follows:

$$(2.5) \quad r = [R^3 + C(t)]^{1/3}, \quad \theta = \Theta, \quad \varphi = \Phi.$$

The first of the above functions of motion results from the assumption that the volume of the surrounding material has to be preserved. The integration function $C(t)$ depends only on time. The remaining functions of motion determine the conditions of spherical symmetry. Differentiating the functions (2.5) with respect to time we obtain the velocity field

$$(2.6) \quad \dot{r} = \frac{1}{3r^2} \dot{C}(t), \quad \dot{\theta} = \dot{\varphi} = 0.$$

The spatial velocity gradient is represented by the matrix

$$(2.7) \quad \text{grad } \mathbf{v} = \begin{bmatrix} -\frac{2}{3r^3} & 0 & 0 \\ 0 & \frac{1}{3r^3} & 0 \\ 0 & 0 & \frac{1}{3r^3} \end{bmatrix} \dot{C}(t).$$

This matrix is symmetrical. Thus, the rotational speed of the material particle vanishes. The deformation rate tensor is equal to the spatial velocity gradient, $\mathbf{d} = \text{grad } \mathbf{v}$. Moreover, the incompressibility condition is satisfied, $\text{tr } \mathbf{d} = \text{tr}(\text{grad } \mathbf{v}) = 0$. The equivalent rate of deformation and equivalent deformation are as follows:

$$(2.8) \quad \dot{\bar{\epsilon}} = \left[\frac{2}{3}(\mathbf{d} : \mathbf{d}) \right]^{1/2} = \frac{2}{3r^3} \dot{C}(t), \quad \bar{\epsilon} = \int_0^t \dot{\bar{\epsilon}} dt = \frac{2}{3} \ln \frac{r^3}{r^3 - C(t)}.$$

The equation of motion described by physical components of the Cauchy stress tensor has the form

$$(2.9) \quad \rho \ddot{r} = \frac{\partial \sigma}{\partial r} + \frac{2}{r} (\sigma_{rr} - \sigma_{\theta\theta}),$$

where ρ is the solid density. Our analysis will be restricted to the case where inertial effects are neglected, i.e. $\rho \ddot{r} = 0$. Equation (2.9) is then integrated from a to b with boundary conditions $\sigma_{rr}(a, t) = p_g$ and $\sigma_{rr}(b, t) = \bar{p}_s$, to give

$$(2.10) \quad \bar{p}_s - p_g = -2 \int_a^b \frac{\Delta S}{r} dr, \quad \Delta S = \sigma_{rr} - \sigma_{\theta\theta}.$$

The rate-dependent matrix material characterized by linear overstress function and nonlinear hardening is assumed. In this case the yield condition is given by the following relation [8]:

$$(2.11) \quad \sqrt{3J_2'} = \sigma^* \left[1 + \Phi^{-1} \left(\frac{\dot{\bar{\epsilon}}}{\gamma_0} \right) \right],$$

where

$$(2.12) \quad \sigma^* = \sigma_s - (\sigma_s - \sigma_0) \exp(-\delta \bar{\epsilon}),$$

is the plastic strain-dependent yield stress due to the work-hardening effects [9]. In Eq. (2.12) σ_0 and σ_s denote the yield and saturation stress of the matrix material, γ_0 is the viscosity constant. We shall apply the linearized form of the relations (2.10) and (2.11), namely

$$(2.13) \quad \sigma_{\theta\theta} - \sigma_{rr} = -\Delta S = \sigma_s - (\sigma_s - \sigma_0) \exp(-\delta\bar{\varepsilon}) + \frac{\sigma_s \dot{\bar{\varepsilon}}}{\gamma_0}.$$

The integral of the above expressions has the form

$$(2.14) \quad \int_a^b \frac{-\Delta S}{r} dr = \sigma_s C_1 - (\sigma_s - \sigma_0) C_2 + \frac{\sigma_s}{\gamma_0} C_3,$$

where

$$(2.15) \quad C_1 = \int_a^b \frac{dr}{r} = \frac{1}{3} \ln \frac{1}{\xi}, \quad C_3 = \int_a^b \frac{\dot{\bar{\varepsilon}}}{r} dr = \frac{2}{9} \frac{\dot{\bar{\varepsilon}}}{\xi}.$$

The integral

$$(2.16) \quad C_2 = \int_a^b \frac{e^{-\delta\bar{\varepsilon}}}{r} dr = \int_a^b e^{-\frac{2}{3}\delta \ln \frac{r^3}{r^3 - C(t)}} \frac{dr}{r}$$

has a non-elementary form, therefore we have to find its approximate value. We make the following change of variables in the expression (2.16):

$$(2.17) \quad x = 1 - \frac{C(t)}{r^3} \Rightarrow x_1 = 1 - \frac{C(t)}{a^3}, \quad x_2 = 1 - \frac{C(t)}{b^3} \quad \text{and} \quad 0 < x_1 < x_2 < 1.$$

Thus the integral C_2 can be rewritten as follows:

$$(2.18) \quad C_2 = \frac{1}{3} \int_{x_1}^{x_2} \frac{x^{\frac{2}{3}\delta}}{1-x} dx.$$

The functions $f_1(x) = \frac{1}{1-x}$ and $f_2(x) = x^{\frac{2}{3}\delta}$ are continuous, bounded and integrable for all points from the interval $[x_1, x_2]$. Therefore, the mean value theorem for integrals gives

$$(2.19) \quad C_2 = \frac{1}{3} y^{\frac{2}{3}\delta} \int_{x_1}^{x_2} \frac{1}{1-x} dx = \frac{1}{3} \ln \frac{1}{\xi} y^{\frac{2}{3}\delta} = h(y) \quad \text{for } y \in [x_1, x_2].$$

The function $h(y)$ is continuous and monotonic over the interval $[x_1, x_2]$ and it has the upper and lower bound values at the end points of this interval. Thus we have

$$(2.20) \quad \frac{1}{3} \ln \frac{1}{\xi} x_1^{\frac{2}{3}\delta} \leq h(y) \leq \frac{1}{3} \ln \frac{1}{\xi} x_2^{\frac{2}{3}\delta}.$$

The function $h(y)$ can be approximated by the mean value of the upper and lower bound values

$$(2.21) \quad h(y) \cong \frac{1}{6} \ln \frac{1}{\xi} \left(x_1^{\frac{2}{3}\delta} + x_2^{\frac{2}{3}\delta} \right) = \frac{1}{6} \ln \frac{1}{\xi} F(\xi, \xi_0),$$

where

$$(2.22) \quad F(\xi, \xi_0) = \left(\frac{\xi_0}{1 - \xi_0} \frac{1 - \xi}{\xi} \right)^{\frac{2}{3}\delta} + \left(\frac{1 - \xi}{1 - \xi_0} \right)^{\frac{2}{3}\delta}.$$

Finally, we obtain

$$(2.23) \quad C_2 = \frac{1}{6} \ln \frac{1}{\xi} F(\xi, \xi_0).$$

Substitution of the determined integrals and Eq. (2.2) into Eq. (2.10) gives the evolution equation for the porosity parameter in the following form:

$$(2.24) \quad \dot{\xi} = \frac{9}{4} \frac{\gamma_0}{\sigma_s} \frac{\xi}{1 - \xi} \left\{ \bar{p} - p_g - \frac{1}{3} (1 - \xi) \ln \frac{1}{\xi} [2\sigma_s - (\sigma_s - \sigma_0) F(\xi_0, \xi)] \right\}.$$

The equilibrium state is reached at $\dot{\xi} = 0$, thus

$$(2.25) \quad p_{eq} = p_g + \frac{1}{3} (1 - \xi) \ln \frac{1}{\xi} [2\sigma_s - (\sigma_s - \sigma_0) F(\xi_0, \xi)].$$

The relation of Eq. (2.25) shows a direct influence of the work-hardening effects on the value of the equilibrium pressure $p_{eq}(\xi)$ for particular porosity ξ .

For infinitesimal strains of the surrounding material, the strain-displacement relations may be written as follows [7]:

$$(2.26) \quad e_{rr} = \frac{\partial u}{\partial r}, \quad e_{\varphi\varphi} = e_{\theta\theta} = \frac{u}{r},$$

where

$$(2.27) \quad u = r - R = r - [r^3 - C(t)]^{1/3}$$

is the radial displacement. The infinitesimal equivalent strain and its rate are given by the expressions

$$(2.28) \quad \bar{\varepsilon} = \frac{2}{3} \left(\frac{\partial u}{\partial r} - \frac{u}{r} \right) = \frac{2}{3} \left\{ \left[1 - \frac{C(t)}{r^3} \right]^{1/3} - \left[1 - \frac{C(t)}{r^3} \right]^{-2/3} \right\},$$

$$\dot{\bar{\varepsilon}} = -\frac{2}{3} \frac{\dot{C}(t)}{r^3} \left\{ \frac{1}{3} \left[1 - \frac{C(t)}{r^3} \right]^{1/3} + \frac{2}{3} \left[1 - \frac{C(t)}{r^3} \right]^{-2/3} \right\}.$$

In this case, the derivation of an evolution equation for the porosity parameter is similar to the previous one. Thus, without going into details, we present the final result

$$(2.29) \quad \dot{\xi} = \frac{9}{4} \frac{\gamma_0}{\sigma_s \bar{F}_1(\xi_0, \xi)} \frac{\xi}{1 - \xi} \left\{ \bar{p} - p_g - \frac{1}{3}(1 - \xi) \ln \frac{1}{\xi} [2\sigma_s - (\sigma_s - \sigma_0) \bar{F}(\xi_0, \xi)] \right\}$$

where

$$(2.30) \quad \bar{F}(\xi_0, \xi) = \exp \left\{ \frac{2}{3} \delta \frac{\xi_0 - \xi}{\xi(1 - \xi_0)} \left[\frac{\xi_0(1 - \xi)}{\xi(1 - \xi_0)} \right]^{-2/3} \right\} + \exp \left[\frac{2}{3} \delta \frac{\xi_0 - \xi}{1 - \xi_0} \left(\frac{1 - \xi}{1 - \xi_0} \right)^{-2/3} \right],$$

$$\bar{F}_1(\xi_0, \xi) = \frac{1}{4} \frac{\xi}{\xi - \xi_0} \left(\frac{1 - \xi}{1 - \xi_0} \right)^{-2/3} \left\{ \frac{1 - \xi}{1 - \xi_0} \left[1 - \left(\frac{\xi_0}{\xi} \right)^{4/3} \right] + 8 \left[1 - \left(\frac{\xi_0}{\xi} \right)^{1/3} \right] \right\}.$$

It can be easily seen that the expressions (2.29) and (2.30) have a more complex structure than those obtained for finite deformation. Furthermore, the function $\bar{F}_1(\xi_0, \xi)$ has a singular point for the initial instant of the growth process ($\xi = \xi_0$). This property demands some additional activities in the numerical integration of the evolution equation (2.29). The proposed function (2.22) has no singular points. The comparison of the described solutions is shown in Figs. 3 and 4. Line 1 denotes the presented solution and line 2 denotes the geometrically linear solution [9]. The following material constants are assumed in numerical calculations:

$$\bar{p} = 800 \text{ MPa}, \quad p_g = 0, \quad \gamma_0 = 100 \text{ s}^{-1}, \quad \sigma_s = 350 \text{ MPa}, \\ \sigma_0 = 40 \text{ MPa}, \quad \delta = 5, \quad \xi_0 = 0.001.$$

The curves in Fig. 3 illustrate the dependence of the equilibrium pressure p_{eq} on the porosity parameter ξ . The character of the analyzed quantity is the same for both discussed solutions. In the first phase of the void growth, the equilibrium pressure increases steadily to reach a maximal value, after that it decreases. Small quantitative differences occur at the maximum of p_{eq} . For a geometrically linearized solution the maximum of p_{eq} is greater than the corresponding value for the solution obtained.

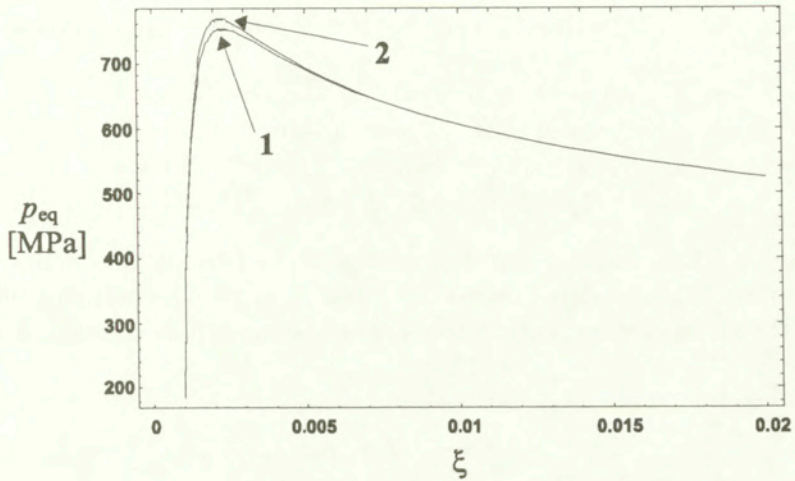


FIG. 3. Dependence of the equilibrium pressure p_{eq} on the porosity parameter ξ : line 1 – proposed solution, line 2 – geometrically linearized solution.

The evolution of the porosity is presented in Fig. 4. For this quantity the differences between the considered solutions are significant. For majority of metals, the loss of local carrying capacity is observed at $\xi \cong 0.3$. In the case of geometrically linear solution (line 2) this value is reached in double time. This result is of great importance to the estimation of the fracture time for structural elements loaded monotonically.

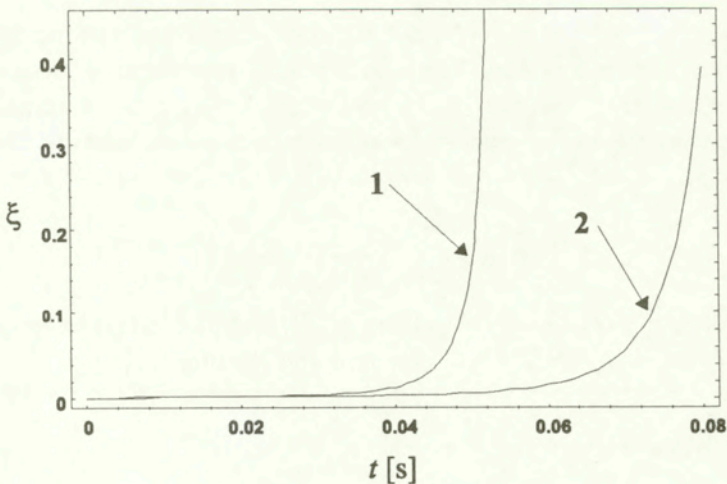


FIG. 4. Evolution of the porosity parameter ξ : line 1 – proposed solution, line 2 – geometrically linearized solution.

3. The microvoids growth equation for the complex state of stress

In the paper [11] the intensity invariant for the growth process in the complex state of stress was postulated in the following form:

$$(3.1) \quad I_g = b_1 J_1 + b_2 \sqrt{J'_2} + b_3 (J'_3)^{1/3},$$

where b_i ($i = 1, 2, 3$) are the material constants, and by J_1 we denote the first invariant of the Cauchy stress tensor σ , J'_2 and J'_3 are the second and third invariants of the stress deviator, respectively. For the growth mechanism we assume [11]

$$(3.2) \quad \dot{\xi}_{\text{grow}} = \frac{g^*(\xi)}{T_m \sqrt{\sigma_0}} [I_g - \sigma_{\text{eq}}(\xi, \bar{\varepsilon}^p)],$$

where $T_m \sqrt{\sigma_0}$ denotes the dynamic viscosity of the material, $g^*(\xi)$ represents the void growth material function and allows for void interaction, and $\sigma_{\text{eq}}(\xi, \bar{\varepsilon}^p)$ is the porosity and equivalent plastic strain-depend void growth threshold stress.

Comparison of Eq. (2.24) and (3.2) shows that

$$(3.3) \quad g^*(\xi) = c_1 \frac{\sqrt{\sigma_0}}{\sigma_s} \frac{\xi}{1 - \xi},$$

$$\sigma_{\text{eq}}(\xi, \bar{\varepsilon}^p) = c_2 (1 - \xi) \ln \frac{1}{\xi} [2\sigma_s - (\sigma_s - \sigma_0) F(\xi_0, \xi)].$$

The material constant c_1 controls the rate of growth and the material constant c_2 determines the level of the threshold stress. The constants σ_0 and σ_s denote the yield and saturation stress of the matrix material. The assumption that the growth process runs in domains of inelastic deformations leads to the particular relation

$$(3.4) \quad c_2 \geq \frac{1}{2(1 - \xi_0) \ln(1/\xi_0)}.$$

The evolution equation in the form (3.2) was also advantageous in certain problems of the plastic flow for cyclic dynamic loading [12].

4. Numerical example

The main objective of this example is the illustration of the fracture process in inelastic materials during dynamic loading. This kind of fracture can occur as a result of the shear-band localization generally attributed to a plastic instability

implied by microdamage softening during dynamic plastic flow process. In the dynamical initial-boundary value problem, the stress and deformation due to wave reflections and interactions are not uniformly distributed, and this kind of heterogeneity can lead to strain localization in the absence of geometrical or material irregularities [14].

The subject of the fracture numerical analysis is a thin rectangular steel plate, Fig. 5a.

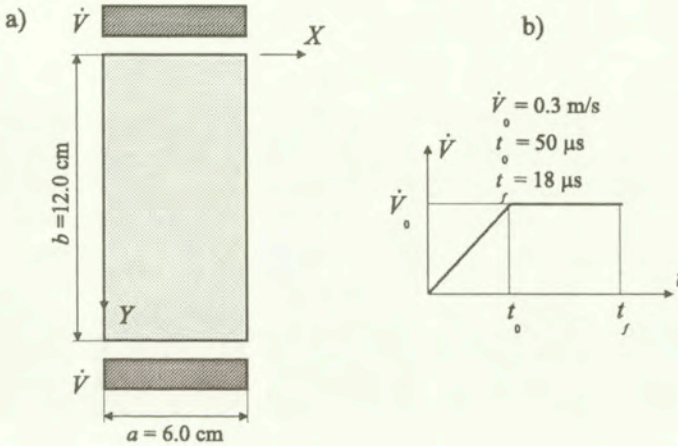


FIG. 5. Dimensions of the plate and variation in time of the kinematic constraints.

The shorter edges of the plate have been subjected to the tensile kinematic constraints, Fig. 5b. The rate-dependent material was assumed, and the effect of the plastic work-hardening was omitted. The porosity evolution has been described by Eq. (3.2) in which the proposed function $F(\xi, \xi_0)$ (2.22) was used. The initial-boundary value problem of this type was the subject of an experimental investigation [13], as well as of a numerical analysis by the finite element method [14]. In the paper [13], different fracture types of sheet specimens were investigated. The plane stress and plane strain conditions were assumed. It was confirmed that the variations in specimen geometry produce significant changes in the stress state, directions of shear bands and in ductility. The final fracture of the plate occurred in the shear bands. Numerical solutions presented in the paper [14] have been obtained by the finite element method. Particular attention has been focused on the thin shear band region of finite width, which undergoes significant deformations and temperature rise. The numerical results are compared with the available experimental observation data.

In this paper we have restricted our attention to the presentation of our own numerical results. Interesting aspects of the initial-boundary problem formulation and of the applied finite difference method have been omitted.

Figure 6 illustrates the evolution of an equivalent plastic deformation in the discretized domain of the plate. In the initial phase of deformation the shear effects (white bands) occur in the region adjacent to the loaded edges. With continued loading process, two cross shear-bands are developed in the center of the plate. Numerical experiments have revealed that the final distribution of shear bands also depends on the rate of deformation, not only on the plate geometry. For the rates larger than those assumed in the example, the shear bands develop in the region adjacent to the loaded edges.

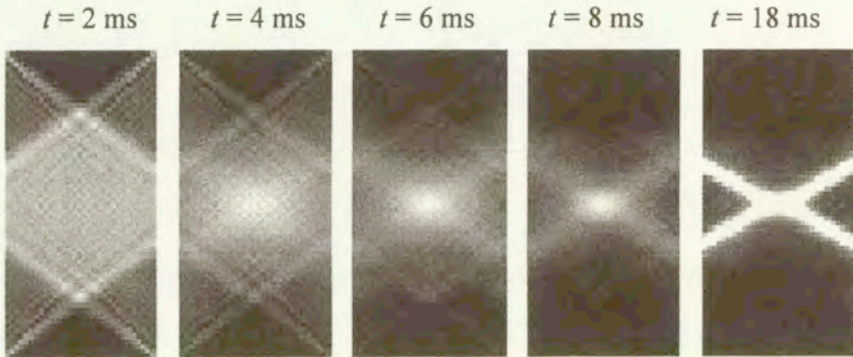


FIG. 6. Evolution of the equivalent plastic deformation in the discretized domain of the plate.

In Fig. 7 we present the distribution of the equivalent plastic deformation along the cross-section $X = a/4$ for chosen instants of the deformation process. It can be observed that the plastic strains develop in the zones of localized viscoplastic flow. The width of these zones does not tend to singular lines as for rate-independent models and depends significantly on the viscosity, which is used in calculations [14]. The obtained results are in good agreement with the experimental observations of CHAKRABARTI and SPERTNAK [13].

The porosity evolution corresponding to the evolution of equivalent plastic deformation (Fig. 7) is shown in Fig. 8.

It can be seen that the intensive increase in the porosity in shear bands occurs shortly before the final fracture of the plate. The process of the void growth, as well as of its coalescence, leads to the nucleation of a macrocrack. The development of macrocracks is illustrated in Fig. 9 by means of three selected instants of the deformation process. The cracking started in the center of a plate, and with continued loading process the macrocracks develop along the shear bands. The deformed configuration for final fracture of a plate ($t_f = 18 \text{ ms}$) is shown in Fig. 10. Figure 11 shows the variation in time of the porosity parameter ξ_{grow} at the mid-point of a plate. This variation is interesting from the viewpoint of

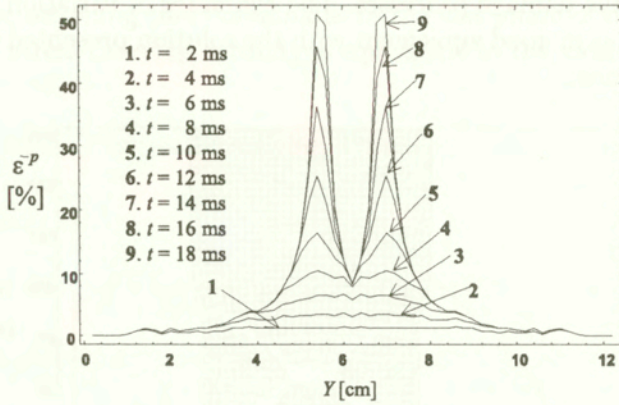


FIG. 7. Distribution of the equivalent plastic deformation along the cross-section $X = a/4$ for chosen instants of the deformation process.

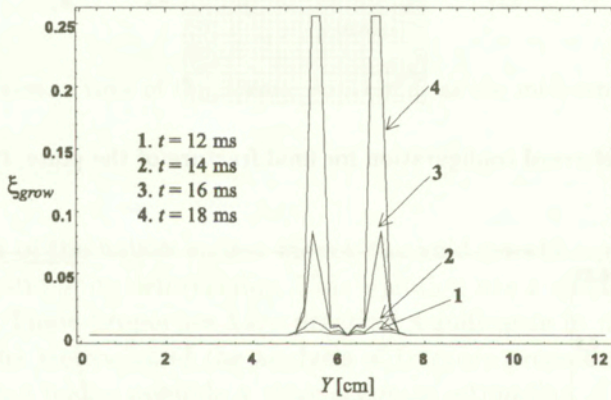


FIG. 8. Distribution of porosity along the cross-section $X = a/4$ for chosen instants of the deformation process.

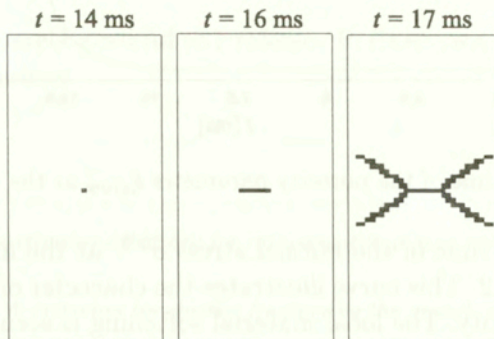


FIG. 9. Development of a macrocrack (black domains).

the analysis of the damage processes. The character of variation of the porosity parameter ξ_{grow} is in good agreement with the solution presented in Section 2 for finite deformations.

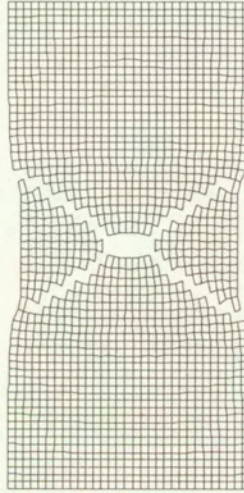


FIG. 10. Deformed configuration for final fracture of the plate, $t_f = 18$ ms.

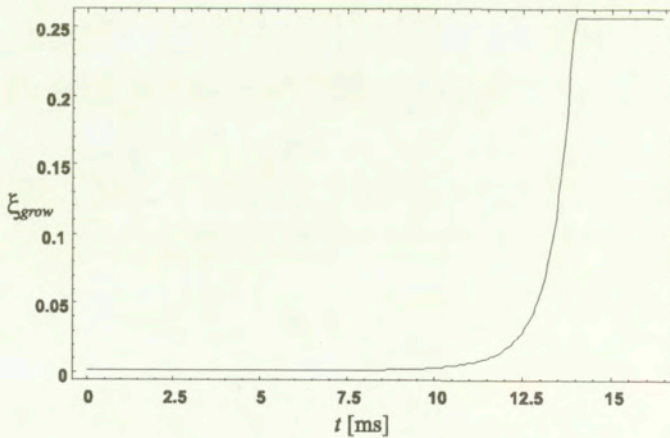


FIG. 11. Variation in time of the porosity parameter ξ_{grow} at the midpoint of the plate.

The variation in time of the normal stress σ^{YY} at the midpoint of the plate is presented in Fig. 12. This curve illustrates the character of changes of the local stress-carrying capacity. The local material softening is seen in the behaviour of inelastic strains. This softening effect depends on the deformation (geometrical softening), as well as on the porosity evolution (physical softening). It can be seen

that the physical softening effect dominates in the last phase of deformations. A complete loss of stress-carrying capacity is equivalent to the local fracture of the material.

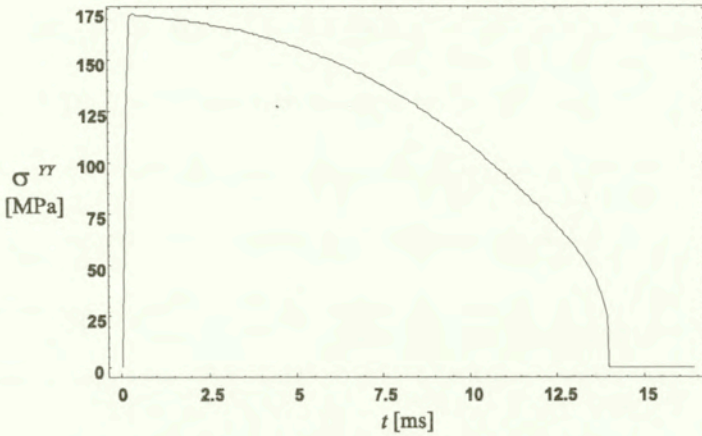


FIG. 12. Variation in time of the normal stress σ^{YY} at the midpoint of the plate.

5. Conclusions

On the basis of the hollow sphere model, the void growth equation has been derived for inelastic finite deformation. This equation has a simple form without singular points. These properties have practical significance in numerical applications. From the viewpoint of the analysis of fracture processes, the proposed evolution equation makes possible a more accurate estimation of fracture course and time for structural elements.

Acknowledgements

The author is sincerely grateful to Professor P. PERZYNA for many interesting and invaluable discussions.

References

1. P. PERZYNA, *The constitutive equations for rate-sensitive plastic materials*, Q. Appl. Math., **20**, 321, 1963.
2. F.A. McCLINTOCK, *A criterion for ductile fracture by the growth of holes*, J. Appl. Mech., **35**, 363, 1968.
3. J.R. RICE, D.M. TRACEY, *On the ductile enlargement of voids in triaxial stress fields*, J. Mech. Phys. Solids, **17**, 201, 1969.

4. B. BUDIANSKY, J.W. HUTCHINSON, S. SLUTSKY, *Void growth and collapse in viscous solids*, H.G. Hopkins, M.J. Sewell, Eds., Mechanics of solids, Pergamon Press, Oxford 1982, 13.
5. Y. HUANG, J.W. HUTCHINSON, V. TVERGAARD, *Cavitation instabilities in elastic-plastic solids*, J. Mech. Phys. Solids, **39**, 223, 1991.
6. M.M. CARROLL, A.C. HOLT, *Static and dynamic pore-collapse relations for ductile porous materials*, J. Appl. Phys., **43**, 1626, 1972.
7. J.N. JOHNSON, *Dynamic fracture and spallation in ductile solids*, J. Appl. Phys., **52**, 2812, 1981.
8. P. PERZYNA, *Internal state variable description of dynamic fracture of ductile solids*, Int. J. Solids Structures, **22**, 797, 1986.
9. J.A. NEMES, J. EFTIS, *Constitutive modeling of the dynamic fracture of smooth tensile bars*, Int. J. Plasticity, **9**, 243, 1993.
10. P. PERZYNA, A. DRABIK, *Influence of thermal effects on micro-damage mechanism in dynamic processes*, Arch. Mech., **40**, 795, 1988.
11. P. PERZYNA, *Constitutive modelling for brittle dynamic fracture in dissipative solids*, Arch. Mech., **38**, 725, 1986.
12. W. DORNOWSKI, P. PERZYNA, *Constitutive modelling of inelastic solids for plastic flow process under cyclic dynamic loading*, 32nd Solid Mechanics Conference, Zakopane, September 1-5, 1998.
13. A.K. CHAKRABARTI, J.W. SPRETNAK, *Instability of plastic flow in the directions of pure shear. II Experimental*, Metallurgical Transactions, **6A** (1975), 1975.
14. T. ŁODYGOWSKI, P. PERZYNA, *Localized fracture in inelastic polycrystalline solids under dynamic loading processes*, Int. J. Damage Mechanics, **6**, 364, 1997.

Received September 16, 1998; new version November 25, 1998.

Friction relations for the Oseen hydrodynamic interactions of spheres at large separations

I. PIENKOWSKA

*Polish Academy of Sciences
Institute of Fundamental Technological Research
Świętokrzyska 21, 00-049 Warszawa, Poland*

WE CONSIDER THE HYDRODYNAMIC FORCES, exerted by the incompressible fluid, having a uniform velocity \mathbf{U} at infinity, on a finite number of fixed rigid spheres. The convective inertia effects of the fluid are described by the Oseen equations. The hydrodynamic interactions between the spheres are treated as multiple scattering events of the perturbations of the uniform velocity \mathbf{U} . The hydrodynamic forces are considered under the assumption that the characteristic Reynolds number is small.

Notations

a	radius of the sphere
A	used to denote a certain estimate
B_1, B_2	coefficients, defined in the Appendix A
d_l^m	coefficients, introduced in the expression (3.1)
$(\mathbf{e}_x, \mathbf{e}_y, \mathbf{e}_z)$	Cartesian coordinate system
E_i	exponential integral
$\mathbf{f}_k(\mathbf{r}_k)$	forces induced on the surface of the k -th sphere
$\mathbf{f}_{k,lm}$	(l, m) component of the induced forces
\mathbf{F}_k	hydrodynamic forces, exerted by the fluid on the k -th sphere
F_4	hypergeometric series of two variables
${}_pF_q$	generalized hypergeometric function
$G_{p,q}^{m,n} \left(x \left \begin{matrix} a_p \\ b_q \end{matrix} \right. \right)$	Meijer's G -function
i	imaginary unit
I_λ	modified Bessel function of the first kind
j_l	spherical Bessel function
$\mathbf{k}(k, \chi, \eta)$	wave-vector (spherical polar coordinates), $\hat{\mathbf{k}} = \mathbf{k}/ \mathbf{k} $
\mathbf{K}_m	vectors, defined by the relations (3.2)
K_λ	modified Bessel function of the second kind
N	number of rigid spheres
$p(\mathbf{r})$	pressure field of the fluid
$\mathbf{P}(\mathbf{r}_j)$	the stress tensor inside the volumes of the spheres
P_l^m	associated Legendre function of the first kind
\mathbf{r}	position vector, specified in a Cartesian coordinate system $(\mathbf{e}_x, \mathbf{e}_y, \mathbf{e}_z)$

	\mathbf{R}_j	position of the surface of j -th sphere
	\mathbf{R}_j^0	position of the centre of j -th sphere
$\mathbf{r}_j = \mathbf{R} - \mathbf{R}_j^0, \mathbf{r}_j(a, \Omega_j)$		in spherical polar coordinates
$\mathbf{R}_{jk} = \mathbf{R}_k^0 - \mathbf{R}_j^0, \mathbf{R}_{jk}(R_{jk}, \Omega_{jk})$		in spherical polar coordinates
	\mathbf{R}_j	position of the surface of j -th sphere
	\mathbf{R}_j^0	position of the centre of j -th sphere
$\mathbf{r}_j = \mathbf{R} - \mathbf{R}_j^0, \mathbf{r}_j(a, \Omega_j)$		in spherical polar coordinates
	$\dot{\mathbf{R}}_j$	velocity of the j -th sphere
	\mathbf{R}	typical distance between the centres of two spheres
	Re	Reynolds number, $\text{Re} = a \mathbf{U} /\nu$
	$\mathbf{T}(\mathbf{r}-\mathbf{r}')$	fundamental tensor, defined by (2.3)
	$\mathbf{T}_{l_1 m_1}^{l_2 m_2}(\mathbf{O}_j)$	self-interaction tensor
	$\tilde{\mathbf{T}}_{l_1 m_1}^{l_2 m_2}(\mathbf{O}_j)$	inverse self-interaction tensor
	$\tilde{\mathbf{T}}_j, \tilde{\mathbf{T}}_j^1$	contributions to the inverse self-interaction tensor
	$\tilde{\mathbf{T}}_{l_1 m_1}^{l_2 m_2}(\mathbf{O}_j)$	
	$\mathbf{T}_{l_1 m_1}^{l_2 m_2}(\mathbf{R}_{jk})$	mutual interaction tensor
$\mathbf{T}_{l_1 m_1, l_3 m_3}^{l_2 m_2}(\mathbf{R}_{jk})$		(l_3, m_3) component of $\mathbf{T}_{l_1 m_1}^{l_2 m_2}(\mathbf{R}_{jk})$
$\mathbf{T}_{jl} = \mathbf{T}_{00}^{00}(\mathbf{R}_{jl})$		
	\mathbf{U}	uniform velocity of the fluid at infinity, $\hat{\mathbf{U}} = \mathbf{U}/ \mathbf{U} $
	$\mathbf{v}(\mathbf{r})$	velocity field of the fluid
	\mathbf{V}_j	relative velocity of the j -th sphere with respect to the fluid
	$\mathbf{V}_{j,lm}$	(l, m) component of the relative velocity \mathbf{V}_j
$x = (R\alpha)^2$		
	Y_l^m	normalized spherical harmonics
	z	quantity, defined by (4.1)
		Greek letters
$\alpha = \mathbf{U} /\nu$		
	β_m	quantity, defined in the expressions (4.1)
	Γ	gamma function
	γ	Euler's constant
	δ	Kronecker delta, Dirac delta function
	η	meridional angle, appearing in $\mathbf{k}(\mathbf{k}, \chi, \eta)$
	θ_{jk}	polar angle, appearing in $\mathbf{R}_{jk}(R_{jk}, \theta_{jk}, \phi_{jk})$
λ, Λ		quantities, introduced in the formulae (3.1)
	μ	dynamic viscosity
	ν	kinematic viscosity
	ξ_{jj}^{TV}	self-friction tensor
	ξ_{jk}^{TV}	mutual-friction tensor
	ξ	$= \cos(\hat{\mathbf{U}}, \hat{\mathbf{k}})$
	ρ	quantity, introduced in the formulae (4.1)
	$\bar{\rho}$	density of the fluid
	σ	$= a/R$
	ϕ_{jk}	meridional angle, appearing in $\mathbf{R}_{jk}(R_{jk}, \theta_{jk}, \phi_{jk})$
	χ	polar angle, appearing in $\mathbf{k}(\mathbf{k}, \chi, \eta)$
	Ω_j	angular variables, describing the vector \mathbf{r}_j
	Ω_{jk}	angular variables, describing the vector \mathbf{R}_{jk}

1. Introduction

THE HYDRODYNAMIC FORCES exerted on small particles, interacting through the ambient fluid, are important, for example, in the small Reynolds number hydrodynamics and in the examination of properties of suspensions or of porous media. We will regard the hydrodynamic forces, exerted on a finite number N of rigid spheres, immersed in an incompressible, unbounded fluid, under the condition of the Reynolds number less than unity. The complexity of the forces, generated by the hydrodynamic interactions, is due to [1]:

- (i) long range of the perturbation of the velocity of the fluid, due to the presence of a body,
- (ii) non-additivity of the interactions.

The known solutions to the problems of the many-sphere hydrodynamic interactions concern mainly the stationary and the transient Stokes interactions [2]. However, even in the range of the Reynolds number less than unity, the hydrodynamic interactions can exhibit the strong dependence on the convective inertia of the fluid [3]. The previous investigations of the inertia effects have been reported, for example, in the author's earlier paper [4].

The present paper is devoted to the examination of the convective effects, appearing in the hydrodynamic interactions of N spheres, held fixed in the flow \mathbf{U} uniform at infinity, of the viscous fluid. The range of the interactions considered is characterized by the following conditions:

$$\begin{aligned}
 & \text{(i)} \quad \text{Re} = a\alpha < 1, \quad \alpha = U/\nu, \quad U = |\mathbf{U}|, \\
 (1.1) \quad & \text{(ii)} \quad \sigma = a/R, \quad \frac{1}{2} < \sigma < \infty, \\
 & \text{(iii)} \quad R\alpha > 1,
 \end{aligned}$$

where Re is the Reynolds number, a – the radius of the sphere, ν – the kinematic viscosity of the fluid, R – the distance between the centres of the spheres. The hydrodynamic interactions are considered in the framework of the Oseen equations, giving an approximate description of the convective inertia of the fluid. In this paper we analyse the so-called friction relations, expressing the dependence of the hydrodynamic forces, exerted by the fluid on the spheres, on the spatial distribution of the spheres and on the Reynolds number Re . To this purpose we use the boundary integral approach, involving the Green tensor, depending on the uniform velocity of the fluid at infinity. The hydrodynamic interactions are treated as the multiple scattering events, conditioned by the configuration of the spheres and the inertia effects. They are characterized by the so-called hydrodynamic interactions tensors, describing the propagation of the perturbations by the fluid. The friction relations are expressed in terms of the series expansion with

respect to the characteristic parameters σ and Re . The series represents different types of the admissible sequences of the hydrodynamic interactions between the spheres. The paper is a continuation of the earlier publication of the author [4], presenting the analysis of the friction relations at the regime:

$$(1.2) \quad \begin{array}{ll} \text{(i)} & a\alpha < 1, \quad \frac{1}{2} < \sigma < \infty, \\ \text{(ii)} & R\alpha < 1. \end{array}$$

Finally, as an illustration, we consider the particular case of the hydrodynamic interactions of three spheres, at large separations, fixed in line with the flow direction.

2. Formulation of the problem

The influence of the spheres on the unperturbed uniform flow is taken into account through the so-called induced forces \mathbf{f}_k , distributed on the surfaces of the spheres \mathbf{R}_k , $k = 1, \dots, N$. We impose the no-slip boundary conditions. The basic relations of the induced forces \mathbf{f}_k to the relative velocities of the spheres with respect to the fluid \mathbf{V}_k can be presented in the form of the set of the boundary integrals over the surfaces of the spheres [4]:

$$(2.1) \quad \dot{\mathbf{R}}_j(\Omega_j) = \mathbf{U} + \int d\Omega'_j \mathbf{T} [\mathbf{R}_j(\Omega_j) - \mathbf{R}'_j(\Omega'_j)] \cdot \mathbf{f}'_j(\Omega'_j) \\ + \sum_{k \neq j}^N \int d\Omega_k \mathbf{T} [\mathbf{R}_j(\Omega_j) - \mathbf{R}_k(\Omega_k)] \cdot \mathbf{f}_k(\Omega_k),$$

$$(2.2) \quad \mathbf{V}_j(\Omega_j) = \dot{\mathbf{R}}_j(\Omega_j) - \mathbf{U}, \quad j = 1, \dots, N,$$

where the velocities of the spheres $\dot{\mathbf{R}}_j$ are assumed to be equal to zero, the induced forces are treated as unknown quantities. The convolution character of the integrals expresses the non-local properties of the interactions.

For further convenience, the fundamental tensor $\mathbf{T}(\mathbf{R}_j - \mathbf{R}_k)$ is expressed in the form of the spatial Fourier transform (presented, for example, in the paper [12]):

$$(2.3) \quad \mathbf{T}(\mathbf{r} - \mathbf{r}') = \int \frac{d\mathbf{k}}{(2\pi)^3} \frac{\exp(i\mathbf{k} \cdot (\mathbf{r} - \mathbf{r}'))}{\mu(k^2 + i\nu^{-1}\mathbf{U} \cdot \mathbf{k})} (1 - \hat{\mathbf{k}}\hat{\mathbf{k}}),$$

where the wave-vector $\mathbf{k} = (k, \chi, \eta)$ in spherical polar coordinates, $\hat{\mathbf{k}} = \mathbf{k}/|\mathbf{k}|$, μ is the dynamic viscosity of the fluid.

Using the technique of the expansions in terms of the normalized spherical harmonics Y_l^m [5], the set of convolution integrals (2.1) can be transformed to the following set of algebraic equations:

$$(2.4) \quad \mathbf{V}_{j,l_1m_1} = \sum_{l_2m_2} \mathbf{T}_{l_1m_1}^{l_2m_2}(\mathbf{O}_j) \cdot \mathbf{f}_{j,l_2m_2} + \sum_{k \neq j} \sum_{l_2m_2} \mathbf{T}_{l_1m_1}^{l_2m_2}(\mathbf{R}_{jk}) \cdot \mathbf{f}_{k,l_2m_2},$$

where $\mathbf{V}_{j,lm}$ and $\mathbf{f}_{k,lm}$ are, respectively, the (l, m) components of the relative velocities \mathbf{V}_j and the induced forces \mathbf{f}_k . The first term on the right-hand side of (2.4), involving the so-called self-interaction tensors $\mathbf{T}_{l_1m_1}^{l_2m_2}(\mathbf{O}_j)$, accounts for the hydrodynamic interactions of a single sphere; the second term, involving the so-called mutual interaction tensors $\mathbf{T}_{l_1m_1}^{l_2m_2}(\mathbf{R}_{jk})$, represents interactions between different spheres through the surrounding fluid. It follows from (2.3) that the self-interaction tensors $\mathbf{T}_{l_1m_1}^{l_2m_2}(\mathbf{O}_j)$, corresponding to the relations between the (l_2m_2) component of the induced force and the (l_1m_1) component of the relative velocity on the surface of the j -th sphere, are equal to:

$$(2.5) \quad \mathbf{T}_{l_1m_1}^{l_2m_2}(\mathbf{O}_j) = \frac{i^{l_1-l_2}}{2\pi^2\mu} \int d\mathbf{k} \frac{(1 - \hat{\mathbf{k}}\hat{\mathbf{k}})}{k^2 + i\nu^{-1}\mathbf{U} \cdot \mathbf{k}} Y_{l_1}^{-m_1} Y_{l_2}^{m_2} j_{l_1}(ak) j_{l_2}(ak),$$

where j_l are the spherical Bessel functions.

The mutual-interaction tensors $\mathbf{T}_{l_1m_1}^{l_2m_2}(\mathbf{R}_{jk})$, describing the relations between the respective quantities on the surfaces of the j -th and k -th sphere, are given by:

$$(2.6) \quad \mathbf{T}_{l_1m_1}^{l_2m_2}(\mathbf{R}_{jk}) = \sum_{l_3m_3} \mathbf{T}_{l_1m_1, l_3m_3}^{l_2m_2}(R_{jk}) Y_{l_3}^{m_3}(\Omega_{jk}),$$

where

$$(2.7) \quad \mathbf{T}_{l_1m_1, l_3m_3}^{l_2m_2} = \frac{2}{\pi\mu} i^{l_1-l_2-l_3} \int d\mathbf{k} \frac{(1 - \hat{\mathbf{k}}\hat{\mathbf{k}})}{k^2 + i\nu^{-1}\mathbf{U} \cdot \mathbf{k}} \times Y_{l_1}^{-m_1} Y_{l_2}^{m_2} Y_{l_3}^{-m_3} j_{l_1}(ak) j_{l_2}(ak) j_{l_3}(R_{jk}k),$$

$\mathbf{R}_{jk} = \mathbf{R}_k^0 - \mathbf{R}_j^0$ is the distance between the centres of relevant spheres, $\mathbf{R}_{jk}(R_{jk}, \Omega_{jk})$ in spherical polar coordinates. To determine the friction relations, we present the (l_1m_1) components of the induced forces in terms of the (l_2m_2) components of the relative velocity \mathbf{V}_{j,l_2m_2} :

$$(2.8) \quad \mathbf{f}_{j,l_1m_1} = \sum_{l_2m_2} \tilde{\mathbf{T}}_{l_1m_1}^{l_2m_2}(\mathbf{O}_j) \cdot \left[\mathbf{V}_{j,l_2m_2} - \sum_{k \neq j} \sum_{l_3m_3} \sum_{l_4m_4} \mathbf{T}_{l_2m_2}^{l_3m_3}(\mathbf{R}_{jk}) \cdot \tilde{\mathbf{T}}_{l_3m_3}^{l_4m_4}(\mathbf{O}_k) \cdot \mathbf{V}_{k,l_4m_4} + \dots \right],$$

where the iterative series describes the multiple scattering character of the interactions between the spheres [9]. The inverse self-interaction tensors $\tilde{\mathbf{T}}_{l_1m_1}^{l_2m_2}(\mathbf{O}_j)$, appearing in the above series, fulfill the relations:

$$(2.9) \quad \sum_{l_3 m_3} \tilde{\mathbf{T}}_{l_1 m_1}^{l_3 m_3}(\mathbf{O}_j) \cdot \mathbf{T}_{l_3 m_3}^{l_2 m_2}(\mathbf{O}_j) = \mathbf{1} \delta_{m_1 m_2} \delta_{l_1 l_2}.$$

In what follows, the properties of the hydrodynamic interaction tensors will be analysed under the assumption of $\text{Re} < 1$. Next, the $(l_0 m_0)$ components of the induced forces, related to the respective vector forces, will be determined within the assumed approximation with respect to σ and Re [4].

3. Properties of the self-interaction tensors

As it follows from Eq.(2.5), the self-interaction tensors are introduced to investigate the consequences of inertia of the fluid in the hydrodynamic interactions. We will consider these consequences in the regime of small values of Re . To examine these effects, the tensors are presented in the following form (for the sake of simplicity, we assume $\mathbf{U}(0, 0, U)$):

$$(3.1) \quad \mathbf{T}_{l_1 m_1}^{l_2 m_2}(\mathbf{O}_j) = \pm \frac{i^{l_1 - l_2 + |l_1 - l_2|}}{\mu a} d_{l_1}^{-m_1} d_{l_2}^{m_2} \int_0^1 d\xi \left[\frac{2}{3} \delta_{m_1, m_2} - \sqrt{\frac{2\pi}{15}} \right. \\ \left. \cdot \sum_{m_6} \mathbf{K}_{m_6} \delta_{m_1, m_2 + m_6} d_2^{m_6} P_2^{m_6}(\xi) \right] P_{l_1}^{-m_1}(\xi) P_{l_2}^{m_2}(\xi) I_\lambda(\text{Re } \xi) K_\lambda(\text{Re } \xi),$$

where I_λ, K_λ denote the modified Bessel function, P_l^m are the associated Legendre functions [6],

$$\Lambda = \max(l_1 + 1/2, l_2 + 1/2), \quad \lambda = \min(l_1 + 1/2, l_2 + 1/2),$$

$$\hat{U} = \mathbf{U}/U, \quad \xi = \cos(\hat{\mathbf{U}}, \hat{\mathbf{k}}),$$

$$d_l^m = (-1)^{(m-|m|)/2} \sqrt{\frac{(2l+1)(l-m)!}{4\pi(l+m)!}}.$$

The signs $\{\pm\}$ refer to the cases $l_1 + l_2 = 2n$ and $l_1 + l_2 = 2n + 1$, respectively. The second order tensors \mathbf{K}_m are cited after [5]:

$$(3.2) \quad \begin{aligned} \mathbf{K}_0 &= \sqrt{\frac{2}{3}}(-\mathbf{e}_x \mathbf{e}_x - \mathbf{e}_y \mathbf{e}_y + 2\mathbf{e}_z \mathbf{e}_z), \\ \mathbf{K}_{\pm 1} &= \mathbf{e}_x \mathbf{e}_z + \mathbf{e}_z \mathbf{e}_x \mp i\mathbf{e}_y \mathbf{e}_z \mp i\mathbf{e}_z \mathbf{e}_y, \\ \mathbf{K}_{\pm 2} &= \mathbf{e}_x \mathbf{e}_x - \mathbf{e}_y \mathbf{e}_y \mp i\mathbf{e}_x \mathbf{e}_y \mp i\mathbf{e}_y \mathbf{e}_x. \end{aligned}$$

<http://rcin.org.pl>

Replacing the Bessel functions by their small argument asymptotic approximations, we obtain the Stokes self-interaction tensors under the condition $l_1 = l_2$:

$$(3.3) \quad \mathbf{T}_{l_1 m_1}^{l_1 m_2}(\mathbf{O}_j) = \frac{1}{6\pi\mu a} \left[\delta_{m_1, m_2} \frac{1}{(2l_1 + 1)} - \sqrt{\frac{3}{8}} \begin{pmatrix} 2 & l_1 & l_1 \\ 0 & 0 & 0 \end{pmatrix} \right. \\ \left. \cdot \sum_{m_6} \delta_{m_6 + m_2, m_1} \begin{pmatrix} 2 & l_1 & l_1 \\ m_6 & -m_1 & m_2 \end{pmatrix} \cdot (-1)^{(|m_1| + |m_6| + |m_1 - m_6|)/2} \mathbf{K}_{m_6} \right],$$

where $\begin{pmatrix} l_1 & l_2 & l_3 \\ m_1 & m_2 & m_3 \end{pmatrix}$ are the Wigner 3- j symbols [6]. The Stokes self-interaction tensors have been introduced, for the first time, by YOSHIKAWA and YAMAKAWA [5], in their paper devoted to an application of the modified Oseen tensor to rigid polymers. The tensors (3.3), being diagonal with respect to l_i , lead to the limitations of the admissible sequences of the hydrodynamic interactions (comp. Eq. (2.8)).

The case of low but nonzero Reynolds number is described by the contributions to the self-interaction tensors, being of the order of $0(\text{Re})$. Firstly, the respective leading order contributions are obtained from Eq. (3.1), under the condition $|l_1 - l_2| = 1$. It implies that the $0(\text{Re})$ tensors are off-diagonal with respect to l_i . They can be presented in the following form:

(i) the case $l_1 - l_2 = -1$;

$$(3.4) \quad \mathbf{T}_{l_1 m_1}^{l_1 + 1 m_2} = -\frac{\text{Re}(-1)^{(-m_1 - |m_1| + m_2 - |m_2|)/2}}{6\pi\mu a \sqrt{(2l_1 + 1)(2l_1 + 3)}} \left\{ \delta_{m_1, m_2} \begin{pmatrix} l_1 & l_1 + 1 & 1 \\ 0 & 0 & 0 \end{pmatrix} \right. \\ \left. \begin{pmatrix} l_1 & l_1 + 1 & 1 \\ -m_1 & m_2 & 0 \end{pmatrix} - \frac{\sqrt{3}}{10\sqrt{2}} \sum_{m_6} \mathbf{K}_{m_6} \delta_{m_1, m_2 + m_6} (-1)^{(m_6 - |m_6|)/2} \right. \\ \left. \cdot \left[\sqrt{9 - m_6^2} \begin{pmatrix} l_1 & l_1 + 1 & 3 \\ 0 & 0 & 0 \end{pmatrix} \begin{pmatrix} l_1 & l_1 + 1 & 3 \\ -m_1 & m_2 & m_6 \end{pmatrix} \right. \right. \\ \left. \left. + \sqrt{4 - m_6^2} \cdot \begin{pmatrix} l_1 & l_1 + 1 & 1 \\ 0 & 0 & 0 \end{pmatrix} \begin{pmatrix} l_1 & l_1 + 1 & 1 \\ -m_1 & m_2 & m_6 \end{pmatrix} \right] \right\},$$

(ii) the case $l_1 - l_2 = 1$;

the tensors $\mathbf{T}_{l_2 + 1 m_1}^{l_2 m_2}$ can be obtained from the expression (3.4) by interchanging the following indices:

$$(3.5) \quad l_1 \rightarrow l_2 + 1; \quad l_1 + 1 \rightarrow l_2.$$

Secondly, the $0(\text{Re})$ contributions appear in the series expansion of the tensor $\mathbf{T}_{00}^{00}(\mathbf{O}_j)$:

$$(3.6) \quad \mathbf{T}_{00}^{00}(\mathbf{O}_j) = \frac{1}{6\pi\mu a} \left[\mathbf{1} - \frac{3}{16} \text{Re}(\mathbf{3} - \hat{\mathbf{U}}\hat{\mathbf{U}}) \right] + \dots$$

The respective inverse self-interaction tensor $\tilde{\mathbf{T}}_{00}^{00}(\mathbf{O}_j)$ reads:

$$(3.7) \quad \tilde{\mathbf{T}}_{00}^{00}(\mathbf{O}_j) = 6\pi\mu a \left[\mathbf{1} + \frac{3}{16} \text{Re}(\mathbf{3} - \hat{\mathbf{U}}\hat{\mathbf{U}}) \right] + \dots$$

The $0(\text{Re})$ contributions to the self- and inverse self-interaction tensors give rise to the particular types of the hydrodynamic interactions, absent at the Stokes regime.

4. The properties of the mutual-interaction tensors

The mutual-interaction tensors, $\mathbf{T}_{l_1 m_1, l_3 m_3}^{l_2 m_2}$, given by (2.6) and (2.7), account for the dependence of the fluid propagated forces on the inertia of the fluid and on the spatial distribution of the spheres. To examine these dependences, the mutual-interaction tensors are presented in the following form:

$$(4.1) \quad \mathbf{T}_{l_1 m_1, l_3 m_3}^{l_2 m_2} = \pm \frac{2(\pi)^{3/2} i^{l_1 - l_2 - l_3}}{a\mu\Gamma(l_1 + 3/2)\Gamma(l_2 + 3/2)} d_{l_1}^{-m_1} d_{l_2}^{m_2} d_{l_3}^{-m_3} \left(\frac{a}{R}\right)^{l_1 + l_2 + 1} \\ \sum_m \beta_m(l_1, l_2) \cdot i^{|l_1 + l_2 + 2m - l_3|} \int_0^1 d\xi \left[\frac{2}{3} \delta_{m_1 + m_3, m_2} - \sqrt{\frac{2\pi}{15}} \right. \\ \left. \cdot \sum_{m_6} \mathbf{K}_{m_6} d_2^{m_6} P_2^{m_6} \delta_{m_6 + m_2, m_1 + m_3} \right] \cdot P_{l_1}^{-m_1} P_{l_2}^{m_2} P_{l_3}^{-m_3} I_z(R\alpha\xi) K_\rho(R\alpha\xi),$$

where the signs $\{\pm\}$ refer to the cases $l_1 + l_2 + l_3 = 2n$ and $l_1 + l_2 + l_3 = 2n + 1$, respectively, $z = \max(l_1 + l_2 + 2m + 1/2, l_3 + 1/2)$, $\rho = \min(l_1 + l_2 + 2m + 1/2, l_3 + 1/2)$,

$$\beta_m = \frac{(l_1 + l_2 + 2m + 1/2)\Gamma(l_1 + l_2 + m + 1/2)}{m!} F_4[-m, l_1 + l_2 + m + 1/2; \\ l_1 + 3/2, l_2 + 3/2; \left(\frac{a}{R}\right)^2, \left(\frac{a}{R}\right)^2],$$

F_4 is the hypergeometric series of two variables.

Similarly, as in the Section 3, we assume $\hat{U}(0, 0, 1)$. We note that the effects of the inertia of the fluid are described in terms of the mutual-interaction parameter $R\alpha$ (analogous of the self-interaction parameter $\alpha\alpha$). Taking into account the properties of the associated Legendre functions P_l^m , expressed by the formulae (A1) and (A2), the mutual interaction tensors can be rewritten in the more convenient form:

$$(4.2) \quad \mathbf{T}_{l_1 m_1, l_3 m_3}^{l_2 m_2} = \pm \frac{2i^{(l_1-l_2-l_3)}(\pi)^{3/2}}{a\mu\Gamma(l_1+3/2)\Gamma(l_2+3/2)} d_{l_1}^{-m_1} d_{l_2}^{m_2} d_{l_3}^{-m_3} \left(\frac{a}{R}\right)^{l_1+l_2+1}$$

$$\sum_{m=0} \beta_m(l_1, l_2) i^{|l_1+l_2+2m-l_3|} \int_0^1 d\xi \left[\frac{2}{3} \sum_{l_4 m_4} \sum_{l_5} B_1 P_{l_5}^0 - \sqrt{\frac{2\pi}{15}} \sum_{m_6} \mathbf{K}_{m_6} d_2^{m_6} \right. \\ \left. \cdot \sum_{l_4 m_4} \sum_{l_7 m_7} \sum_{l_8} B_2 P_{l_8}^0 \right] \cdot I_z(R\alpha\xi) K_\rho(R\alpha\xi),$$

where the general formulae for the coefficients B_1 and B_2 are derived in the Appendix A. From the expression (4.2) we obtain, in particular, the uniform estimate:

$$(4.3) \quad \mathbf{T}_{l_1 m_1, l_3 m_3}^{l_2 m_2} \sim A(R\alpha) \left(\frac{a}{R}\right)^{l_1+l_2+1}.$$

The estimation of the type of $\left(\frac{a}{R}\right)^{l_1+l_2+1}$ is common to all hydrodynamic interactions at $Re < 1$, both the quasi-stationary and the time-dependent ones [10]. The integral with respect to ξ can be calculated with the help of the formula (2.24.6.1) from [7]:

$$(4.4) \quad \int_0^1 d\xi P_l^0(\xi) I_z(R\alpha\xi) K_\rho(R\alpha\xi) = \frac{1}{4\sqrt{\pi}} G_{4,6}^{2,4}$$

$$\cdot \left((R\alpha)^2 \left| \frac{z+\rho}{2}, \frac{z-\rho}{2}, \frac{-z+\rho}{2}, \frac{-z-\rho}{2}, \frac{-1-l}{2}, \frac{l}{2} \right. \right),$$

where $G_{p,q}^{m,n}$ is Meijer's function. Meijer's function has been applied to obtain the compact form of the integral (4.4). We assume that the parameters of the $G_{p,q}^{m,n} \left(\begin{matrix} a_p \\ b_q \end{matrix} \right)$ functions fulfill the conditions [8]:

$$(4.5) \quad \begin{aligned} a_k - b_j & \text{ is not a positive integer,} \\ k = 1, \dots, n; & \quad j = 1, \dots, m. \end{aligned}$$

The properties of the mutual-interaction tensors in the range of small values of $R\alpha$ are governed by the following estimate [8]:

$$(4.6) \quad \begin{aligned} G_{p,q}^{m,n} \left((R\alpha)^2 \left| \begin{array}{l} a_p \\ b_q \end{array} \right. \right) & \simeq (R\alpha)^{2\gamma}, \quad p \leq q, \quad \gamma = \min(b_h), \\ h = 1, \dots, m, & \quad R\alpha < 1. \end{aligned}$$

Hence it can be readily verified that for $R\alpha \ll 1$, the Stokes hydrodynamic interaction tensors are recovered [4].

As an example, using the described procedure we have calculated the tensors $\mathbf{T}_{00,l_3 0}^{00}$. Due to the properties of the tensors \mathbf{K}_m (3.2), the Cartesian components of the tensors $\mathbf{T}_{00,l_3 0}^{00}$ fulfill the relations:

$$(4.7) \quad \begin{aligned} \mathbf{T}_{00,l_3 0}^{00} |_{xy} & = \mathbf{T}_{00,l_3 0}^{00} |_{xz} = \mathbf{T}_{00,l_3 0}^{00} |_{yz} = 0, \\ \mathbf{T}_{00,l_3 0}^{00} |_{xx} & = \mathbf{T}_{00,l_3 0}^{00} |_{yy}. \end{aligned}$$

The respective diagonal components are equal to:

$$(4.8) \quad \mathbf{T}_{00,l_3 0}^{00} |_{zz} = \pm \frac{\sqrt{2l_3 + 1}(i)^{-l_3}}{4\pi\mu R\sqrt{\pi}} \sum_{m=0}^{\infty} \beta_m(0,0) i^{|2m-l_3|}$$

$$\begin{aligned} & \left[G_{4,6}^{2,4} \left((R\alpha)^2 \left| \begin{array}{l} -1, 1/2, \quad 0, 1/2 \\ \frac{z+\rho}{2}, \quad \frac{z-\rho}{2}, \quad \frac{-z+\rho}{2}, \quad \frac{-z-\rho}{2}, \quad \frac{-1-l_3}{2}, \quad \frac{l_3}{2} \end{array} \right. \right), \right. \\ & \left. -G_{4,6}^{2,4} \left((R\alpha)^2 \left| \begin{array}{l} 0, 1/2, \quad 0, 1/2 \\ \frac{z+\rho}{2}, \quad \frac{z-\rho}{2}, \quad \frac{-z+\rho}{2}, \quad \frac{-z-\rho}{2}, \quad \frac{-3-l_3}{2}, \quad \frac{-2+l_3}{2} \end{array} \right. \right) \right], \end{aligned}$$

$$\mathbf{T}_{00,l_3 0}^{00} \left| \begin{array}{l} xx \\ yy \end{array} \right. = \pm \frac{\sqrt{2l_3 + 1}(i)^{-l_3}}{8\pi\sqrt{\pi}\mu R} \sum_{m=0}^{\infty} \beta_m(0,0) i^{|2m-l_3|}$$

$$\left[G_{4,6}^{2,4} \left((R\alpha)^2 \left| \begin{array}{l} 0, 1/2, 0, 1/2 \\ \frac{z+\rho}{2}, \quad \frac{z-\rho}{2}, \quad \frac{-z+\rho}{2}, \quad \frac{-z-\rho}{2}, \quad \frac{-1-l_3}{2}, \quad \frac{l_3}{2} \end{array} \right. \right) \right]$$

$$(4.8) \quad +G_{4,6}^{2,4} \left((R\alpha)^2 \left[\begin{array}{c} -1, -1/2, 0, 1/2 \\ \frac{z+\rho}{2}, \frac{z-\rho}{2}, \frac{-z+\rho}{2}, \frac{-z-\rho}{2}, \frac{-3-l_3}{2}, \frac{-2+l_3}{2} \end{array} \right] \right).$$

Some other properties of the mutual-interaction tensors are discussed in the Appendix B.

5. Friction relations at $R\alpha > 1$

From (2.8) it follows that the hydrodynamic forces $\mathbf{F}_j, j = 1, \dots, N$, exerted by the fluid on the immersed spheres, can be presented in the following form [4]:

$$(5.1) \quad \mathbf{F}_j = \sum_{k=1}^N \xi_{jk}^{TV} \cdot \mathbf{U},$$

where the second-rank friction tensors ξ_{jk}^{TV} , describing the hydrodynamic interactions between the spheres as the multiple scattering process, take into account the effects of the inertia of the fluid and of the geometrical distribution of the spheres. The explicit expressions for the self-friction tensors ξ_{jj}^{TV} and the mutual-friction tensors ξ_{jk}^{TV} , can be obtained through the rearrangement of the contributions to the multiple scattering series (2.8). The rearrangements lead to the following formulae for the self-friction tensors ξ_{jj}^{TV} (including the contributions up to the first order with respect to Re and the second order with respect to σ):

$$(5.2) \quad \xi_{jj}^{TV} = \tilde{\mathbf{T}}_j + \tilde{\mathbf{T}}_j^1 + \sum_{l \neq j} \left[\tilde{\mathbf{T}}_j \cdot \mathbf{T}_{jl} \cdot \tilde{\mathbf{T}}_l \cdot \mathbf{T}_{lj} \cdot \tilde{\mathbf{T}}_j + \tilde{\mathbf{T}}_j^1 \cdot \mathbf{T}_{jl} \cdot \tilde{\mathbf{T}}_l \cdot \mathbf{T}_{lj} \cdot \tilde{\mathbf{T}}_j \right. \\ \left. + \tilde{\mathbf{T}}_j \cdot \mathbf{T}_{jl} \cdot \tilde{\mathbf{T}}_l^1 \cdot \mathbf{T}_{lj} \cdot \tilde{\mathbf{T}}_j + \tilde{\mathbf{T}}_j \cdot \mathbf{T}_{jl} \cdot \tilde{\mathbf{T}}_l \cdot \mathbf{T}_{lj} \cdot \tilde{\mathbf{T}}_j^1 \right] + \dots$$

The above contributions depend on the interaction of a single sphere and a pair of spheres. Hence, in contrast with the self-friction tensors, obtained under the assumption $R\alpha < 1$ [4], here the non-additivity of the interactions does not affect the forces considered.

The mutual-friction tensors read:

$$(5.3) \quad \xi_{jk}^{TV} = -\tilde{\mathbf{T}}_j \cdot \mathbf{T}_{jk} \cdot \tilde{\mathbf{T}}_k - \tilde{\mathbf{T}}_j \cdot \tilde{\mathbf{T}}_{jk} \cdot \mathbf{T}_k^1 - \tilde{\mathbf{T}}_j^1 \cdot \mathbf{T}_{jk} \cdot \tilde{\mathbf{T}}_k \\ - \sum_m \tilde{\mathbf{T}}_{00}^{1m}(O_j) \cdot \mathbf{T}_{1m}^{00}(\mathbf{R}_{jk}) \cdot \tilde{\mathbf{T}}_k - \tilde{\mathbf{T}}_j \cdot \sum_m \mathbf{T}_{00}^{1m}(\mathbf{R}_{jk}) \cdot \tilde{\mathbf{T}}_{1m}^{00}(O_k) \\ + \sum_{l \neq k} \sum_{l \neq j} \left[\tilde{\mathbf{T}}_j \cdot \mathbf{T}_{jl} \cdot \tilde{\mathbf{T}}_l \cdot \mathbf{T}_{lk} \cdot \tilde{\mathbf{T}}_k + \tilde{\mathbf{T}}_j^1 \cdot \mathbf{T}_{jl} \cdot \tilde{\mathbf{T}}_l \cdot \mathbf{T}_{lk} \cdot \tilde{\mathbf{T}}_k + \tilde{\mathbf{T}}_j \right. \\ \left. \mathbf{T}_{jl} \cdot \tilde{\mathbf{T}}_l^1 \cdot \mathbf{T}_{lk} \cdot \tilde{\mathbf{T}}_k + \tilde{\mathbf{T}}_j \cdot \mathbf{T}_{jl} \cdot \tilde{\mathbf{T}}_l \cdot \mathbf{T}_{lk} \cdot \tilde{\mathbf{T}}_k^1 \right] + \dots$$

They depend on the interactions of a pair and of three spheres. Hence, in comparison with the case of $R\alpha < 1$, we have here a smaller number of the spheres, participating in the hydrodynamic interactions. The non-additivity appears starting from the terms of the order of $O(\sigma^2)$.

From (5.2) and (5.3) it follows that in the range $R\alpha > 1$, the non-additivity effects are weaker than in the range $R\alpha < 1$. In the above relations we have introduced the following short-hand notation:

(i) for the self-interaction tensors,

$$(5.4) \quad \tilde{\mathbf{T}}_{00}^{00}(\mathbf{O}_j) = \tilde{\mathbf{T}}_j + \tilde{\mathbf{T}}_j^1 + \dots,$$

$$(5.5) \quad \tilde{\mathbf{T}}_j = 6\pi\mu a \mathbf{1}, \quad \tilde{\mathbf{T}}_j^1 = 6\pi\mu a \left[\frac{3}{16} \text{Re}(\mathbf{3} - \hat{\mathbf{U}}\hat{\mathbf{U}}) \right],$$

$$(5.6) \quad \tilde{\mathbf{T}}_{00}^{1m}(\mathbf{O}_j) = 2\sqrt{3}\pi\mu a \text{Re} \delta_{m0} \mathbf{1}; \quad \tilde{\mathbf{I}}_{1m}^{00}(\mathbf{O}_j) = -\tilde{\mathbf{I}}_{00}^{1m}(\mathbf{O}_j)$$

(ii) for the mutual-interaction tensors,

$$(5.7) \quad \mathbf{T}_{jk} = \mathbf{T}_{00}^{00}(\mathbf{R}_{jk}) = \sum_{l_3=0}^3 \sum_{m_3} \mathbf{T}_{00,l_3m_3}^{00}(R_{jk}) Y_{l_3}^{m_3}(\Omega_{jk}),$$

$$(5.8) \quad \mathbf{T}_{10}^{00}(\mathbf{R}_{jk}) = \sum_{l_3=0}^4 \sum_{m_3} \mathbf{T}_{10,l_3m_3}^{00}(R_{jk}) Y_{l_3}^{m_3}(\Omega_{jk}).$$

In (5.7) and (5.8) the upper limits of the summations with respect to l_3 follow from the fact that we confine our attention to the hydrodynamic interactions at $\text{Re} < 1$ (comp. App.B).

Here we use the friction tensors (5.2) and (5.3) to calculate the drag forces on the three spheres, rigidly held in the external uniform flow $\mathbf{U}(0, 0, U)$. The centre line of the spheres is parallel to the direction of the external flow. The relative distances between the centres of the spheres are specified in terms of the vectors $\mathbf{R}_{12}(R_{12}, \theta_{12} = 0^\circ, \phi_{12} = 0^\circ)$ and $\mathbf{R}_{13}(R_{13}, \theta_{13} = 0^\circ, \phi_{13} = 0^\circ)$.

The drag forces, obtained according to the expansions (5.2) and (5.3), read:

$$(5.9) \quad F_j \Big|_z = \sum_{k=1}^3 \xi_{jk}^{TV} \Big|_{zz} U_z, \quad j = 1, 2, 3,$$

where the respective components of the friction tensors in the approximation considered are given by:

$$(5.10) \quad \xi_{jj}^{TV} |_{zz} = 6\pi\mu a \left\{ 1 + \frac{3}{8}\text{Re} + \left[(6\pi\mu a)^2 + 6\pi\mu a \frac{9}{8}\text{Re} \right] \sum_{l \neq j} T_{jl} |_{zz} T_{lj} |_{zz} + \dots \right\},$$

$$(5.11) \quad \xi_{jk}^{TV} |_{zz} = 6\pi\mu a \left\{ -6\pi\mu a T_{jk} |_{zz} \left[1 + \frac{3}{4}\text{Re} \right] - 4\sqrt{3}\pi\mu a \text{Re} T_{10}^{00} |_{zz} + \left[(6\pi\mu a)^2 + 6\pi\mu a \frac{9}{8}\text{Re} \right] \sum_{l \neq k} \sum_{l \neq j} T_{jl} |_{zz} T_{lk} |_{zz} + \dots \right\}.$$

For this particular configuration we have:

$$(5.12) \quad \mathbf{T}_{jk} = \sum_{l_3=0}^3 \mathbf{T}_{00,l_3 0}^{00} Y_{l_3}^0, \quad \mathbf{T}_{10}^{00} = \sum_{l_3=0}^4 \mathbf{T}_{10,l_3 0}^{00} Y_{l_3}^0.$$

From (4.1) it follows that

$$(5.13) \quad \mathbf{T}_{00,l_3 0}^{10} |_{zz} = -\mathbf{T}_{10,l_3 0}^{00} |_{zz}, \quad l_3 = 0, 1, 2, 3, 4.$$

The relevant mutual interaction tensors are treated in more detail in the Appendix B. We recall that the friction tensors are obtained under the assumptions:

$$(5.14) \quad a/R < 1/2, \quad \text{Re} < 1, \quad R\alpha > 1.$$

It is a direct consequence of (5.10) and (5.11) that the drag forces, exerted on the spheres under the condition of finite but small values of Re, are differentiated stronger than the relevant Stokes drag forces. The inertial contributions to the considered forces are generated both by the self-interactions and the mutual interactions of the spheres. The non-additivity of the interactions affects the mutual-friction tensors ξ_{jk}^{TV} .

According to the results which have been established in ref. [11], in the case of free-fall motion of micron-order particles, the Stokes motion is observed at Re below 0.05 and the Oseen range motion, respectively, at $0.05 < \text{Re} < 0.5$. Hence the convective inertia effects considered here can, in particular cases, affect the hydrodynamic interactions at surprisingly low Re.

Appendix A. The calculations of the coefficients B_1 and B_2 , entering the relation (4.2)

In view of the properties of the normalized surface spherical harmonics Y_l^m , described by the formula (4.6.5) from [6], the product $P_{l_1}^{-m_1} P_{l_2}^{m_2} P_{l_3}^{-m_3} \delta_{m_1+m_3, m_2}$ can be expressed in terms of the sum of the P_l^0 functions:

$$(A.1) \quad P_{l_1}^{-m_1} P_{l_2}^{m_2} P_{l_3}^{-m_3} \delta_{m_1+m_3, m_2} = \sum_{l_4 m_4} \sum_{l_5} B_1 P_{l_5}^0,$$

where

$$B_1 = \frac{(-1)^{m_3} (2l_4 + 1)(2l_5 + 1)}{4\pi} \sqrt{\frac{(l_1 - m_1)!(l_2 + m_2)!(l_3 - m_3)!}{(l_1 + m_1)!(l_2 - m_2)!(l_3 + m_3)!}}$$

$$\begin{pmatrix} l_1 & l_2 & l_4 \\ -m_1 & m_2 & -m_3 \end{pmatrix} \begin{pmatrix} l_1 & l_2 & l_4 \\ 0 & 0 & 0 \end{pmatrix} \begin{pmatrix} l_3 & l_4 & l_5 \\ -m_3 & m_2 - m_1 & 0 \end{pmatrix}$$

$$\begin{pmatrix} l_3 & l_4 & l_5 \\ 0 & 0 & 0 \end{pmatrix} \delta_{m_1+m_3, m_2}, \quad \begin{array}{l} |l_1 - l_2| \leq l_4 \leq l_1 + l_2, \\ |l_3 - l_4| \leq l_5 \leq l_3 + l_4. \end{array}$$

Similarly, the product $P_2^{m_6} P_{l_1}^{-m_1} P_{l_2}^{m_2} P_{l_3}^{-m_3} \delta_{m_6+m_2, m_1+m_3}$ can be presented in the following form:

$$(A.2) \quad P_{l_1}^{-m_1} P_{l_2}^{m_2} P_{l_3}^{-m_3} P_2^{m_6} \delta_{m_1+m_3, m_2+m_6} = \sum_{l_4 m_4} \sum_{l_7 m_7} \sum_{l_8} B_2 P_{l_8}^0,$$

where

$$B_2 = (2l_4 + 1)(2l_7 + 1)(2l_8 + 1) \sqrt{\frac{(l_1 - m_1)!(l_2 + m_2)!(l_3 - m_3)!(2 + m_6)!}{(l_1 + m_1)!(l_2 - m_2)!(l_3 + m_3)!(2 - m_6)!}}$$

$$\begin{pmatrix} l_1 & l_2 & l_4 \\ -m_1 & m_2 & m_4 \end{pmatrix} \begin{pmatrix} l_1 & l_2 & l_4 \\ 0 & 0 & 0 \end{pmatrix} \begin{pmatrix} l_3 & 2 & l_7 \\ -m_3 & m_6 & m_7 \end{pmatrix} \begin{pmatrix} l_3 & 2 & l_7 \\ 0 & 0 & 0 \end{pmatrix}$$

$$\begin{pmatrix} l_4 & l_7 & l_8 \\ -m_4 & -m_7 & 0 \end{pmatrix} \begin{pmatrix} l_4 & l_7 & l_8 \\ 0 & 0 & 0 \end{pmatrix} \delta_{m_1+m_3, m_2+m_6},$$

$$\begin{array}{l} |l_1 - l_2| \leq l_4 \leq l_1 + l_2, \\ |l_3 - 2| \leq l_7 \leq l_3 + 2, \\ |l_4 - l_7| \leq l_8 \leq l_4 + l_7. \end{array}$$

The above expressions yield the information needed to calculate the mutual-interaction tensors $\mathbf{T}_{l_1 m_1, l_3 m_3}^{l_2 m_2}$ for the arbitrary range of $R\alpha$.

Appendix B. Some properties of the mutual-interaction tensors

In what follows we will calculate a few examples of the tensors $\mathbf{T}_{l_1 m_1, l_3 m_3}^{l_2 m_2}$, which in the range $R\alpha < 1$ describe the Stokes and the 0(Re) hydrodynamic

interactions. As it has been discussed in the paper [4], the first group of the tensors is characterized by the following sets of their indices:

$$(B.1) \quad \begin{aligned} (i) \quad & l_3 = l_1 + l_2, m = 0, \\ (ii) \quad & l_3 = l_1 + l_2 + 2, m = 1. \end{aligned}$$

As an example, we present the zz -component of the tensor $\mathbf{T}_{00,00}^{00}$:

$$(B.2) \quad \begin{aligned} \mathbf{T}_{00,00}^{00} |_{zz} = & \frac{1}{8\sqrt{\pi}R\mu} \left\{ {}_4F_2 \left(x \left| \begin{matrix} 1/2 \\ 3/2, 3/2 \end{matrix} \right. \right) - \frac{4}{3} {}_0F_1 (x | 5/2) \right. \\ & \left. + x^{1/2} \left[-{}_2F_3 \left(x \left| \begin{matrix} 1, 1 \\ 3/2, 2 \end{matrix} \right. \right) + {}_1F_2 \left(x \left| \begin{matrix} 1 \\ 3/2, 3 \end{matrix} \right. \right) \right] \right\}, \\ x = & (R\alpha)^2, \end{aligned}$$

where the appropriate $G_{p,q}^{m,n}$ functions, appearing in (4.4), have been expressed in terms of the generalized hypergeometric functions ${}_pF_{q-1}$ [8, § 5.2]. To establish the asymptotic properties of $\mathbf{T}_{00,00}^{00} |_{zz}$ at $R\alpha > 1$, we can use the relations for the ${}_pF_{q-1}$ functions, given in § 7 of [7]. Thus we obtain:

$$(B.3) \quad \begin{aligned} \mathbf{T}_{00,00}^{00} |_{zz} = & \frac{1}{8\sqrt{\pi}\mu R^2\alpha} \left\{ \gamma + \ln 2\sqrt{x} - Ei(-2\sqrt{x}) \right. \\ & \left. + \frac{1}{4x} \left[1 - 2x - (1 + 2\sqrt{x})e^{-2\sqrt{x}} \right] \right\}, \end{aligned}$$

where γ is the Euler constant, $-Ei(-2\sqrt{x})$ is the exponential integral [8, §6.2].

The asymptotic series for the exponential integral for large values of $R\alpha$ reads:

$$(B.4) \quad Ei(-2R\alpha) = e^{-2R\alpha} \left[\sum_{k=1}^n (-1)^k \frac{(k-1)!}{(2R\alpha)^k} + R_n \right], \quad R_n < \frac{n!}{|2R\alpha|^{n+1}}.$$

Hence we obtain that for $R\alpha \ll 1$

$$(B.5) \quad \mathbf{T}_{00,00}^{00} |_{zz} \sim \frac{1}{R^2\alpha}.$$

On the other hand, the expression (B.3) may be rewritten in the following form:

$$(B.6) \quad \mathbf{T}_{00,00}^{00}|_{zz} = \frac{1}{2\sqrt{\pi}\mu R} \sum_{k=0}^{\infty} \frac{(k+2)(-2R\alpha)^k}{(k+1)(k+3)!}.$$

From (B.6) it follows that for $R\alpha \ll 1$

$$(B.7) \quad \mathbf{T}_{00,00}^{00}|_{zz} \sim \frac{1}{R}.$$

The above example illustrates the diverse properties of the hydrodynamic interactions in the regime $R\alpha < 1$, considered in [4], in comparison with the regime $R\alpha > 1$, analysed in the present paper.

The second group of the tensors has the following characteristic indices:

$$(B.8) \quad \begin{aligned} l_3 &= l_1 + l_2 - 1, & m &= 0, \\ l_3 &= l_1 + l_2 + 1, & m &= 0, 1, \\ l_3 &= l_1 + l_2 + 3, & m &= 1, 2. \end{aligned}$$

Here we present, for example, the zz -components of the tensor $\mathbf{T}_{10,00}^{00}$:

$$(B.9) \quad \mathbf{T}_{10,00}^{00}|_{zz} = -\frac{\sqrt{3}a}{2\sqrt{\pi}\mu R^4\alpha^2} \left[-1 - \frac{2}{3}\sqrt{x} + \gamma + \ln 2\sqrt{x} - Ei(-2\sqrt{x}) \right. \\ \left. + \frac{1}{2x} - \frac{1}{2x} (1 + 2\sqrt{x}) e^{-2\sqrt{x}} \right].$$

Further examples are given in compact forms, involving the functions ${}_pF_q$:

$$(B.10) \quad T_{00,20}^{00}|_{zz} = \frac{5\sqrt{5}}{96\sqrt{\pi}\mu R} \left[1 - 2 \left(\frac{a}{R} \right)^2 \right] \cdot \left\{ x \frac{d}{dx} \left[x^{5/2} \frac{d^2}{dx^2} \right. \right. \\ \cdot \left. \left. \left[{}_2F_3 \left(x \left| \begin{matrix} 1, 1 \\ 3/2, 4, 3 \end{matrix} \right. \right) - \frac{64}{15} x^{-1/2} {}_1F_2 \left(x \left| \begin{matrix} 1/2 \\ 5/2, 7/2 \end{matrix} \right. \right) \right] \right] \right\} \\ \left. - \frac{d}{dx} \left[x^{7/2} \frac{d^2}{dx^2} \left[{}_2F_3 \left(x \left| \begin{matrix} 2, 1 \\ 3/2, 4, 4 \end{matrix} \right. \right) - \frac{64}{15} x^{-1/2} {}_1F_2 \left(x \left| \begin{matrix} 3/2 \\ 7/2, 7/2 \end{matrix} \right. \right) \right] \right] \right\},$$

$$\begin{aligned}
 \text{(B.11)} \quad \mathbf{T}_{00,10}^{00}|_{zz} = & -\frac{\sqrt{3}}{8\sqrt{\pi}\mu R} \left\{ x \frac{d}{dx} \left[-{}_2F_3 \left(x \left| \begin{matrix} 1, 1 \\ 3/2, 2, 2 \end{matrix} \right. \right) \right. \right. \\
 & + 4x^{-1/2} \left({}_1F_2 \left(x \left| \begin{matrix} 1/2 \\ 3/2, 3/2 \end{matrix} \right. \right) - 1 \right) - \frac{8}{15} x^{1/2} {}_1F_2 \left(x \left| \begin{matrix} 1 \\ 2, 7/2 \end{matrix} \right. \right) \\
 & + {}_1F_2 \left(x \left| \begin{matrix} 1 \\ 3/2, 3 \end{matrix} \right. \right) \left. \right] + \frac{5}{2} \left[1 - 2 \left(\frac{a}{R} \right)^2 \right] \cdot \frac{x^2 d^2}{dx^2} \left[{}_2F_3 \left(x \left| \begin{matrix} 1, 1 \\ 3/2, 3, 2 \end{matrix} \right. \right) \right] \\
 & - \frac{8}{3} x^{1/2} \left({}_1F_2 \left(x \left| \begin{matrix} 1/2 \\ 3/2, 5/2 \end{matrix} \right. \right) - 1 \right) - \frac{1}{2} {}_2F_3 \left(x \left| \begin{matrix} 2, 1 \\ 3/2, 3, 3 \end{matrix} \right. \right) \\
 & \left. \left. - \frac{8}{9} x^{-1/2} \left({}_1F_2 \left(x \left| \begin{matrix} 3/2 \\ 5/2, 5/2 \end{matrix} \right. \right) - 1 \right) \right] \right\}.
 \end{aligned}$$

Similarly, as for the case of the components $\mathbf{T}_{00,00}^{00}|_{zz}$ and $\mathbf{T}_{10,00}^{00}|_{zz}$, the above hypergeometric functions can be rewritten in the more explicit forms, using the formulae of the Chapter 7 of [7].

Appendix C. On the integral equations (2.1)

The integral equations (2.1) are obtained, starting from the Oseen equations of the motion of the viscous, incompressible fluid

$$\begin{aligned}
 \text{(C.1)} \quad \bar{\rho} \mathbf{U} \cdot \nabla \mathbf{v} - \mu \Delta \mathbf{v} + \nabla p = & \sum_{j=1}^N \int d\Omega_j \delta[\mathbf{r} - \mathbf{R}_j(\Omega_j)] \mathbf{f}_j(\Omega_j), \\
 \nabla \cdot \mathbf{v} = & 0,
 \end{aligned}$$

and the no-slip boundary conditions on the surfaces of the spheres:

$$\text{(C.2)} \quad \dot{\mathbf{R}}_j(\Omega_j) = \mathbf{v}(\mathbf{R}_j(\Omega_j)).$$

Inside the volumes of the spheres, the following relation holds [12]:

$$\text{(C.3)} \quad \nabla \cdot \mathbf{P}(\mathbf{r}_j) = 0, |\mathbf{r}_j| < a.$$

In the case considered, the velocity field of the fluid can be expressed in terms of the fundamental tensor $\mathbf{T}(\mathbf{r} - \mathbf{r}')$, acting on the induced forces \mathbf{f}_j :

$$\text{(C.4)} \quad \mathbf{v}(\mathbf{r}) = \mathbf{U} + \int d\mathbf{r}' \mathbf{T}(\mathbf{r} - \mathbf{r}') \cdot \sum_{j=1}^N \int d\Omega'_j \delta[\mathbf{r}' - \mathbf{R}'_j(\Omega'_j)] \mathbf{f}'_j(\Omega'_j).$$

Applying the boundary conditions (C.2) to the formula (C.4), we arrive at N coupled integral equations (2.1). Starting from these equations, the hydrodynamic interactions can be described as multiple scattering processes of the perturbations of the uniform velocity \mathbf{U} . The multiple scattering is the main physical phenomenon, examined in connection with the hydrodynamic drag, exerted by the fluid on the spheres. The scattering events are specified by the series (2.8), describing the dependence of the hydrodynamic forces on the geometrical distribution of the spheres and on the convective inertia of the fluid, expressed in terms of the parameters σ and Re . The subsequent contributions to the series are due to the interaction of a single sphere with the surrounding fluid, the one-fold interactions between two different spheres, the two-fold interactions between two or three different spheres, and so on. The contributions present the series expansion of the induced forces with respect to the parameters σ and Re , where $\sigma < 1$ and $Re < 1$. Hence the hydrodynamic forces can, in general, be calculated within the required approximation with respect to σ and Re . In this paper, we confine our attention to the first order Oseen effects.

References

1. S. KIM, S.J. KARRILA, *Microhydrodynamics*, Butterworth-Heinemann.
2. F. FEUILLEBOIS, *Some theoretical results for the motion of solid spherical particles in a viscous fluid*, [in:] *Multiphase Science and Technology*, vol. 4, [Eds.:] G.F. Hewitt, J.M. Delhaye, N. Zuber, Hemisphere 1989.
3. T. KUMAGAI, *JSME Int. J. Ser. B*, **38**, 563, 1995.
4. I. PIEŃKOWSKA, *Arch. Mech.*, **48**, 231, 1996.
5. T. YOSHIZAKI, H. YAMAKAWA, *J. Chem. Phys.*, **73**, 578, 1980.
6. A. R. EDMONDS, *Angular momentum in quantum mechanics*, Princeton University Press, 1974.
7. A.P. GRUDNIKOV, YU.A. BRYČKOW, O.I. MARIČEV, *Integrals and Series [in Russian]*, Nauka, Moskva 1986.
8. Y. L. LUKE, *The spherical functions and their approximations*, vol. I, Academic Press, 1969.
9. P. MAZUR, W. VAN SAARLOOS, *Physica A*, **115**, 21, 1982.
10. I. PIEŃKOWSKA, *Arch. Mech.*, **36**, 749, 1984.
11. T. KUMAGAI, *Revaluation of Oseen's approximation for prediction of motions of a cluster of spheres in fluid at low Reynolds number*, [in:] XIXth Int. Congress of Theoretical and Applied Mechanics, Kyoto, Japan, August 25-31, 1996.
12. P. MAZUR, A. J. WEISENBORN, *Physica A*, **123**, 209, 1984.

Received September 28, 1998; revised version December 4, 1998.

Quasi-homoclinic solutions to a system of ODEs

B. KAŹMIERCZAK

Polish Academy of Sciences

Institute of Fundamental Technological Research

Centre of Mechanics IFTR-PAS

Świętokrzyska 21, 00-049 Warszawa, Poland

THIS PAPER considers the problem of existence of “quasi-homoclinic” solution to a system of three first order ODEs containing a small parameter. These equations describe travelling wave solutions to a one-temperature model of laser-sustained plasma with absorption. This solution is homoclinic with respect to the first two variables. We use the methods of geometric singular perturbation theory to prove the existence of strictly homoclinic trajectory and then prove that it implies the existence of the desired solution.

Key words: Homoclinic solution, singular perturbation, exchange lemma, laser-sustained plasma.

1. Introduction

PLASMA SUSTAINED by a laser beam occurs naturally in different processes in which laser radiation is used, e.g. in laser welding. The full systems of equations modelling such phenomena are very complicated and it is impossible to know the quantitative details of their solutions. In this work we are looking for solutions in a form of homoclinic travelling waves of temperature. Such waves, though one-dimensional, may serve as a local approximation of the real solution and may supply us with some qualitative relations between the basic magnitudes characterizing the considered system (e.g. the speed of the moving boundary of plasma region and the intensity of the laser radiation). In this paper we consider the same problem as in [1], however the proof is simpler. *The one-temperature model of laser-maintained plasma with absorption is sketched in Sec. 3.*

2. Formulation of the problem

In this paper we consider the following system of ODEs:

$$(2.1) \quad \tilde{u}' = \tilde{v},$$

$$(2.2) \quad \tilde{v}' = qc(\tilde{u})\tilde{v} - f(\tilde{u}) - \kappa(\tilde{u})\tilde{I},$$

$$(2.3) \quad \tilde{I}' = -\varepsilon \kappa(\tilde{u}) \tilde{I},$$

where $' := \frac{d}{d\xi}$, $\xi \in (-\infty, \infty)$, $\tilde{u}, \tilde{v}, \tilde{I}: R^1 \rightarrow R^1$ and $q \in R^1$, $\varepsilon \in R^1$ with $0 < \varepsilon \ll 1$.

ASSUMPTION 1. The functions $c, f, \kappa: R^1 \rightarrow R^1$ are sufficiently smooth.

ASSUMPTION 2. $c(u) > 0$ for all $u \in (-\infty, \infty)$. There exists $u_0 > 0$, such that $\kappa(u) \equiv 0$ for $u \leq u_0$, and $\kappa(u) > 0$ for $u > u_0$.

We assume that for I from some appropriate interval, the source function $(f(u) + \kappa(u)I)$ behaves qualitatively like a cubic polynomial, i.e. that:

ASSUMPTION 3. There exist numbers $I_c > 0$, and $I^c > I_c$ such that for $I \in (I_c, I^c)$ the equation $F(u, I) = f(u) + \kappa(u)I = 0$ has exactly three solutions: $0, u_1(I) > u_0$, and $u_2(I) > u_1(I)$ such that $F_{,u}(0, I) < 0$, $F_{,u}(u_1(I), I) > 0$, $F_{,u}(u_2(I), I) < 0$, $F(u, I) > 0$ for $u < 0$, $F(u, I) < 0$ for $u \in (0, u_1(I))$, $F(u, I) > 0$ for $u \in (u_1(I), u_2(I))$ and $F(u, I) < 0$ for $u > u_2(I)$.

REMARK 1. Due to ASSUMPTION 3 and the implicit function theorem we note that $u_{1,I}(I) < 0$ and $u_{2,I}(I) > 0$ for $I \in (I_c, I^c)$ (see Fig. 1). \square

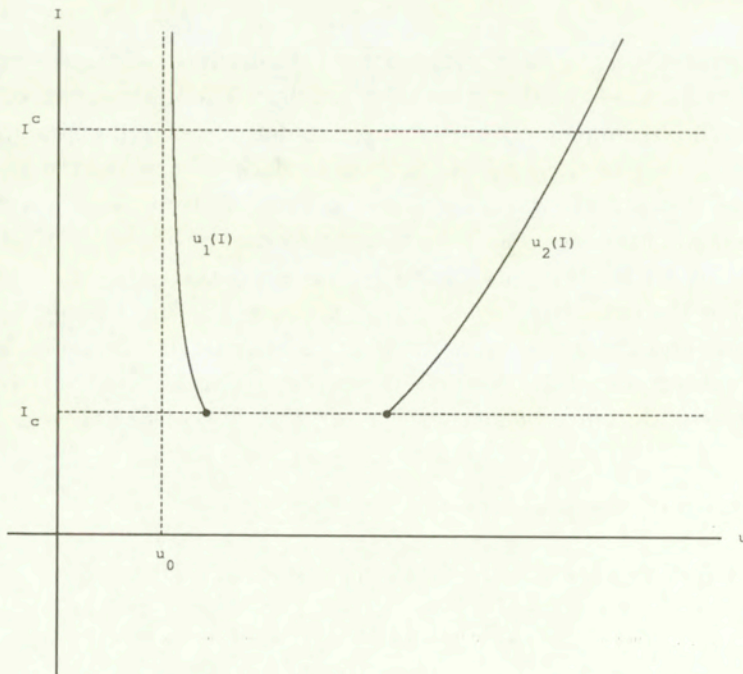


FIG. 1. The three branches of solutions to the equations $F(u, I)$.

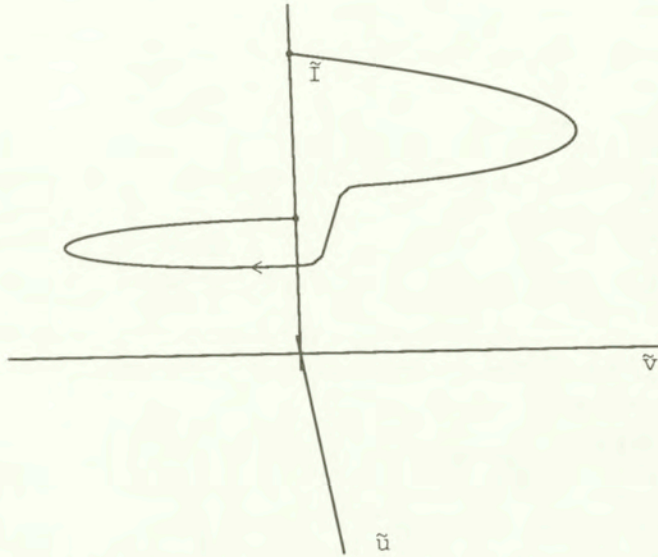


FIG. 2. A possible trajectory satisfying the conditions (2.4) and (2.5).

Our problem consists in showing that for all I_0 from some subinterval of (I_c, I^c) and for all sufficiently small $\varepsilon > 0$, there exists at least one q such that the system (2.1) – (2.3) has a solution defined for $\xi \in R^1$ and satisfying the conditions:

$$(2.4) \quad \tilde{I}(-\infty) = I_0, \quad \tilde{v}(\pm\infty) = 0,$$

$$(2.5) \quad \tilde{u}(\pm\infty) = 0, \quad \max_{\xi \in R^1} \tilde{u}(\xi) > u_2(I_0) + O(\varepsilon) \quad \text{as } \varepsilon \searrow 0.$$

Such a problem occurs e.g. in a simplified one-dimensional analysis of plasma sustained by a laser beam. This example is shortly described in the next section.

On the one hand this problem is simpler than seeking a solution homoclinic to the point $(\tilde{u}, \tilde{v}, \tilde{I}) = (0, 0, I_0)$, because we do not demand the condition $\tilde{I}(-\infty) = \tilde{I}(\infty)$. On the other hand it is, in a way, not standard as we have to do with the whole line of nonseparate singular points of the form $(\tilde{u}, \tilde{v}, \tilde{I}) = (0, 0, \tilde{I})$. We are looking for a solution starting from one point of this line and arriving at another one (with smaller \tilde{I} ; see Fig. 2). Our idea to solve the problem is to modify the considered system, so that the line of singular points shrinks to one singular point $(0, 0, I_0)$, and to apply the efficient methods of asymptotic analysis of existence of homoclinic orbits (see [2], [3], [4]). Then we prove that the obtained homoclinic solution can be modified in turn to become a solution to the system (2.1) – (2.3).

To construct the homoclinic orbit, we must make two crucial assumptions about the existence of forward and backward heteroclinic solutions for $\varepsilon = 0$ limit of the system (2.1) – (2.3).

ASSUMPTION 4. There exists exactly one $q_0 > 0$ such that for $q = q_0$ and $\tilde{I} = I_0$ there exists a unique (modulo shifts in ξ) heteroclinic solution $h_f(\xi) = (u_f(\xi), v_f(\xi))$ to the system (2.1) – (2.2) connecting the points $(0, 0) = h_f(-\infty)$ and $(u_2(I_0), 0) = h_f(\infty)$ such that $v_f(\xi) > 0$ for $|\xi| < \infty$.

ASSUMPTION 5. There exists $I^* \in (I_c, I_0)$ such that for $q = q_0$ and $\tilde{I} = I^*$ there exists a unique (modulo shifts in ξ) heteroclinic solution $h_b(\xi) = (u_b(\xi), v_b(\xi))$ to the system (2.1) – (2.2) connecting the points $(u_2(I^*), 0) = h_b(-\infty)$ and $(0, 0) = h_b(\infty)$ such that $v_b(\xi) < 0$ for $|\xi| < \infty$.

REMARK 2. It is necessary to comment on the validity of the existence assumptions (ASSUMPTIONS 4 and 5). First, the necessary conditions for ASSUMPTIONS 4 and 5 to hold are:

$$\int_0^{u_2(I_c)} (f(s) + \kappa(s)I_c) ds < 0, \quad \int_0^{u_2(I^c)} (f(s) + \kappa(s)I^c) ds > 0.$$

Now, let $I_l > I_c$ be such that

$$\int_0^{u_2(I_l)} (f(s) + \kappa(s)I_l) ds = 0$$

and

$$\int_0^{u_2(I)} (f(s) + \kappa(s)I) ds < 0$$

for all $I \in (I_c, I_l)$. A possible range of I_0 may be estimated in the following way. Let us consider the system (2.1), (2.2) for $\tilde{I} = I_\vartheta \in (I_c, I_l)$. Let q_ϑ denote the corresponding value of q for which the (unique) heteroclinic solution $h_b(\xi)$ (such that $h_b(-\infty) = (u_2(I_\vartheta), 0)$, $h_b(\infty) = (0, 0)$) exists. Since $(-f(u) - \kappa(u)\tilde{I})$ increases for every $u > u_0$ as \tilde{I} decreases, then it is easy to note that q_ϑ increases. Thus, if I_ϑ tends to I_c from above, then $q_\vartheta(I_\vartheta) \nearrow q_c > 0$.

Now, we may estimate I^u – the upper bound for the value of I_0 . It is just the value of I , for which there exists a (unique) heteroclinic $h_f(\xi)$ (such that $h_f(-\infty) = (0, 0)$, $h_f(\infty) = (u_2(I_\vartheta), 0)$) for $q = q_c$. (Again, one notes that if $h_f(\xi)$ exists for two pairs (q_1, \tilde{I}_1) and (q_2, \tilde{I}_2) and $q_2 > q_1$, then we also have $\tilde{I}_2 > \tilde{I}_1$.) If $I^u \leq I^c$ then ASSUMPTIONS 4, 5 will be valid for $I_0 \in (I_l, I^u) \subseteq (I_c, I^c)$. \square

3. Physical example

The system (2.1) – (2.3) arises naturally, when we look for travelling wave solutions to partial differential equations describing plasma sustained by a laser

beam. Under the assumption of constant pressure, the temperature field in plasma maintained by a laser radiation may be modelled by means of a nonlinear heat conduction equation (see e.g. [6] or [7]):

$$(3.1) \quad \rho C(\partial_t T + \mathbf{v}_k \cdot \text{grad}_x T) = \text{div}_x(\sigma \text{grad}_x T) + W(T, \mathbf{x}),$$

where $\mathbf{x} \in R^3$, ρ is the mass density, C is the heat capacity per unit mass at constant pressure, $\sigma(T)$ is the total heat conductivity coefficient and $W(T, \mathbf{x})$ is the nonlinear source function responsible for the energy balance: the gain of energy from the laser beam and its losses through radiation, and \mathbf{v}_k is the local velocity of the gas stream. Eq. (3.1) was analyzed in many papers (see e.g. [7], [8]). The source term has the form:

$$(3.2) \quad W(T, \mathbf{x}) = -L(T) + \kappa(T)\tilde{I}(\mathbf{x}).$$

$L(T)$ denotes the energetic losses of plasma. They are negligible below a certain temperature $T = \eta$ of the order of 10^3K . $\tilde{I}(\mathbf{x})$ is the intensity of the laser beam at the point \mathbf{x} and $\kappa(T)$ is the coefficient of energy absorption from the laser radiation. The magnitude of $\kappa(T)$ is negligible below a certain temperature $T = \eta_* \approx 10^4\text{K}$. In optically thin plasma the dependence of \tilde{I} on \mathbf{x} is described by the equation:

$$(3.3) \quad \text{div}(\mathbf{n}_p(t, \mathbf{x})\tilde{I}) = -\kappa(T)\tilde{I},$$

where $\mathbf{n}_p(t, \mathbf{x})$ is a unit vector parallel to the Poynting vector of the electromagnetic wave at point \mathbf{x} . The equations (3.1), (3.3) may be written in an dimensionless form. Let us choose a typical $\tilde{I} = J$ and let τ be the first root of the equation

$$-L(T) + \kappa(T)J = 0$$

such that $\tau > \eta_*$. Let

$$U = U(T) = (T - \eta)(\tau - \eta)^{-1}.$$

Then

$$T(U) = (\tau - \eta)U + \eta.$$

Let us set

$$\underline{\rho}(U) = \rho_0^{-1}\rho(T(U)), \quad \underline{C} = C_0^{-1}C(T(U)), \quad \underline{\sigma}(U) = \sigma(T(U))\sigma_0^{-1},$$

$$\underline{L}(U) = L(T(U))(L(\tau))^{-1}, \quad \underline{\kappa}(U) = \kappa(T(U))\kappa_0^{-1},$$

$$\rho_0 = \rho(\tau), \quad C_0 = C(\tau), \quad \sigma_0 = \sigma(\tau), \quad L_0 = L(\tau)(\tau - \eta)^{-1},$$

$$\kappa_0 = \kappa(\tau), \quad \underline{\mathbf{x}} = \kappa_0\mathbf{x}, \quad \underline{t} = \frac{L_0}{C_0\rho_0} t.$$

Then Eq. (3.1) takes the form:

$$(3.4) \quad \underline{\rho} \underline{C} (\partial_t U + \varepsilon \mathbf{v} \cdot \text{grad}_{\underline{\mathbf{x}}} U) = \varepsilon^2 \text{div}_{\underline{\mathbf{x}}} (\underline{\sigma} \text{grad}_{\underline{\mathbf{x}}} U) + \underline{W}(U, \underline{\mathbf{x}}),$$

where

$$\varepsilon^2 = \sigma_0 \frac{\kappa_0^2}{L_0}, \quad \mathbf{v} = \mathbf{v}_k \rho_0 C_0 (L_0 \sigma_0)^{-\frac{1}{2}},$$

$$\underline{W}(U, \underline{\mathbf{x}}) = -\underline{L}(U) + \underline{\kappa}(U) \underline{I}(\underline{\mathbf{x}}),$$

$$\underline{I}(\underline{\mathbf{x}}) = \kappa_0 I(\underline{\mathbf{x}}) \frac{1}{L(\tau)},$$

$$\underline{\rho}(U) = \rho_0^{-1} \rho(T(U)), \quad \underline{C} = C_0^{-1} C(T(U)), \quad \underline{\sigma}(U) = \sigma(T(U)) \sigma_0^{-1}.$$

In a similar way, Eq. (3.3) may be written in the form:

$$(3.5) \quad \text{div}_{\underline{\mathbf{x}}} (\mathbf{n}_p(\underline{\mathbf{x}}) \tilde{I}(\underline{\mathbf{x}}) - \underline{\kappa}(U) \tilde{I}(\underline{\mathbf{x}})).$$

In most experiments with laser-sustained plasma, the value of ε is relatively small. For example, for argon plasma (for pressure equal to 1 atm) it is of the order of 0.1 (see [9, 10]).

Under suitable conditions (sufficiently large laser radiation intensity and properly chosen speed of the gas stream), in a certain region of space we can cause the gas ionization. Here the gas may be in the state of plasma – its temperature is equal to T_2 ($\approx 2 \cdot 10^4 \text{K}$ for argon plasma and pressure equal to 1 atm). Out of this region the inflowing gas is cold, unionized and its temperature is equal to η ($\approx 10^3 \text{K}$). (See [6, 7, 8] and references therein). We can examine the qualitative character of the temperature profile as well as the motion of the plasma boundaries by assuming that ε is (sufficiently) small. Moreover, we will confine ourselves to the axis of symmetry of the problem, which has the simplifying property: $\mathbf{n}_p(\underline{\mathbf{x}})$ is parallel to it at every $\underline{\mathbf{x}}$, i.e. the laser beam propagates along this axis. Also $\underline{\mathbf{v}}(\underline{\mathbf{x}})$ can be assumed to be parallel to it. This 1-dimensional analysis may serve as an initial point to a more advanced consideration of the problem. So, let us look for solutions in the form of a travelling wave moving with the speed χ in the direction \mathbf{n} parallel to the axis of symmetry. Let:

$$U(\underline{t}, \underline{\mathbf{x}}) = U(\xi),$$

where

$$\xi = \varepsilon^{-1} \mathbf{n} \cdot (\underline{\mathbf{x}} - \underline{\mathbf{x}}_0) + \chi \underline{t},$$

$\underline{\mathbf{x}}_0$ lies at the axis of symmetry and $\mathbf{n} \in R^3$ is a fixed unit vector parallel to it. Thus one arrives at the system:

$$(3.6) \quad C(U)qU' = (\sigma(U)U')' + W(U, I) ,$$

$$(3.7) \quad \tilde{I}' = -\varepsilon\kappa(U)\tilde{I},$$

where $q = \rho(U)(\chi + \mathbf{v} \cdot \mathbf{n})$, $' = \frac{d}{d\xi}$, $\xi \in (-\infty, \infty)$, where we have omitted bars under the coefficients symbols. One can easily check that, due to the continuity equation and the assumed symmetry of the problem, $q = \text{const}$, q can be interpreted as the mass speed of the wave (in the direction of decreasing ξ) in the system of coordinates moving with the gas.

Finally, after introducing the relative heat potential:

$$\tilde{u}(U) := \int_0^U \sigma(y)dy$$

we arrive at the following system of equations:

$$(3.8) \quad \tilde{u}' = \tilde{v},$$

$$(3.9) \quad \tilde{v}' = qC(\tilde{u})(\sigma(\tilde{u}))^{-1}\tilde{v} + L(\tilde{u}) - \kappa(\tilde{u})\tilde{I},$$

$$(3.10) \quad \tilde{I}'(\xi) = -\varepsilon\kappa(\tilde{u})\tilde{I}(\xi),$$

where $C(\tilde{u}) = C(U(\tilde{u}))$, $L(\tilde{u}) = L(U(\tilde{u}))$ and $\kappa(\tilde{u}) = \kappa(U(\tilde{u}))$. Due to the second law of thermodynamics $\sigma(y) > 0$ for all $y > 0$, so the above transformation is invertible, i.e. there exists a smooth function $U = U(\tilde{u})$.

When we denote:

$$c(\tilde{u}) := C(\tilde{u})(\sigma(\tilde{u}))^{-1} ,$$

$$f(\tilde{u}) := -L(\tilde{u}),$$

then we obtain the system (2.1) – (2.3). We can modify slightly the function $f(u)$ for $u \in (-\infty, \delta)$, δ small, and choose I_c and I^c in such a way that ASSUMPTIONS 2, 3, 4 and 5 are satisfied. The roots u_0 and u_2 of ASSUMPTION 3 correspond to the temperatures of cold incoming gas and T_2 , respectively.

4. Modified system

First, we will analyze the system:

$$(4.1) \quad u' = v,$$

$$(4.2) \quad v' = qc(u)v - f(u) - \kappa(u)I,$$

$$(4.3) \quad I' = -\varepsilon(\kappa(u)I + k(u)(I - I_0)) ,$$

where $k(u)$ is a function with its support disjoint with the support of $\kappa(u)$ and $I_0 = \tilde{I}(-\infty)$. To this system we add the auxilliary equation:

$$(4.4) \quad q' = 0.$$

As we have mentioned, our plan is to prove the existence of an orbit homoclinic to the point $(0, 0, I_0)$ for the system (4.1) – (4.3), and then to prove that it implies the existence of a solution to our initial system (2.1), (2.2), (2.3). We assume that the function $k(u)$ is sufficiently smooth and satisfies the condition:

ASSUMPTION 6. $k : R^1 \rightarrow R^1$, $k(u) \equiv 0$ for $u \geq \frac{1}{2}u_0$, and $k(u) > 0$ for $u < \frac{1}{2}u_0$.

5. Singular orbit

The system (4.1) – (4.4) has two different time scales. By changing the “time” scale from ξ to $\tau = \xi\varepsilon$ we obtain the so-called slow system:

$$(5.1) \quad \varepsilon \dot{u} = v,$$

$$(5.2) \quad \varepsilon \dot{v} = qc(u)v - f(u) - \kappa(u)I,$$

$$(5.3) \quad \dot{I} = -(\kappa(u)I + k(u)(I - I_0)),$$

$$(5.4) \quad \dot{q} = 0,$$

where $\dot{(\)}$ denotes differentiation of $(\)$ with respect to the variable τ . On the other hand, the system (4.1) – (4.4) is called the fast system.

In the limit as $\varepsilon \rightarrow 0$ the set of critical points of the fast system (4.1) – (4.4) is determined by the set of equations:

$$(5.5) \quad v = 0,$$

$$(5.6) \quad f(u) + \kappa(u)I = 0.$$

The manifold determined by the above system will be denoted below by S . Let us note that S is invariant with respect to q , so $S = \bigcup_{q \in R^1} S(q)$. Note that the limiting flow (as $\varepsilon \rightarrow 0$) for the slow system takes place on S . According to ASSUMPTION 3, in the strip $I \in (I_c, I^c)$ every $S(q)$ consists of three branches corresponding to the three solutions to the Eq. (5.6). These branches will be denoted respectively by $\mathcal{M}^0(q)$, $\mathcal{M}^1(q)$ and $\mathcal{M}^2(q)$. Thus $\mathcal{M}^0(q) = \{(u, v, I, q) : u = 0, v = 0, I \in (I_c, I^c)\}$, $\mathcal{M}^1(q) = \{(u, v, I, q) : u = u_1(I), v = 0, I \in (I_c, I^c)\}$ and $\mathcal{M}^2(q) = \{(u, v, I, q) : u = u_2(I), v = 0, I \in (I_c, I^c)\}$. Let us denote

$$\mathcal{M}^i = \bigcup_{q \in R^1} \mathcal{M}^i(q), \quad i = 0, 1, 2.$$

Every $\mathcal{M}^i(q)$, $i = 0, 1, 2$, is parametrized by $I \in (I_c, I^c)$. Consequently, the limiting (as $\varepsilon \rightarrow 0$) flow on S (for $I \in (I_c, I_0 + \delta)$) is in fact determined by a single autonomous equation for I (with $v = 0$ and q fixed) of the form:

$$(5.7) \quad \dot{I} = -k(0)(I - I_0)$$

on \mathcal{M}^0 , and

$$(5.8) \quad \dot{I} = -\kappa(u_i(I))I$$

on \mathcal{M}^i , $i = 1, 2$.

Under the assumption $\varepsilon \ll 1$ our aim is to show the existence of an orbit homoclinic to the point $(u, v, I, q) = (0, 0, I_0, q(\varepsilon, I_0))$, where I_0 is from some open interval and $q(\varepsilon, I_0)$ is to be chosen appropriately. This will be done by the use of the geometric singular perturbations theory developed e.g. in [3], [4], [2], [5]. The starting point of the proof is the construction of a singular homoclinic orbit, i.e. an orbit consisting of solutions to the $\varepsilon = 0$ limit of the fast system, with their "ends" joined by trajectories of the $\varepsilon = 0$ limit of the slow system. More precisely:

DEFINITION 1. Let \mathcal{H}_f denote the orbit in the (u, v, I, q) -space corresponding to the solution (h_f, I_0, q_0) of $\varepsilon = 0$ limit of the system (4.1) - (4.4). Let \mathcal{H}_b denote the orbit in the (u, v, I, q) -space corresponding to the solution (h_b, I^*, q_0) of $\varepsilon = 0$ limit of the system (4.1) - (4.4).

DEFINITION 2. The singular homoclinic orbit consists of:

- (1) Heteroclinic orbits \mathcal{H}_f and \mathcal{H}_b joining the points $(0, 0, I_0, q_0)$ with $(u_2(I_0), 0, I_0, q_0)$ and $(u_2(I^*), 0, I^*, q_0)$ with $(0, 0, I^*, q_0)$.
- (2) Singular trajectories of the $\varepsilon = 0$ limit of the slow system lying on the manifolds $\mathcal{M}^0(q_0)$, and $\mathcal{M}^2(q_0)$ joining the "ends" of the heteroclinics: the right orbit \mathcal{J}_1 (lying on $\mathcal{M}^2(q_0)$) joins the point $(u_2(I_0), 0, I_0, q_0)$ with $(u_2(I^*), 0, I^*, q_0)$, and the left orbit \mathcal{J}_2 (lying on $\mathcal{M}^0(q_0)$) joins the point $(0, 0, I^*, q_0)$ with $(0, 0, I_0, q_0)$.

6. Existence of a homoclinic solution

Let us recall that two manifolds \mathcal{N}_1 and \mathcal{N}_2 , both in R^m , $m \geq 1$, are said to intersect transversely at point $p \in \mathcal{N}_1 \cap \mathcal{N}_2$ if

$$T_p\mathcal{N}_1 + T_p\mathcal{N}_2 = T_pR^m \equiv R^m.$$

The basic question undertaken by the geometric singular perturbation theory for ODEs consists in finding conditions sufficient for the existence of an orbit which stays near the singular one for sufficiently small $\varepsilon \neq 0$. One of the

possible answers is given by the following theorem (Theorem of Section 4 in [2], Theorem 8 in [4]):

THEOREM 1. *Consider the system:*

$$(6.1) \quad x' = X(x, y, q, \varepsilon),$$

$$(6.2) \quad y' = \varepsilon Y(x, y, q, \varepsilon),$$

$$(6.3) \quad q' = 0,$$

where $x \in R^{k+l}, y \in R^n$. Assume that for each $q \in R^1$ and $\varepsilon > 0$, there is a locally unique hyperbolic equilibrium point $P(q)$. Suppose that the linearization matrix at $P(q)$ possesses k positive and $l+n$ negative eigenvalues and that exactly n negative eigenvalues tend to 0 together with ε . Let $\{S^i\}, i = 0, \dots, N$ denote a family of slow manifolds for $\varepsilon = 0$ equations (with the equilibrium point for $\varepsilon \neq 0$ in S^0) and assume that for each i , S^i is normally hyperbolic with splitting: k stable and l unstable. Assume further that there is a singular homoclinic orbit, with finitely many heteroclinic orbits $\mathcal{H}_{i,i+1}$, each from S^i to S^{i+1} for some i , and trajectories \mathcal{J}_{i+1} of the $\varepsilon = 0$ limit flow of the slow system corresponding to (6.1) – (6.3) connecting the ends of heteroclinic orbits (lying on S^{i+1}). Let $\hat{\mathcal{J}}_i$ denote the trajectories \mathcal{J}_i extended beyond these jump points. Finally, assume that the following transversality conditions hold for the $\varepsilon = 0$ system:

Let $[P(q), q] \subset S^0$ denote the graph as q is varied of the $\varepsilon = 0$ limit of the $\varepsilon \neq 0$ equilibrium point. Let $S^{N+1} \equiv S^0$. We require that:

- $W^u([P(q), q])$ transversely intersects $W^s(S^1)$ in (x, y, q) – space along $\mathcal{H}_{0,1}$.
- $W^u(\hat{\mathcal{J}}_i)$ transversely intersects $W^s(S^{i+1})$ in (x, y, q) – space along $\mathcal{H}_{i,i+1}$.

Then for $\varepsilon > 0$ sufficiently small, there is a locally unique homoclinic solution to the considered system near the singular orbit.

REMARK 3.

1. This theorem was slightly changed in that we assumed that $\varepsilon \geq 0$. But, one may easily note that it does not affect its validity. (Formally, we can satisfy the conditions of the Theorem of Section 4 in [2] by substituting $\varepsilon = \varepsilon_*^2$ and considering ε_* as a small parameter)

2. Let \mathcal{A} denote a subset of a slow manifold of the system (6.1) – (6.3). By the stable (unstable) manifold of $\mathcal{A} \subset S$ (at $\varepsilon = 0$) we mean the sum:

$$W_0^s(\mathcal{A}) = \bigcup_{p \in \mathcal{A}} W_0^s(p), \quad (W_0^u(S) = \bigcup_{p \in \mathcal{A}} W_0^u(p)),$$

where $W_0^s(p)$ ($W_0^u(p)$) denotes the stable manifold of the point p with respect to the $\varepsilon = 0$ limit of the system (6.1) – (6.3).

3. In the context of the above system, a slow manifold S^i is said to be normally hyperbolic if the matrix $D_{\mathbf{x}}X(x_0, y_0, q_0, 0)$ has only eigenvalues with nonzero real parts for all $(x_0, y_0, q_0) \in S^i$ (see [2] p. 67, [4] p. 49).

4. “Near the singular orbit” means that the trajectory of the homoclinic solution lies within the $O(\varepsilon)$ neighbourhood of the singular orbit (see [4] Theorem 8 p. 102). \square

According to Assumptions 2 and 3 we have:

LEMMA 1. For all $\varepsilon > 0$, $I_0 \in (I_e, I^c)$, the point $(u, v, I) = (0, 0, I_0)$ is an equilibrium point of the system (4.1) – (4.3) for all $q \in R^1$ with $k = 1$, $l = 1$, and $n = 1$.

To apply the theorem we will take:

$$N = 1, \quad S^0 = S^2 = \mathcal{M}^0, \quad S^1 = \mathcal{M}^2, \quad \mathcal{H}_{01} = \mathcal{H}_f, \quad \mathcal{H}_{12} = \mathcal{H}_b .$$

Thus to prove the existence of a locally unique homoclinic orbit, we have to verify the transversality condition. The proof of this transversality may be found in [4], [2] or [3], but for the reader’s convenience we will sketch it below.

6.1. Transversality of $W^u(S^0)|_{[P(q),q]}$ and $W^s(S^1)$

In our case $W^u(S^0)|_{[P(q),q]}$ is just the set of points $\{(u, v, I, q) : u = v = 0, I = I_0, q \in R^1\}$. Of course, according to Assumption 4, the manifolds $W^u(S^0)|_{[P(q),q]}$ and $W^s(S^1)$ intersect in the plane $\{(u, v, I, q) : q = q_0, I = I_0\}$ along the heteroclinic orbit \mathcal{H}_f . Let $v^*(q, u)$ denote the unstable manifold of the singular point $(0, 0, I_0, q)$ with respect to the $\varepsilon = 0$ limit of the system (4.1) – (4.4) (for $I = I_0$ and q fixed). We have the following relations:

$$(6.4) \quad \frac{1}{2}v^{*2}(q, u) = \int_0^u \{qc(y)v^*(q, y) - f(y) - \kappa(y)I_0\}dy ,$$

$$(6.5) \quad \frac{1}{2}v_*^2(q, u) = - \int_u^{u_2(I_0)} \{qc(y)v_*(q, y) - f(y) - \kappa(y)I_0\}dy .$$

In fact, in Eq. (6.4), for q near q_0 , we must confine ourselves to $u \in [0, u^*(q)]$, where $u^*(q) \rightarrow u_2(I_0)$ as $q \rightarrow q_0$. In the same way, in Eq. (6.5) $u \in [u_*(q), u_2(I_0)]$, $u_*(q) \rightarrow 0$ as $q \rightarrow q_0$.

By differentiating with respect to q at $q = q_0$ one obtains the relations:

$$(6.6) \quad v_{,q}^*(q_0, u)v^*(q_0, u) = \int_0^u c(y)\{q_0v_{,q}^*(q_0, y) + v^*(q_0, y)\}dy ,$$

$$(6.7) \quad v_{*,q}(q_0, u)v_*(q_0, u) = - \int_u^{u_2(I_0)} c(y)\{q_0v_{*,q}(q_0, y) + v_*(q_0, y)\}dy ,$$

which are valid for all $u \in (0, u_2(I_0))$. As every trajectory in $W^s(S^1)$ stays in a plane $I = \text{const}$, thus to prove the desired transversality, it suffices to show that the projection of $W^s(S^1)$ onto the space $I = I_0$ intersects $W^u(S^0) |_{[P(q),q]}$ along the curve $u \rightarrow (u, v^0(q_0, u), I_0, q_0)$, for $u \in (0, u_2(I_0))$ (corresponding to \mathcal{H}_f) transversely in the plane $\{(u, v, I, q) : I = I_0\}$ which is isomorphic to R^3 . Here $v^0(q_0, u) := v^*(q_0, u) = v_*(q_0, u)$. At any point (u_0, v, I_0, q_0) , $v = v^0(q_0, u_0)$, an arbitrary vector from the space tangent to the surface $(u, q) \rightarrow (u, v^*(q, u), I_0, q)$ has the form

$$[du, v_{*,u}^0(q_0, u_0)du + v_{*,q}^*(q_0, u_0)dq, 0, dq]$$

and a vector from the space tangent to the surface $(u, q) \rightarrow (u, v_*(q, u), I_0, q)$ has the form

$$[du, v_{*,u}^0(q_0, u_0)du + v_{*,q}(q_0, u_0)dq, 0, dq].$$

One notes that all vectors from R^3 can be expressed in terms of these vectors iff $v_{*,q}^*(q_0, u_0) \neq v_{*,q}(q_0, u_0)$.

LEMMA 2. For $u \in (0, u_2(I_0))$:

$$v_{*,q}^*(q_0, u) > 0 \quad \text{and} \quad v_{*,q}(q_0, u) < 0.$$

Moreover,

$$\lim_{u \nearrow u_2(I)} v_{*,q}^*(q_0, u) \rightarrow \infty, \quad \lim_{u \searrow 0} v_{*,q}(q_0, u) \rightarrow -\infty .$$

Proof. Let us note that $v_{*,q}^*(q_0, 0) = v_{*,q}(q_0, u_2(I_0)) = 0$, $v_{*,qu}^*(q_0, 0) > 0$ and $v_{*,qu}(q_0, u_2(I_0)) > 0$. Hence, $v_{*,q}^*(q_0, u) > 0$ for $u \in (0, \delta)$ whereas $v_{*,q}(q_0, u) < 0$ for $u \in (u_2(I_0) - \delta, u_2(I_0))$ for some $\delta > 0$ sufficiently small. Now, suppose that u_m is the largest u in $(0, u_2(I_0))$, such that $v_{*,q}(q_0, u_m) = 0$. As $v_{*,q}(q_0, u)$ satisfies the equation of the form:

$$v_{*,qu}v + v_{*,q}v_u = q_0c(u)v_{*,q} + cv ,$$

this would imply that $v_{*,qu}(q_0, u_m) = c(u_m) > 0$ - a contradiction. Thus $v_{*,q}(q_0, u) < 0$ for all $u \in (0, u_2(I_0))$. In the same way we prove that $v_{*,q}^*(q_0, u) > 0$ for all $u \in (0, u_2(I_0))$. Also $m := \lim_{u \searrow 0} v_{*,q}(q_0, u) < 0$ and

$\lim_{u \nearrow u_2(I)} v_{*,q}^*(q_0, u) > 0$. Using (6.6) we obtain the third relation of this lemma.

Now, we will prove that the last relation is true. Suppose to the contrary that $m \in (-\infty, 0)$. Then both sides of Eq. (6.) are (in the limit) equal to 0 for $u = 0$ and we obtain for $u \searrow 0$:

$$[\lambda_- + o(1)][m + o(1)]u = q_0[c(0) + o(1)][m + o(1)] + O(u^2),$$

$$[\lambda_- - q_0c(0) + o(1)] = O(u^2),$$

where λ_- is the positive eigenvalue of linearization matrix at $(u, v) = (0, 0)$. As $\lambda_- > q_0c(0)$, then passing to the limit $u \searrow 0$ we arrive at a contradiction. The lemma is proved. \square

6.2. Transversality of $W^u(S^1)|_{sing.orbit}$ and $W^s(S^0)$

The intersection of these two manifolds takes place in the set $\{(u, v, I, q) : q = q_0, I = I^*\}$ along the orbit corresponding to \mathcal{H}_b . It is easy to note that this intersection is transversal, if it is transversal in the $\{(u, v, I, q) : q = q_0\}$ space. So, as above, for I from some neighbourhood of I^* , let us denote by $\sigma^*(I, u)$ the stable manifold of the singular point $(0, 0, I, q_0)$ with respect to the $\varepsilon = 0$ limit of the system (4.1) – (4.4) (for $q = q_0$ and I fixed) parametrized locally by u . Analogically, let $\sigma_*(q, u)$ denote the unstable manifold of the point $(u_2(I^*), 0, I, q_0)$. Then, for I from some neighbourhood of I^* we have:

$$(6.8) \quad \frac{1}{2}\sigma_*^2(I, u) = \int_{u_2(I)}^u \{q_0c(y)\sigma_*(I, y) - f(y) - \kappa(y)I\}dy ,$$

$$(6.9) \quad \frac{1}{2}\sigma^{*2}(I, u) = \int_0^u \{q_0c(y)\sigma^*(I, y) - f(y) - \kappa(y)I\}dy .$$

Equation (6.8) is valid for $u \in [u_*(I), u_2(I)]$, where $u_*(I) \rightarrow 0$ as $I \rightarrow I^*$. In the same way Eq. (6.9) is valid for $u \in [0, u^*(I)]$, where $u^*(I) \rightarrow u_2(I^*)$ as $I \rightarrow I^*$. For $I = I^*$, $\sigma^*(I, u) = \sigma_*(I, u)$. Of course $\sigma^*(I^*, u) = \sigma_*(I^*, u)$ is negative for $u \in (0, u_2(I^*))$. Differentiation with respect to I at $I = I^*$ gives us the relations:

$$(6.10) \quad \sigma_{*,I}(I^*, u)\sigma_*(I^*, u) = \int_u^{u_2(I^*)} \{-q_0c(y)\sigma_{*,I}(I, y) + \kappa(y)\}dy ,$$

$$(6.11) \quad \sigma_{*,I}^*(I^*, u)\sigma^*(I^*, u) = - \int_0^u \{-q_0c(y)\sigma_{*,I}^*(I, y) + \kappa(y)\}dy .$$

Now, it easy to see that the following lemma holds:

LEMMA 3. $\sigma_{*,I}(I^*, u)$, and $\sigma_{*,I}(I^*, u)$ satisfy the relations:

$$\sigma_{*,I}(I^*, u) < 0 \quad \text{for} \quad u \in (0, u_2(I^*)),$$

$$\begin{aligned} \sigma_{*,I}^*(I^*, u) &= 0 & \text{for } u \in [0, u_0], \\ \sigma_{*,I}^*(I^*, u) &> 0 & \text{for } u \in (u_0, u_2(I^*)), \\ \lim_{u \searrow 0} \sigma_{*,I}^*(I^*, u) &= -\infty, & \lim_{u \nearrow u_2(I^*)} \sigma_{*,I}^*(I^*, u) = \infty. \end{aligned}$$

P r o o f. Due to Assumption 3 we note that $\sigma_{*,I}^*(I^*, u_2(I^*)) = 0$. Thus, by (6.10), we infer that $\sigma_{*,I}^*(I^*, u) < 0$ for $u \in (0, u_2(I^*))$. Moreover, $\sigma_{*,I}^*(I^*, u) \searrow -\infty$ as $u \searrow 0$. It follows from (6.11) that $\sigma_{*,I}^*(I^*, u) = 0$ for $u \in [0, u_0]$. Suppose that $\sigma_{*,I}^*(I^*, \eta) \leq 0$ for some $\eta > u_0$. Then, by (6.11), $\sigma_{*,I}^*(I^*, u) < 0$ for $u < \eta$, sufficiently close to η , so it cannot become 0 for $u = u_0$. Hence $\sigma_{*,I}^*(I^*, u) > 0$ for $u \in (u_0, u_2(I^*))$. Finally, as $\kappa(u_2(I^*)) > 0$, then $\lim_{u \nearrow u_2(I^*)} \sigma_{*,I}^*(I^*, u) \neq 0$, as otherwise the right-hand side of Eq. (6.11) cannot tend to 0 as $u \nearrow u_2(I^*)$. Now, as in the proof of Lemma 2, one can show that $\lim_{u \nearrow u_2(I^*)} \sigma_{*,I}^*(I^*, u) = \infty$. The lemma is proved. \square

This lemma guarantees the transversality of the considered manifolds.

7. Existence of a solution to the initial system

Below, we will prove that from the homoclinic solution obtained by means of Theorem 1 we can construct a solution to the system (2.1) – (2.3) satisfying the conditions (2.4) – (2.5). First, we will state some properties of the solution homoclinic to the point $(0, 0, I_0)$ obtained by means of Theorem 1.

LEMMA 4. Let $(u(\xi), v(\xi), I(\xi))$ be a solution to the system (4.1) – (4.3) homoclinic to the point $(0, 0, I_0)$. Then:

1. $u(\xi) > 0$ for $|\xi| \neq 0$.
2. Let $(1, w_-)$ and $(1, w_+)$ denote eigenvectors corresponding to the eigenvalues $\lambda_- > 0$ and $\lambda_+ < 0$ of the linearization matrix of Eqs. (4.1), (4.2) for $q = q(\varepsilon, I_0)$ at $(0, 0)$. Then $w_- = \lambda_-$, $w_+ = \lambda_+$ and $(u(\xi), v(\xi)) = u(\xi)(1, w_{\pm} + o(1))$ as $\xi \rightarrow \pm\infty$.

P r o o f. Suppose to the contrary that the first part of the lemma is not true. Then there must exist such ξ that $u(\xi)$ is a negative minimum. So, $-f(u(\xi)) - \kappa(u(\xi))I(\xi) \geq 0$. This is, however, impossible according to Assumption 3. The second part is obvious as, due to Assumption 2, $\kappa(u) \equiv 0$ for $u \in [0, u_0]$. \square

LEMMA 5. For $\varepsilon > 0$ sufficiently small, the u -component of the homoclinic solution to Eqs. (4.1) – (4.3) may have only one maximum and no minimum.

P r o o f. As $\varepsilon \searrow 0$, then homoclinic solution to Eqs. (4.1) – (4.4) obtained by Theorem 1 tends to the singular solution defined in Section 5. The projection

of the singular orbit onto the (u, v) space touches the $v = 0$ axis for $u = 0$ and $u \in [u_2(I^*), u_2(I_0)]$. Suppose that the function u attains a maximum different from the global maximum (or from a fixed global maximum if there are more than one) at some point ζ_M . According to Lemma 4, for ε small, $u(\zeta_M)$ must be close to the set $[u_2(I^*), u_2(I_0)]$. As there is another maximum, the function u must attain a minimum at some point ζ_m , where $\zeta_m < u^*$ and $u^* \rightarrow u_1(I^*)$ for $\varepsilon \rightarrow 0$. However, due to Assumption 3, $u_2(I^*) > u_1(I^*) + d$, $d > 0$, for $I \in (I_c, I^c)$. This would imply that the distance between the considered solution and the singular solution would not tend to 0 as $\varepsilon \searrow 0$. Hence we arrive at a contradiction with Theorem 1. The lemma is proved. \square

LEMMA 6. Let $u(\xi) < u_0$ for $\xi < \xi_-$. Then $I(\xi) \equiv I_0$ for $\xi \in (-\infty, \xi_-)$.

P r o o f. Suppose that this is not true and that for some $\zeta < \xi_-$ we have $I(\zeta) \neq I_0$. Then $I(\xi) = I_0 + (I(\zeta) - I_0) \exp(-\varepsilon \int_{\zeta}^{\xi} k(u(s)) ds)$ and consequently, $I(\xi)$ would diverge as $\xi \rightarrow -\infty$ unless $(I(\zeta) - I_0) = 0$. \square

In view of Lemma 4, 5 and 6, the following theorem of existence is valid:

THEOREM 2. Let Assumptions 1-5 be fulfilled. Then for each $\varepsilon > 0$ sufficiently small there exists $q(\varepsilon, I_0)$ such that for $q = q(\varepsilon)$ there exists a (locally unique modulo shifts in ξ) solution to the system (2.1) – (2.3) satisfying the conditions (2.4), (2.5).

P r o o f. Fix $\varepsilon > 0$ sufficiently small. Let ξ_- be the same as in Lemma 6 and let ξ_+ be such that $u(\xi) < u_0$ for $\xi > \xi_+$. (Of course ξ_- and ξ_+ may depend on ε .) Then a solution to our problem can be determined by the equations:

$$\tilde{u}(\xi) = u(\xi), \quad \tilde{v}(\xi) = v(\xi) \quad \text{for} \quad \xi \in (-\infty, \infty) ,$$

$$\tilde{I}(\xi) = I(\xi) = I_0 \quad \text{for} \quad \xi \in (-\infty, \xi_-) ,$$

$$\tilde{I}(\xi) = I(\xi) \quad \text{for} \quad \xi \in [\xi_-, \xi_+) ,$$

$$\tilde{I}(\xi) = I(\xi_+) \quad \text{for} \quad \xi \in [\xi_+, \infty) .$$

The theorem is proved. \square

Acknowledgements

This work was supported by grant KBN 7 T07A 02113.

References

1. B. KAŻMIERCZAK, *Travelling waves in a system modelling laser-sustained plasma*, to be published in *J. Appl. Math. Phys.*
2. C.K.R.T. JONES, N. KOPELL, *Tracking invariant manifolds with differential forms in singularly perturbed systems*, *J. Differential Equations*, **108**, 64–88, 1994.
3. P. SZMOLYAN, *Heteroclinic and homoclinic orbits in singular perturbation problems*, *J. Differential Equations*, **92**, 252–281, 1991.
4. C.K.R.T. JONES, *Geometric singular perturbation theory*, in *Dynamical Systems*, Montecatini Terme, 1994, Lecture Notes in Mathematics, 1609, 45–118, 1994.
5. B. DENG, *The existence of infinitely many traveling front and back waves in the FitzHugh-Nagumo Equations* *SIAM J. Math. Anal.*, **22** (1991) (1631–1650).
6. Iu.P. RAIZER, *Fizika gazovogo razrjada* (in Russian), Moskva, Nauka, 1987.
7. Z. PERADZYŃSKI, *Continuous Optical Discharge, Properties and Modelling*, III, ICPIG XXI, Ruhr-Universität Bochum (1993), 227–236.
8. W. ECKHAUS, A. van HARTEN, Z. PERADZYŃSKI, *A Singularly Perturbed Free Boundary Problem Describing a Laser Sustained Plasma*, *SIAM J. Appl. Math.*, **45** (1985), 1–31.
9. J. KURZYNA, *Numerical Modelling of Laser Sustained Plasma and Its Comparison with Experiments* (in Polish)—Ph.D. thesis, IFTR-PAS, Warsaw, 1992.
10. R.S. DEVOTO, *Transport coefficients of partially ionized argon*, *Physics of Fluids*, **10** (1967), 354–364.

Received October 9, 1998; revised version January 8, 1999.

DIRECTIONS FOR THE AUTHORS

The journal *ARCHIVES OF MECHANICS (ARCHIWUM MECHANIKI STOSOWANEJ)* deals with the printing of original papers which should not appear in other periodicals.

As a rule, the volume of a paper should not exceed 40 000 typographic signs, that is about 20 type-written pages, format: 210×297 mm, leaded. The papers should be submitted in two copies. They must be set in accordance with the norms established by the Editorial Office. Special importance is attached to the following directions:

1. The title of the paper should be as short as possible.
2. The text should be preceded by a brief introduction; it is also desirable that a list of notations used in the paper should be given.
3. The formula number consists of two figures: the first represents the section number and the other the formula number in that section. Thus the division into subsections does not influence the numbering of formulae. Only such formulae should be numbered to which the author refers throughout the paper, and also the resulting formulae. The formula number should be written on the left-hand side of the formula; round brackets are necessary to avoid any misunderstanding. For instance, if the author refers to the third formula of the set (2.1), a subscript should be added to denote the formula, viz. (2.1)₃.
4. All the notations should be written very distinctly. Special care must be taken to write small and capital letters as precisely as possible. Semi-bold type should be underlined in black pencil. Explanations should be given on the margin of the manuscript in case of special type face.
5. It has been established to denote vectors by semi-bold type. Trigonometric functions are denoted by sin, cos, tg and ctg, inverse functions – by arc sin, arc cos, arc tg and arc ctg; hyperbolic functions are denoted by sh, ch, th and cth, inverse functions – by Arsh, Arch, Arth and Arcth.
6. Figures in square brackets denote reference titles. Items appearing in the reference list should include the initials of the first name of the author and his surname, also the full title of the paper (in the language of the original paper); moreover;

- a) In the case of books, the publisher's name, the place and year of publication should be given, e.g.,
 5. S. Ziemia, *Vibration analysis*, PWN, Warszawa 1970;
 - b) In the case of a periodical, the full title of the periodical, consecutive volume number, current issue number, pp. from ... to ..., year of publication should be mentioned; the annual volume number must be marked in black pencil so as to distinguish it from the current issue number, e.g.,
 6. M. Sokolowski, *A thermoelastic problem for a strip with discontinuous boundary conditions*, Arch. Mech., **13**, 3, 337–354, 1961.
7. The authors should enclose a summary of the paper. The volume of the summary is to be about 100 words.

8. The authors are kindly requested to enclose the figures prepared on diskettes (format PCX, BitMap or PostScript).

Upon receipt of the paper, the Editorial Office forwards it to the reviewer. His opinion is the basis for the Editorial Committee to determine whether the paper can be accepted for publication or not.

The printing of the paper completed, the author receives 25 copies of reprints free of charge. The authors wishing to get more copies should advise the Editorial Office accordingly, not later than the date of obtaining the galley proofs.

The papers submitted for publication in the journal should be written in English. No royalty is paid to the authors.

Please send us, in addition to the typescript, the same text prepared on a diskette (floppy disk) 3 1/2" as an ASCII file, preferably in the T_EX or L_AT_EX format in Dos or Unix format.

EDITORIAL COMMITTEE
ARCHIVES OF MECHANICS
(ARCHIWUM MECHANIKI STOSOWANEJ)

Archives of Mechanics

Contents of issue 1 vol. 51

- 3 R. WOJNAR, *Distortion equation of motion in linear incompatible elastodynamics*
- 15 I. ADLURI, *Some exact solutions of steady plane MHD non-Newtonian power-law fluid flows*
- 33 A. CIARKOWSKI, *Frequency dependence on space-time for elastomagnetic propagation in dispersive medium*
- 47 M. CIARLETTA and F. PASSARELLA, *Domain of influence theorem in the theory of bending of micropolar elastic plates with stretch*
- 59 S. MAY, *Two-point Padé approximants to the effective heat conduction coefficient of non-uniform media*
- 71 W. DORNOWSKI, *Influence of finite deformations on the growth mechanism of microvoids contained in structural metals*
- 87 I. PIEŃKOWSKA, *Friction relations for the Oseen hydrodynamic interactions of spheres at large separations*
- 105 B. KAŻMIERCZAK, *Quasi-homoclinic solutions to a system of ODDEs*